



***Cyto-molecular investigations to analyse the
synaptonemal complex of rye standard and B
chromosomes during meiosis and to evaluate the
potential of a new FISH probe labelling system***

**Dissertation
zur Erlangung des
Doktorgrades der Naturwissenschaften (Dr. rer. nat.)**

der
Naturwissenschaftlichen Fakultät III
Agrar- und Ernährungswissenschaften,
Geowissenschaften und Informatik
der Martin-Luther-Universität Halle-Wittenberg

vorgelegt von

Susann Kerstin Hesse-Bikbaeva
Geb. am 21.07.1982 in Berlin-Buch, Deutschland

Gutachter

Prof. Dr. Neil Jones
Prof. Dr. Andreas Houben

Verteidigt am

20.01.2020

Halle/Saale

In memoriam callidi avi mei.

Werner Hesse

22.05.1937 - 24.12.2018

Acknowledgments

This work was funded by the baseclick GmbH, Neuried, Germany and the Leibniz Institute of Plant Genetics and Crop Plant Research, Gatersleben, Germany and was carried out in the research group of 'Chromosome Structure and Function (CSF)' at the Leibniz Institute of Plant Genetics and Crop Plant Research.

I had the pleasure to work with a lot of wonderful people that helped and supported me and made this PhD a very special time of my life, so many thanks to all of you!

I want to thank my three supervisors, Andreas Houben, Veit Schubert and Antonio Manetto for their support during this dissertation. To Andreas and Antonio for giving me the opportunity to become the first 'Doctor' in my family and to Veit for hosting me in the cosiest of our labs with lovely temperatures, a moody SIM microscope, the best chocolate supply in Saxony-Anhalt and the most delicious honey available "weit und breit".

To Oda, Karla, Sylvia and Katrin our beloved fairies of the lab, without your magic pixie dust for me a functional and social lab life wouldn't have been possible, thanks girls!

To Jana and Jörg, the best running companions I could have wished for in my wildest dreams! Thank you for all this endless laughing, highly professional running experiences, lunch-cheese cake-coffee rituals, wonderful concerts, theatre visits... and all the time we spend together until now! Don't you even hope you will get rid of me just because I move to Mainz! ;D

Also many thanks to my amazing lab mates! To Wei and Maja who made the 'big office' a place to feel home.

To Lala, thank you for all the lovely talks we had and for your amazing humour which is as black, sarcastic and dry as mine and made me laugh so much!

To Mateusz, sorry man, but in all this years you did not convince me that bison food added to polish vodka makes it anyhow more drinkable.

To Ishii-Sun, at least to me you have proven that you deserve your position as a sensei in your own group. It was my biggest pleasure to work and learn from you! For the sake of your employees, I hope you're improving your motivation skills. "You need to do it a thousand times before you will do it right!" is not as motivating as you might think, when someone is down because of non-working chromosome preps.

To Celia, thank you for the lovely time we spent in the "small office", outside of the lab and for "synchronizing" in so many respects!

And to all other CSF members and guest that made my time at IPK so interesting and nice!

Beside the IPK, I also have a wonderful family who supported me all my way long.

Thank you so much mom and dad! I might have been incapable to tell you what I was actually doing in this mysterious labs all the years but without you I wouldn't be here at this point ;D

To my beautiful, beautiful two daughters, Leo and Elli, thank you for teaching me what really matters in life!

And last but not least, Artur, my beloved Russian scientist without a proper accent! "Let's me speak from my heart": throughout all this years we have shared wonderful highs and you never gave up on me at my lows. Thank you for that, my love! Without you, the past 9 years would not have been the greatest of my life so far...Okay, if you would have went with me to Paris, they would have been the greatest x 2 but since we in future live closer to Paris than to Berlin, I do not give up hope! Apart from that, I always love you twice more...infinitely...endlessly...unconditionally♥

Contents

Table of figures	7
Abstract	8
Abbreviations	9
0. Preface	11
1. The dynamics of synaptonemal complex components during meiotic pairing/synapsis of standard (A) and accessory (B) rye chromosomes	11
1.1 Introduction	11
1.1.1 Meiosis	11
1.1.2 Prophase I of meiosis	12
1.1.7. Meiosis of rye B chromosomes	21
1.3 Materials and Methods	24
1.3.1 Plant material and cultivation	24
1.3.2 FISH probe preparation	24
1.3.3 Assessment of B chromosome number in individual rye plants	24
1.3.4 Characterization of the NDJ-deficient B isoform by FISH	25
1.3.5 Immunostaining followed by FISH on meiotic chromosomes	26
1.3.6 Characterization of the SC of B chromosomes	26
1.3.7 NSE4A antibody specificity test	27
1.3.8 Super-resolution microscopy	27
1.4 Results	28
1.4.1 Characterization of a rye NDJ-deficient B chromosome	28
1.4.2 Rye B chromosomes participate in the 'bouquet' formation	30
1.4.3 The use of structured illumination microscopy (SIM) for meiotic studies in rye	32
1.4.5 The SMC5/6 complex δ -kleisin NSE4 colocalizes to ZYP1 within the SC during synapsis	36
1.4.6 The SC is a protein structure embedded in chromatin	39
1.4.7 HEI10 localizes to the SC during synapsis and indicates the location of recombination sites at late diakinesis	41
1.4.8 Centromeres and the SC structure of rye A and B chromosomes do not differ	43
1.4.9 Prophase I pairing configurations of B chromosomes depend on their number	46
1.5 Discussion	48
1.5.1 The dynamics of ASY1 and ZYP1 indicates the SC assembly and disassembly during prophase I	48
1.5.2 The SMC5/6 complex δ -kleisin NSE4 seems to be required for synapsis and recombination	50

1.5.3 HEI10, a marker for class I crossovers in rye?	50
1.5.4 A model for the behaviour of rye chromosomes during prophase I.....	51
1.5.5 B chromosomes behave like A chromosomes during prophase I	55
1.6 Summary.....	57
1.7 Outlook.....	58
2. Fluorescent labelling of <i>in situ</i> hybridization probes through the copper-catalyzed azide-alkyne cycloaddition reaction	59
2.1 Introduction.....	59
2.1.1 Fluorescence <i>in situ</i> hybridization (FISH)	59
2.1.2 General introduction to click chemistry.....	61
2.1.3 Application of click-chemistry to nucleic acids.....	62
2.1.4 Click-chemistry-labelled oligonucleotides as probes for FISH.....	63
2.2 Aims of the PhD work.....	65
2.3 Materials and methods	66
2.3.1 Plant materials.....	66
2.3.2 Preparation of mitotic chromosomes for non-single copy FISH	66
2.3.3 Preparation of mitotic chromosomes for single copy FISH (standard method)	67
2.3.4 Preparation of mitotic chromosomes for single copy FISH (alternative method)	67
2.3.5 Preparation and sorting of isolated nuclei	67
2.3.6 FISH probe preparation	68
2.3.7 Treatment of oligonucleotide FISH probes by ammonia for pH change.....	69
2.3.8 Fluorescence <i>in situ</i> hybridization using <i>pre-</i> or <i>post-</i> hybridization click probes	69
2.3.9 Single-copy fluorescence <i>in situ</i> hybridization	70
2.3.10 Combined 5-Ethynyl-deoxyuridine (EdU)-based DNA replication analysis and FISH using <i>pre-</i> clicked probes	70
2.3.11 Combined immunohistochemistry and hybridization of <i>pre-</i> hybridization CuAAC-labelled FISH probes.....	71
2.3.12 Quantification of telomeric FISH signals	71
2.4 Results	72
2.4.1 Characterization of <i>Arabidopsis</i> -type telomere-specific CuAAC-labelled oligonucleotide probes.....	72
2.4.2 The use of CuAAC-labelled probes in combination with immuno-histochemistry and EdU labelling	73
2.4.3 Detection of a single copy sequence of <i>H. vulgare</i> chromosome 3H by CuAAC-labelled oligonucleotide probes.....	76
2.6 Discussion	86

2.6.1 CuAAC-labelled probes are suitable for reliable detection of repetitive sequences	86
2.6.2 Single copy FISH using CuAAC-labelled oligonucleotide probes requires optimization.....	88
2.6 Summary.....	91
2.7 Outlook.....	92
3. References.....	93
Curriculum vitae.....	109
Eidesstattliche Erklärung/ Declaration under Oath	112
Erklärung über bestehende Vorstrafen und anhängige Ermittlungsverfahren / Declaration concerning Criminal Record and Pending Investigations	113

Table of figures

Figure 1 Meiosis in monocentric eukaryotes	12
Figure 2 Cytological substages of meiotic prophase I in rye microsporocytes	14
Figure 3 The structure of the synaptonemal complex (SC)	16
Figure 4 Characterization of a rye B chromosome isoform harbouring a deletion of the nondisjunction control region (NDJ)	29
Figure 5 Bouquet formation of rye carrying 1B, 2B and 4B chromosomes.....	31
Figure 6 SIM improves the resolution and thus the identification of SC nanostructures significantly	33
Figure 7 The behaviour of ASY1 and ZYP1 during prophase I	35
Figure 8 Characterization of the Nse4A antibody in rye	37
Figure 9 ZYP1 and NSE4A colocalize at the SCs of rye A and B chromosomes.....	38
Figure 10 SIM identifies the SC as a complex protein structure embedded in chromatin	40
Figure 11 HEI10 behaviour in comparison to ASY1 and ZYP1 dynamics during prophase I.....	42
Figure 12 Bilby repeats and CENH3 identify the centromeres of A and B chromosomes	43
Figure 13 The SC structure of B chromosomes does not differ from that of As	45
Figure 14 Pairing configurations of B chromosomes at pachytene	47
Figure 15 Scheme showing the behaviour of two homologous chromosomes, together with the localization of the SC proteins ASY1, ZYP1, NSE4A and HEI10 during prophase I.....	53
Figure 16 The principles of fluorescence <i>in situ</i> hybridization (FISH)	60
Figure 17 Proposed reaction mechanism of the copper (I)-catalysed azide-alkyne cycloaddition (CuAAC)	62
Figure 18 The CuAAC reaction can be used to functionalise alkyne-modified DNA nucleobases	63
Figure 19 Different DNA labelling strategies based on CuAAC	64
Figure 20 CuAAC-labelled DNA probes are suitable for FISH	72
Figure 21 Workflow of <i>pre</i> - and <i>post</i> -hybridization CuAAC	74
Figure 22 Combination of <i>pre</i> - and <i>post</i> -hybridization CuAAC-labelled probes on wheat metaphase chromosomes.....	75
Figure 23 Combination of CuAAC-labelled microsatellite probes with immunohistochemistry and labelling of replication <i>via</i> 5-Ethynyl-deoxyuridine (EdU).....	76
Figure 24 Detection of a 7670 bp single copy sequence of the barley chromosome 3H by FISH.....	78
Figure 25 Detection of a single copy sequence on 3H of barley by CuAAC-labelled FISH probes	80
Figure 26 Purification of the CuAAC-labelled oligonucleotide FISH probe did not result in specific hybridization signals	81
Figure 27 Characterization of the uniform labelling of the CuAAC-labelled oligonucleotide FISH probes by splitting the mix.....	83
Figure 28 Alternative strategies to prevent the uniform binding of the CuAAC-labelled oligonucleotide FISH probe mix	84

Abstract

The first part of the thesis addresses the dynamics of the synaptonemal complex (SC) of standard and accessory rye chromosomes (As and Bs, respectively). While the assembly of the SC was extensively studied in *Arabidopsis thaliana* and cereals, the process of SC disassembly, which is essential for correct chromosome segregation, gained less attention. Intriguingly, the cereal species rye (*Secale cereale* L.) contains not only the standard A chromosomes, but also dispensable B chromosomes. The Bs are characterized by several striking peculiarities: the number of Bs varies between individuals of a population, Bs do not pair or recombine with As at meiosis and exhibit a non-Mendelian mode of inheritance. Previous electron microscopy studies showed differences between As and Bs in their synaptic behaviour. In addition to bivalent formation, Bs may also perform intrachromosomal synapsis leading to formation of multivalents. Given that the SC protein composition of Bs remains elusive, we monitored the ultrastructural dynamics of the SC assembly and disassembly in rye plants containing Bs. Using immunohistochemistry and super resolution microscopy, we tracked four meiotic proteins ASY1 (a marker for axial element (AE)/lateral element (LE)), ZYP1 (a transverse filament protein), HEI10 (a structure-based signal transduction protein involved in recombination) and NSE4A (a δ -kleisin of the SMC5/6 complex) during prophase I. The combined approach revealed that all four proteins were present at the SC until its complete disassembly. Their distinct spatio-temporal distribution reflects extensive changes in the SC structure. Moreover, we found that Bs participate in the bouquet formation, and characterized the extent of the long arm deletion of a B chromosome variant.

In the second part, the labelling of *in situ* hybridization probes through the copper-catalysed azide-alkyne cycloaddition reaction was investigated. Fluorescent *in situ* hybridization (FISH) is a powerful tool to study the genome and chromosome architecture, with nick translation (NT) being widely used to label DNA probes. While NT is applicable for long double-stranded DNA, it generally fails to label single-stranded and short DNA, e.g. oligonucleotides. An alternative technique is the copper (I)-catalysed azide-alkyne cycloaddition (CuAAC), at which azide and alkyne functional groups react in a multistep process catalysed by copper (I) ions to give 1, 4-distributed 1, 2, 3-triazoles at a high yield (also called "click reaction"). We successfully applied CuAAC to label short single-stranded DNA probes and tested them by FISH on plant chromosomes and nuclei. The alternatively labelled probes were subsequently compared with those obtained by conventional labelling techniques in respect of hybridization efficiency. We found that CuAAC-labelled probes reliably detect different types of repetitive sequences in chromosomes. A combination of FISH based on such probes with other techniques, e.g. immunohistochemistry and cell proliferation assays using 5-Ethynyl-deoxyuridine is feasible. However, despite multiple efforts the application of CuAAC-labelled FISH probes to detect a single copy sequences was not achieved and requires further optimization.

Abbreviations

AE	axial element
As	A chromosomes
ASY1	asynapsis 1
Bs	B chromosomes
bp	base pair
CO	crossover
CuAAC	Cu (I)-catalysed azide-alkyne cycloaddition
CR	central region
DAPI	4', 6-diamidino-2-phenylindole
delB	NDJ-deficient B chromosome
DMC1p	disrupted meiotic cDNA 1p
DNA	deoxyribonucleic acid
dNTP	deoxyribonucleic triphosphate
DS	dextran sulphate
DSB	double strand break
dUTP	desoxyuridine triphosphate
EdU	5-Ethynyl-2'deoxyuridine
Fig	Figure
FISH	Fluorescence <i>in situ</i> hybridization
GSD	ground state depletion microscopy
h	hour
HEI10	human enhancer of invasion-10 protein
HOP1	Homolog pairing 1
HORMA	Hop1p, Rev7p and MAD2 proteins
ISH	<i>in situ</i> hybridization
KASH domain	Klarsicht, Anc-1, and Syne Homology domain
LE	lateral element

LINC complex	linker of the cytoskeleton and nucleoskeleton complexes
µm	micrometre
mg	milligram
min	minute
MTOC	cytoplasmatic microtubule organization centre
NDJ	nondisjunction control region
NE	nuclear envelop
nm	nanometre
NT	nick translation
NSE	non-SMC element
PCR	Polymerase chain reaction
PMC	Pollen mother cell
RING	really interesting new gene
RNA	ribonucleic acid
RT	room temperature
SC	synaptonemal complex
SCP1	synaptonemal complex protein 1
SIM	structural illumination microscopy
SMC5/6	structural maintenance of chromosome 5/6 complex
sSMC	small supernumerary marker chromosome
SPO11	sporulation-specific protein 11
SUN	Sad1p/UNC-84 homology domain
TAMRA	carboxy-tetramethyl-rhodamine
TF	transverse element
ZMM	ZIP1/ZIP2/ZIP3/ZIP4, MSH4/MSH5 and MER3 protein family
ZIP1/ ZYP1	Zipper 1 orthologues

0. Preface

The thesis is arranged in two parts, each includes an introduction, the experimental questions and aims, the materials and methods, the results, the discussion, the summary and an outlook. The first part addresses the organization of the synaptonemal complex of rye A and B chromosomes. The second part describes the development of a copper (I)-catalysed azide-alkyne cycloaddition (CuAAC)-based method to label DNA probes suitable for fluorescence *in situ* hybridization.

1. The dynamics of synaptonemal complex components during meiotic pairing/synapsis of standard (A) and accessory (B) rye chromosomes

1.1 Introduction

1.1.1 Meiosis

During the late 19th century, Carl Rabl demonstrated in salamander cells the permanence and orientation of somatic chromosomes (known as ‘Rabl orientation’) and scientists realized that a mechanism compensating for genome doubling at fertilization is needed, to maintain a constant number of chromosomes in somatic cells from individuals of the same species (van Beneden 1883, Rabl 1885, Scherthan 2001). Despite the first observation of meiosis in sea urchins in 1876 by Oscar Hertwig, it still took additional 11 years, until August Weismann introduced the concept of a ‘Reduktionsteilung’ (reductional division), which halves the diploid chromosome number in germ cells (Hertwig 1876, Weismann 1887). A year later, Eduard Strasburger demonstrated the reduction of the diploid to a haploid chromosome set also in germ cells of angiosperms (Strasburger 1888). The term ‘maiosis’ (Greek μείωσις, ‘diminution’) was proposed by Farmer and Moore in 1905, to cover the whole series of nuclear changes and to emphasize the importance of the two divisions for sexual reproduction (Farmer and Moore 1905). Nowadays, meiosis is known as a specialized cell division found in all sexually reproducing eukaryotes including plants. By reduction of the chromosome number from a diploid set to the gametic haploid set, meiosis ensures the maintenance of the stability and constancy of chromosomal numbers during fertilisation in successive generations. Furthermore, meiosis leads to genetic and phenotypic diversity in the offspring by shuffling the parental genes in gametes. Despite intense studies, the evolution of meiosis remains largely enigmatic (Wilkins et al. 2009, Niklas et. al. 2014). While it is widely accepted that meiosis presumably evolved from mitosis, the gain of novel steps, e.g. the pairing of homologous chromosomes and the recombination between non-sister chromatids, challenges any Darwinian explanation of the meiotic origin, as a simultaneous creation of such complex new features in one step seems impossible. Given that the entire sequence of new features is obligatory for the

successful production of haploid gametes, even a stepwise evolution of meiosis appears to be highly unlikely (Wilkins et al. 2015). Additionally, in diverse organisms the evolved meiotic process differs substantially. However, in most eukaryotes one initial round of DNA replication (S phase) is followed by two subsequent cell divisions, called meiosis I and II (Zickler et al. 2016). Meiosis I is critical for the segregation of homologous chromosomes and is characterized by a highly dynamic prophase I, which involves crucial processes related to meiotic chromosome structure, including sister chromatid cohesion, homologous chromosome alignment, pairing, synapsis, and recombination (Hamant et al. 2006). During the first meiotic division an increase in cell and nucleus size is observable. Meiosis II resembles in monocentric species, a mitotic division in terms of sister chromatid separation, leading to the formation of four haploid daughter cells (Figure 1).

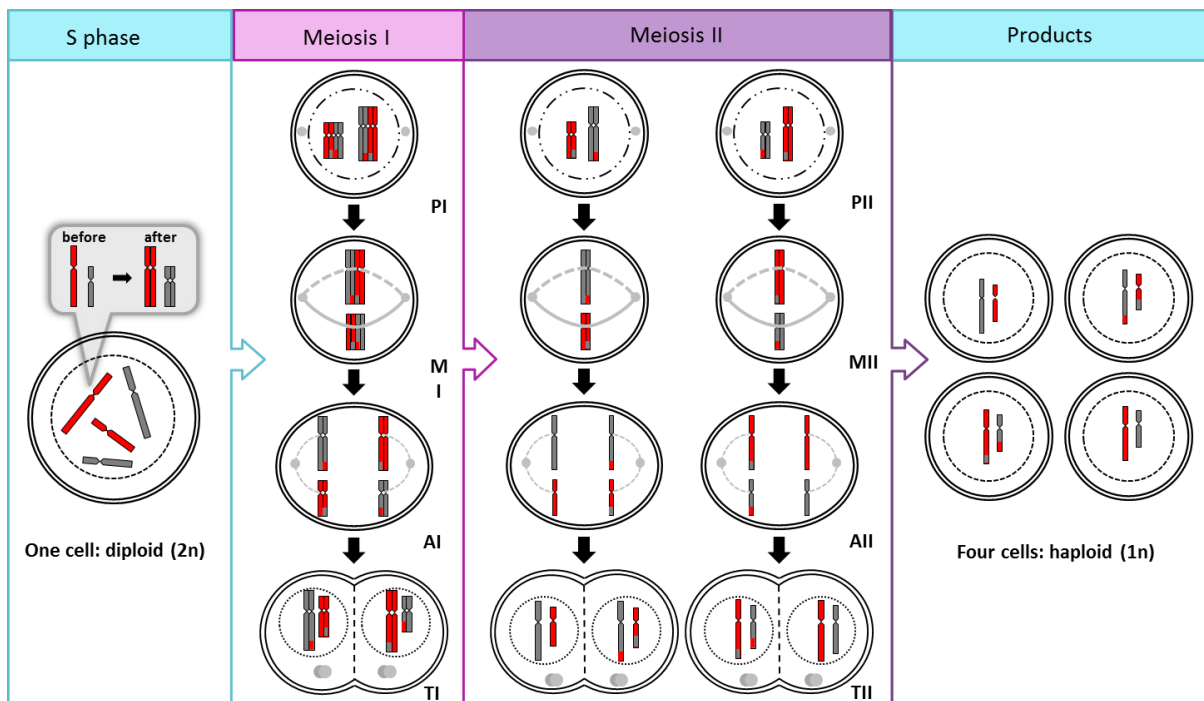


Figure 1 | Meiosis in monocentric eukaryotes. The meiotic cell cycle is initiated at pre-meiotic S phase of interphase I by one round of DNA replication. Two rounds of cell division follow: meiosis I and meiosis II. Both cell divisions are characterized by the four stages of prophase (PI/II), metaphase (MI/II), anaphase (AI/II) and telophase (TI/II), analogous to mitosis. In many organisms a resting stage, named interkinesis/interphase II takes place between both divisions. Meiosis I is characterized by a prolonged and complex prophase that shuffles the parental genes *via* recombination and is crucial for the segregation of the homologous chromosomes to two daughter cells. Because of the reduction of ploidy from diploid to haploid, meiosis I is referred to as reductional division. Subsequently, during meiosis II both daughter cells undergo an equational division separating sister chromatids of each chromosome and giving rise to four haploid gametes.

1.1.2 Prophase I of meiosis

To ensure a regular segregation of homologous chromosomes, several unique processes occur during meiosis I, in a prolonged and complex prophase I. First, sister chromatid cohesion becomes established during S phase by cohesin complexes. Second, the chromosome axis condenses and

pairing of homologous chromosomes takes place. Third, the synaptonemal complex (SC) is formed *via* synapsis and fourth, recombination occurs eventually leading to crossover formation (Sanchez-Moran et al. 2008). In addition, homology-dependent or -independent interactions, e.g. centromere and/or telomere clustering can prelude and/or complement these processes (Zickler et al. 2015). Only few organisms exhibit a deviating program of prophase I events. In most species SC formation depends on double strand break (DSB) formation and strand invasion. However, e.g. in *Caenorhabditis elegans* and *Drosophila* females, SC formation occurs without DSB formation (Zickler et al. 2015). In *Schizosaccharomyces pombe* and *Aspergillus nidulans* no SCs become established and pairing occurs recombination-independent and recombination-mediated, respectively (Olson et al. 1978, Egel-Mitani et al. 1982, Bahler et al. 1993).

Based on the morphology of the chromosomes, prophase I was historically defined into five substages (Figure 2), each characterized by a specific chromosome conformation (Winiwarter 1901). The initiation of prophase I can be cytologically recognized at leptotene (Greek λεπτός ‘thin’ and ταινία, ‘ribbon’), as chromatin condensation begins and chromosomes form thin, long, separated threads in the nucleus. The axial element, a protein fibrous core involved in the subsequent formation of the SC, is loaded on each homolog and the formation of DSBs is detectable (Zickler et al. 2015). The chromosome ends, called telomeres (Greek τέλος, ‘end’ and μέρος, ‘part’; (Muller 1938)), attach scattered to the inner membrane of the nuclear envelope and a spatial coalignment of the whole homologous chromosomes (pairing or conjugation (Boveri 1892)) occurs (Zickler et al. 1999, Scherthan 2007, Zickler et al. 2015). In some species also a coupling and clustering of the centromeres can be observed (Da Ines and White 2015). At the transition to the next substage, zygotene (Greek ζυγόν, ‘yoke’ and ταινία, ‘ribbon’), telomeres adopt a polar orientation named the ‘chromosomal bouquet’ (Eisen 1900). During zygotene, homologous chromosomes become tightly associated along their length by the formation of a robust, proteinaceous structure, the synaptonemal complex. This process is referred to as ‘synapsis’ and defines this substage (Moore 1895, Zickler et al. 2015). Beside synapsed homologous chromosomes, also unconnected chromosome regions are still visible in zygotene. When synapsis is completed, only a single set of chromosomes can be cytologically visualized. This substage is defined as pachytene (Greek παχύς, ‘thick’ and ταινία, ‘ribbon’). In the context of the established SC, the latter steps of recombination take place and recombination-mediated interhomolog interaction result in crossovers (COs) (Zickler et al. 2015). Diplotene (Greek διπλῦς, ‘double’ and ταινία, ‘ribbon’) is characterized by the disassembly of the SC, which results in the separation of the homologs along their whole lengths, except at sites of COs. These visible, physical connections are called chiasmata (Greek χιάσμα, ‘cross’; (Janssens 1909)) and remain until the end of prophase I. The condensation of the chromosomes continuously progresses. At diakinesis (Greek δια, ‘through’ and κίνησις, ‘movement’) threads at the

chromosome periphery become visible, therefore the chromosomes are also named as ‘lamp brush chromosomes’ (Rückert 1882). The physical connection is replaced by an end-to-end connection of the homologues resulting in a typical chromosome structure, e.g. circular bivalents visible at the end of diakinesis (Figure 2).

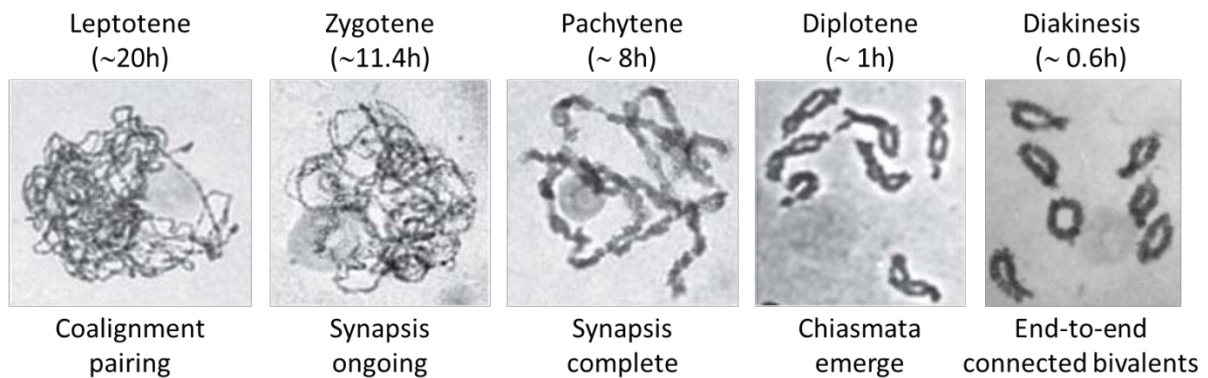


Figure 2 | Cytological substages of meiotic prophase I in rye microsporocytes. Chromosomes are stained by hematoxylin and the corresponding timing of each substage in rye as well as the crucial processes is indicated. During leptotene homologous chromosomes coalign and pair. The establishment of a proteinaceous structure that connects both homologs, the synaptonemal complex (SC, not visible at this resolution), characterizes the zygotene substage. At pachytene synapsis is completed and the ongoing chromosome condensation is clearly visible. The disassembly of the SC takes place at diplotene and the homologs remain connected only by chiasmata. During diakinesis chiasmata are replaced by end-to-end connections resulting in a typical circular bivalent morphology (modified from (Bennett et al. 1973, Zickler et al. 1998, Zickler et al. 2015)).

1.1.3 The ‘chromosomal bouquet’

The ‘chromosomal bouquet’ is a polarized arrangement of one or both ends of prophase I chromosomes at a limited area of the nuclear periphery (Scherthan 2001). Discovered shortly after the chromosomes itself, the ‘chromosomal bouquet’ owes its name to the imagination of Gustav Eisen, who compared this arrangement to the stems of flowers in a bouquet (Platner 1886, Eisen 1900). Highly conserved among all eukaryotes and unique to meiosis, the ‘bouquet’ does not reflect a modification of the ‘Rabl’ chromosome arrangement, which is a product of anaphase chromosome movement and arranges telomeres and centromeres on opposite sides of the somatic interphase nucleus. By contrast, the telomeres of the ‘bouquet’ cluster tightly, whereas the centromeres are distributed throughout the nucleus (Harper et al. 2004). In animals and fungi, the telomeres cluster adjacent to the cytoplasmatic microtubule organization centre (MTOC) (Zickler et al. 1998). In higher plants such as rye and wheat, which lack an obvious MTOC, ‘bouquet’ formation occurs at the microtubule-poor nuclear envelop (NE) region, furthest away from the centre of the anther (Cowan et al. 2002, Richards et al. 2012).

The ‘Bouquet’ formation involves two distinct phases. First, upon entry into meiosis, the premeiotic nuclear architecture is dissolved and repositioning and attachment of telomeres to the nucleoplasmic

face of the inner nuclear membrane of the NE occurs (Gelei 1921, Moens 1969, Esponda and Gimenez-Martin 1972, Byers and Goetsch 1975, Scherthan 2007). Second, the cluster of the NE-associated telomeres in a small subregion is formed; in most species *de novo* at the leptotene/zygotene transition and usually persists until pachytene (Chikashige et al. 1994, Scherthan et al. 1994, Bass et al. 1997, Zickler et al. 1998). Notably, the degree of clustering varies from highly pronounced, e.g. in *Saccharomyces pombe*, to a more loose polarization as seen in *Zea mays* (Chikashige et al. 1994, Bass et al. 1997). The exact mechanism of the 'bouquet' formation is still unknown. Studies in rye and wheat suggest that the clustering is not a result of pure diffusion, but requires a directed process of telomere movements at the NE (Carlton et al. 2003, Richards et al. 2012). As the attachment of the telomeres is strong enough to resist pulling forces applied by centrifugation or micromanipulation, a tight connection to the NE is needed (Gelei 1922, Hiraoka 1952). In most organisms, 'bouquet' formation is thought to be mediated by telomeric repeats, telomere-associated proteins and NE components (Bhalla et al. 2008). Recent studies in animals, yeast and plants revealed a conserved family of NE bridge proteins, harbouring a Sad1p/UNC-84 homology (SUN) domain that forms a functional link between the nucleoplasm and the cytoplasm. On the inner nuclear membrane, SUN proteins interact with other proteins that contain a Klarsicht, Anc-1 and Syne Homology (KASH) domain to build a linker of the cytoskeleton and nucleoskeleton (LINC) complexes that couple the telomeres to the cytoskeleton and thereby mediate telomere tethering and movement during chromosome pairing and recombination (Hiraoka et al. 2009, Starr et al. 2010, Starr 2011, Zhou et al. 2013, Luxton et al. 2014, Murphy et al. 2014).

So far, the exact role of the chromosomal 'bouquet' has not been firmly determined in any species. Current studies suggest that telomere clustering facilitates chromosome movements to reduce the complexity of the homology search process and promotes the regular homolog juxtaposition and pairing, as well as the elimination of inappropriate chromosome linkages or entanglements. Moreover, in some species the 'bouquet' seems to be involved in evaluation of the chromosome status and/or recombination process and works as a checkpoint sensor before allowing completion of synapsis (Chikashige et al. 1994, Golubovskaya et al. 2002, White et al. 2004, Zickler 2006, Scherthan et al. 2007, Conrad et al. 2008, Sheehan et al. 2009, Lee et al. 2012, Rog et al. 2015, Varas et al. 2015, Zickler et al. 2016).

1.1.4 The synaptonemal complex

An essential feature of meiosis is the ability to identify and pair homologous chromosomes to recombine and establish a physical linkage between homologues, which is essential for correct meiotic chromosome segregation (Zickler et al. 2016). Already in 1892, the zoologist Theodor Boveri suggested that ahead of the reductional division, homologous chromosomes should pair up (Boveri 1892). Shortly after, Johannes Rückert detected in copepods that the chromosomes appear in pairs during the first meiotic division of oogenesis (Rückert 1894). In 1895, John E. S. Moore observed the same phenomenon during prophase I of meiosis in rays and sharks and named it 'synapsis' (Greek συνάπτω, 'join together'), a term still used to describe the process of connecting the two homologous chromosomes along their length (Moore 1895, Scherthan 2001). More than half a century later, the proteinaceous structure, which is called synaptonemal complex (SC), connecting the paired chromosomes was independently discovered by Fawcett and Moses in pigeon, cat, man and crayfish (Fawcett 1956, Moses 1956, Moses 1968). Subsequently, intense studies across yeast, mammals and plants indicated that the SC structure is as highly conserved as meiosis itself (Figure 3A) (Zickler et al. 1999, Page et al. 2004, Zickler et al. 2015).

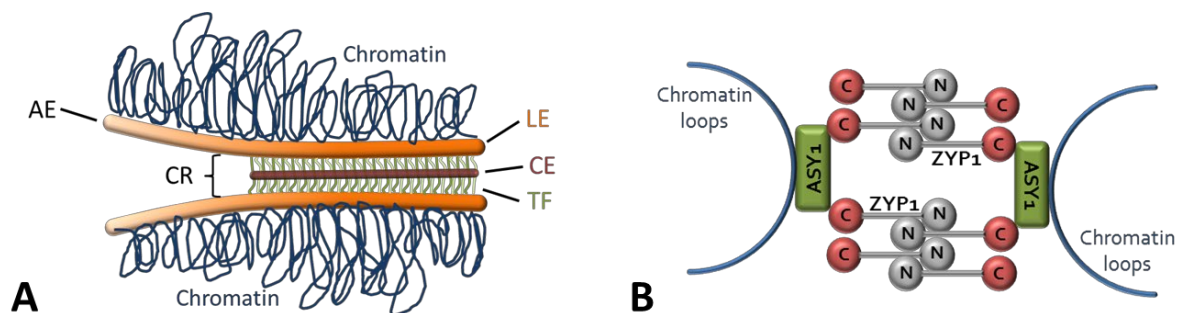


Figure 3 | The structure of the synaptonemal complex (SC). (A) A model of the tripartite structure of the SC. Prior SC assembly, homologous chromosomes associate with a proteinaceous structure termed axial element (AE, \varnothing ~50 nm). Within the SC, the AEs are referred to as lateral elements (LEs). The assembly of components of the central region (~100 nm) results in the appearance of SCs as structurally conserved tripartite ribbon-like structures between the homologues. In some organisms, substructures of the CR, i.e. transverse filaments (TFs) and the central element (CE) can be identified. (B) Proposed model of ASY1 and ZYP1 structure in barley. ASY1 (green) associates with chromatin loops (blue). The C-terminus of ZYP1 (red) contacts ASY1 (adapted from (Phillips et al. 2012)).

Early electron microscopy studies revealed the basic SC organization as a tripartite structure consisting of two lateral elements (LEs) flanking a ~100 nm wide central region (CR) (Fawcett 1956, Moses 1956, Moses 1968). Prior to SC formation at leptotene, axial element (AE) components assemble alongside the cohesin-based chromosome axis mediating sister chromatid cohesion, to establish the meiotic chromatin loop-axis structure (Zickler et al. 1999). During synapsis, homologous AEs are linked in a zipper-like manner by CR components along their entire length. With a diameter

of about 50 nm, the AEs are called LEs within the SC (Moses 1968, Westergaard et al. 1972). The CR consists of two functional units, namely the transverse filament (TF) proteins that span the CR to link both homologous chromosomes, as well as central region proteins acting tentatively to stabilize the CR (de Vries et al. 2005, Bolcun-Filas et al. 2007, Hamer et al. 2008, Page et al. 2008, Bolcun-Filas et al. 2009, Schramm et al. 2011, Humphryes et al. 2013, Collins et al. 2014, Hernandez-Hernandez et al. 2016). Noteworthy, in some species, e.g. barley, the CR consists only of one protein representing both functional units (Figure 3B) (Phillips et al. 2012). Recent genomic and proteomic studies, e.g. in yeast, identified multiple genes and proteins, such as SPO11, RAD51p, DMC1p, ZIP1 and HOP1, which are involved in SC formation and meiotic processes and appear to have orthologues across various eukaryotes (Zickler et al. 1999, Caryl et al. 2000, Page et al. 2004, Gerton et al. 2005, Zickler et al. 2015). Despite the common basic structural similarity between SCs, primary amino acid sequence comparison of orthologues components shows a substantial dissimilarity. For example, the TF protein ZYP1 of *A. thaliana* (L.) Heynh. shares only 18-20% sequence identity and 36-40% similarity with the corresponding proteins of budding yeast (ZIP1), *Drosophila* (C(3)G) and rat (SCP1) (Meuwissen et al. 1992, Sym et al. 1993, Page et al. 2001, Higgins et al. 2005). Furthermore, orthologous genes do not necessarily encode proteins with equivalent functions. For instance, electron microscopy confirmed that the ASY1 protein of *A. thaliana* belongs to the axis-associated proteins, whereas its orthologue of budding yeast (HOP1) is crucial for AE formation (Hollingsworth et al. 1997, Armstrong et al. 2002). In summary, the studies of SC components suggest that their evolution was driven by the need to fulfil a structural role, rather than conserving a catalytic one (Zickler et al. 2015).

Beside ASY1 and ZYP1, additional components, such as subunits of the structural maintenance of chromosome SMC5/6 complex and human enhancer of invasion-10 (HEI10) proteins associated with the chromosome axis have been identified. Similarly to other organisms, components of plant chromosome axis comprise in addition HORMA domain containing proteins (Armstrong et al. 2002, Nonomura et al. 2006), coiled-coil proteins (Wang et al. 2011, Ferdous et al. 2012, Lee et al. 2015) and cohesins (Cai et al. 2003, Yamada et al. 2004).

The conserved SMC5/6 complex, belonging to the SMC family, is formed *via* the interaction of the hinge domains of the SMC5 and SMC6 subunits resulting in a heterodimer connected by the δ -kleisin NSE4 (non-SMC element 4) at the head domains of SMC5 and SMC6 (Kawamoto et al. 2001, Kusama et al. 2004, Palecek et al. 2006, Taylor et al. 2008). In addition to functions of SMC5/6 in somatic tissues, various essential roles during meiosis were found in yeasts, worm, mouse and human. SMC5/6 subunits were proven to play a role in meiotic processes such as in response to DSBs, meiotic recombination, heterochromatin maintenance, centromere cohesion, homologous chromosome synapsis and meiotic sex chromosome inactivation (Verver et al. 2016). In *A. thaliana*,

due to the presence of two alternative SMC6 (SMC6A and SMC6B) and NSE4 (NSE4A and NSE4B) subunits, different SMC5/6 complexes may be composed (Schubert et al. 2009, Zolkowski et al. 2019).

HEI10 is a member of the ZMM (ZIP1/ZIP2/ZIP3/ZIP4, MSH4/MSH5 and MER3) protein family, originally identified as a growth regulator and essential for meiotic recombination in different eukaryotes (Toby et al. 2003, Whitby 2005, Osman et al. 2011, Chelysheva et al. 2012, Wang et al. 2012). Possessing a RING-finger motif, coiled-coil and tail domains, HEI10 functions as an E3 ligase catalysing post-translational protein modifications *via* ubiquitination proteins, and thereby integrates information from the SC, the state of the recombination complexes and the cell cycle for successful recombination (De Muyt et al. 2014, Qiao et al. 2014).

Whereas extensive studies focused on the assembly of SCs, little is known about the process of SC disassembly, which is essential for correct chromosome segregation. In particular, a detailed analysis of the SC composition of rye chromosomes and the identification of recombination markers are missing.

1.1.5 B chromosomes - a general introduction

Beside a set of standard chromosomes, also called A chromosomes (As), many eukaryotes exhibit supernumerary chromosomes causing a numerical chromosome variation (Jones et al. 1982). Apart from small supernumerary marker chromosomes (sSMC) another class of dispensable chromosomes exist, the B chromosomes (Bs). They were first described in 1907 by the American geneticist Edmund B. Wilson as “supernumerary chromosomes” in the leaf footed bug *Acanthocephala* (formally *Metapodius*) *terminalis*, later studies also referred to Bs as (*extra*) *diminutive*, *accessory* or *extra fragment* chromosomes (Wilson 1907, Stevens 1908, Lutz 1916, Östergren 1945, Cleland 1951). Until now, 736 animal species carrying B chromosomes are known, including all major taxonomic groups, including molluscs, arthropods, amphibians, reptiles and mammalian species (Jones et al. 1982, Vujosevic et al. 2004, D'Ambrosio et al. 2017). Additionally, Bs were described in 14 fungi, pteridophytes, bryophytes and in more than 2000 seed plants including taxa from both gymnosperms and angiosperms (Muntzing 1946, Jones et al. 1993, Covert 1998, Jones et al. 2005, D'Ambrosio et al. 2017). . The number of Bs varies between individuals of a population from zero to 34 Bs found in experimental material of *Zea mays* (Jones et al. 1982). In some species, B chromosomes are present only in particular organs, e.g. in *Aegilops speltoides* where they are present exclusively in aerial parts of the plant, but not in roots (Mendelson et al. 1972). The distribution of Bs is neither related to taxonomic ranking nor restricted to a certain level of ploidy (Gill et al. 1972, Zeleny 1974, Jones et al. 1982, Palestis et al. 2004, Trivers et al. 2004). In striking

contrast to As, B chromosomes are dispensable and not essential to normal growth and development. Many attempts to find an adaptive significance of Bs in natural populations resulted in no or very little evidence supporting this assumption (Semple 1989).

Another important feature of Bs is that they do not pair and recombine with As during meiosis and do not follow the Mendelian inheritance pattern. Beside this common feature, there is a great species-to-species variability in Bs' behaviour in meiosis in terms of different rates of pairing, elimination and accumulation, which makes a generalization of Bs' role in meiosis virtually impossible (Jones et al. 1982). For example, pairing behaviour and chiasma formation ranges among Bs from complete failure (e.g., *Plantago serraria* (Fröst 1959), *Allium cernuum* (Grun 1959)) to ~90% bivalents in two B-carrying individuals of *Locusta migratoria* (Kayano 1971) or *S. cereale* (Kishikawa 1965). The elimination rate of Bs during meiotic divisions and their transmission rate was shown to depend on the non-pairing rate during meiotic division (Jimenez et al. 1997). The fate of univalent B chromosomes at meiosis also varies between different species. In general, the lag in Bs' movement at the first meiotic division, to some extent causes a failure in reaching the metaphase plate and their loss as micronuclei (Mendelson et al. 1972, Jones et al. 1982). Additionally, the centromeres of univalents are sensitive to premature separation of the sister chromatids in anaphase I, which are then incapable of division at anaphase II and are likely to be also lost as micronuclei (Jones et al. 1982). To circumvent their own elimination, Bs possess an independent 'selfish' accumulation mechanism, so called 'drive'. Our knowledge about this mechanism is still very limited. The 'drive' mechanisms revealed so far involves preferential accumulation of Bs in germ-line cells that occurs either before (*Calliptamus palaestinensis*), during (*Lilium callosum*), or after (*S. cereale*) meiosis (Müntzing 1946, Kayano 1957, Nur 1963).

The origin of B chromosomes remains enigmatic. Comparison between A and B chromosomes led to the commonly accepted view that Bs originated either from A chromosomes and/or sex chromosomes, or from rearrangements following interspecific hybridization (Sapre et al. 1987, Page et al. 2001, Dhar et al. 2002, Cheng et al. 2003, Bugrov et al. 2007, Martis et al. 2012, Klemme et al. 2013). When compared with As, the size of Bs varies from exceeding the size of the biggest A chromosomes (e.g., *Apodemus peninsulae* (Kartavtseva 2000)), being of the same size (e.g., *Clarkia elegans* (Lewis 1951)) or much smaller (e.g., *Allium schoenoprasum* (Bougourd et al. 1975)). Moreover, in some species different isoforms of B chromosomes were also found, e.g., in *S. cereale* and *Nectria haematococca* (Müntzing 1944, Covert 1998).

1.1.6 The B chromosomes of rye (*S. cereale* L.)

S. cereale L. and *Zea mays* L. were the first and remain until now the best studied plants in which B chromosomes were identified (Gotoh 1924, Kuwada 1925). The Bs in rye were discovered unintentionally by M. Nakao in 1911. Looking for the chromosome complement of rye, wheat and barley, he stated that 'the number of chromosomes is 8 in wheat and rye, and 7 in barley' (Nakao 1911). Likely, Nakao observed rye plants carrying 1 B chromosome. Thirteen years later, Kazuo Gotoh published a detailed study where he investigated rye with two small extra 'k-chromosomes' (Gotoh 1924).

S. cereale belongs to the higher plants owning a polymorphic B system. The most frequent variant is an acrocentric so called 'standard' B chromosome, but several isoforms can be found in addition. Presumably, rye B chromosome isoforms are of monophyletic origin and originated from deletions, centric misdivision and isochromosome formation of the standard B (Müntzing 1944, Müntzing 1948, Müntzing 1948, Müntzing et al. 1952, Müntzing et al. 1953, Puertas 1973, Niwa et al. 1995, Marques et al. 2012, Martis et al. 2012, Klemme et al. 2013). The transmission of Bs to the gametophytes in rye is a post-meiotic process taking place at first pollen mitosis. At anaphase I of the first pollen mitosis, B chromosomes undergo directed nondisjunction. Both sister chromatids of Bs do not separate and are directed to the generative nucleus, whereas the As undergo normal disjunction resulting in equal numbers of chromosomes in the generative and vegetative nucleus (Hasegawa 1934, Müntzing 1945, Müntzing 1946, Müntzing 1948). Such directed nondisjunction of rye Bs is highly effective with an average frequency of ~80% in microspores and consequently non-disjoined Bs are found exclusively in the generative nucleus (Matthews et al. 1983). In the second pollen mitosis, the Bs undergo normal disjunction at anaphase II. The consequence of this rye B 'drive' mechanism is a doubled number of Bs and their equal distribution in the generative nuclei. Detailed studies showed that B isoforms, which lack the terminal region of the long arm containing the so-called nondisjunction control region (NDJ), do not undergo directed nondisjunction at the first pollen mitosis (Hasegawa 1934, Müntzing et al. 1952, Müntzing et al. 1953, Lima-De-Faria 1962, Beliveau et al. 2015).

Up to eight B chromosomes are tolerated by rye plants (Jones et al. 1982). Each standard B chromosome adds ~580 Mbp to the normal complement of seven pairs of As (1C ~7,917 Mbp) (Martis et al. 2012). Early studies on the DNA composition of rye B chromosomes were based on the comparison between plants with and without Bs. DNA/DNA hybridization studies did not reveal a difference between A and B chromosomes in heterogeneity and proportion of repetitive sequences (Rimpau et al. 1975). *In situ* hybridization analysis using 0B- and +B-genomic DNA as a probe showed that the majority of the rye B chromosome is labelled except the heterochromatic terminal region of

the long arm that harbours the NDJ (Tsujiimoto et al. 1992, Wilkes et al. 1995). In the beginning of 1990s, the presence of two B-specific repeat families (D1100 and E3900) in this region was demonstrated (Sandery et al. 1990, Blunden et al. 1993, Houben et al. 1996, Houben et al. 2001). Interestingly, the terminal heterochromatic region is simultaneously marked with conflicting histone modifications for hetero- and euchromatin (H3K27m3 and H3K4m3, respectively) and shows non-coding RNA transcripts (Carchilan et al. 2007). Recent studies combining next generation sequencing approaches and FISH allowed a detailed mapping of high-copy sequences on the standard B chromosome and revealed a stepwise evolution of rye B chromosomes as a mosaic of A chromosome- and organelle-derived sequences (Martis et al. 2012, Klemme et al. 2013). The gain of a 'drive' mechanism, on-going sequence amplification and accumulation resulted in the standard B chromosome (Martis et al. 2012).

1.1.7. Meiosis of rye B chromosomes

First meiotic studies on rye B chromosomes by Kazuo Gotoh revealed that at diakinesis the Bs either pair themselves to form bivalents, or stay as univalents and lag behind the A chromosomes (Gotoh 1924). Moreover, in Swedish rye varieties a varying degree of pairing and subsequently different transmission rates of the B chromosomes were observed (Müntzing 1945). Later genetic analysis of the B chromosome transmission properties of rye revealed two different genotypes, namely plants with high or low B transmission rates. The investigation of the pairing behaviour of 2B plants of each rye line showed that in case of low transmission, the bivalents were only formed in 20% of the pollen mother cells (PMCs) at metaphase I. In contrast, the high transmission line showed in 90% of the cells a formation of bivalents, and the B chromosomes were present in 85% of the pollen grains (Jimenez et al. 1997). Crosses between high and low transmission lines verified that the transmission rate-controlling element is located on the B chromosome itself (Puertas et al. 1998). In general, rye plants carrying two or more Bs form bi- or multivalents with a single terminal chiasma (Jones et al. 1982). Bivalents with two chiasmata were found rarely (Sybenga et al. 1972). In case of univalent Bs, already Gotoh observed irregularities in meiosis I and II, e.g. random distribution of Bs to the poles or abnormal separation behaviour at anaphase I and II causing often a loss of the B chromosomes (Gotoh 1924). Occasionally, univalents manage to reach the poles at anaphase I and divide normal at anaphase II, explaining the low transmission rate of 1B plants (Müntzing 1945, Jones et al. 1982).

Analysis of the synaptic pattern of rye B chromosomes revealed pachytene configurations, which include intra-arm as well as non-homologous inter-arm pairing (Müntzing et al. 1952, Müntzing et al. 1953, Santos et al. 1993, Jimenez et al. 1994, Santos et al. 1995, Beliveau et al. 2015). Moreover, the different isoforms (standard-, deficient-, iso-Bs) were always located on the periphery of surface-

spread nuclei and were delayed in their pairing related to the A chromosomes (Santos et al. 1993, Jimenez et al. 1994, Santos et al. 1995).

Thus, B chromosomes represent a very peculiar class of supernumerary chromosomes. However, limited knowledge is available concerning the synapsis of rye B chromosomes. The SC protein composition of neither the standard, nor the NDJ-deficient B isoforms, has been yet investigated in detail or compared to A chromosomes.

1.2 Aims of the PhD work

Despite intense studies across yeast, mammals and plants, the dynamics of the chromosome axis during prophase I is far from being understood. To investigate the SC structure in higher plants, we chose *S. cereale* as a model plant possessing supernumerary B chromosomes. The most frequent variant is an acrocentric ‘standard’ B chromosome, but seven additional isoforms of Bs were described (Endo et al. 2008). Despite being one of the best studied B chromosome models in the past 90 years, the dynamics of rye Bs at early meiosis remained elusive. Newly available antibodies developed against meiotic proteins and new B-specific FISH probes allow addressing the following aims:

1. Monitoring of the structural dynamics of the SC during prophase I through imaging of different SC components and associated proteins.
2. Comparison of the dynamics of standard A and B chromosomes at prophase I using a combination of immunohistochemistry and FISH.
3. Characterization of the extent of the subtelomeric deletion of a NDJ-deficient B chromosome variant and evaluation of structural SC dynamics during prophase I.

1.3 Materials and Methods

1.3.1 Plant material and cultivation

Rye (*S. cereale* L. cv. Paldang; $2n= 14+0-4$ supernumerary Bs) plants carrying standard (Romera et al. 1989) or NDJ-deficient B chromosomes (Ribeiro et al. 2004) were grown under greenhouse conditions (22° C, 16 h light/ 8 h dark cycle) to obtain anthers containing pollen mother cells during prophase I. The number of Bs in individual plants was determined by FISH using the rye B chromosome-specific probes Sc11, D1100 and E3900.

1.3.2 FISH probe preparation

The retrotransposon Bilby (Francki 2001) was used as rye centromere-specific probe, and the repeats Sc11, Sc55c1, Sc63c34, D1100, E3900 and Sc36c82 were employed as rye B chromosome-specific probes (Sandery et al. 1990, Blunden et al. 1993, Klemme et al. 2013). Vectors containing the repeat-specific sequences were kindly provided by Dr. Sonja Klemme (Klemme et al. 2013) and the labelling was done by nick translation using the Atto550 or Atto647N NT Labelling Kits (Jena Bioscience GmbH, Germany). The two high-copy sequences Sc380 (Appels, Moran et al. 1986) and Sc250 (Vershinin et al. 1995) were detected using a mix of oligonucleotides, which were 5'-end labelled with TAMRA (Sc380: GGGCCAGACGGCCTTTTTGGG and GCCCAGGTCCTGAACACCAAAGG; Sc250: GAGCAAGTTACCTTGGAAGCCGG and GCAAGCCCTA-CATGCTAGTCTGG; Eurofins Genomics, Ebersberg Germany).

1.3.3 Assessment of B chromosome number in individual rye plants

Root tips of each rye plant were cut and fixed in ethanol/glacial acid (3:1) for 48 h at room temperature. Fixed roots were stained in 1% acetocarmine solution (1% carmine in 45% acetic acid, 12-24 h at room temperature). For slide preparation, the roots were carefully heated up in the acetocarmine solution over an open flame until they became soft. Then, the softened roots were placed on a slide, the root tip cap was cut off with a razor blade and the meristem was carefully extracted on the slide by using a preparation needle. The extracted meristem was squashed in 45% acetic acid using a coverslip. After coverslip removal using liquid nitrogen, the slides were stored in 100% ethanol (4° C). Subsequently, the slides were air-dried and the FISH probe-containing hybridization mix (FISH probes diluted in 20% dextran sulphate (Sigma-Aldrich, cat. no. D 8906), 50% deionized formamide, 300 mM NaCl, 30 mM tri-sodium citrate dehydrate, 50 mM phosphate buffer, pH 7.0) was applied. Then, the slides were incubated for denaturation for 2 min on a hot plate at 80° C in darkness. FISH was performed at 37° C in darkness overnight. Slides were washed 3x5 min in

1× phosphate buffer saline (PBS, pH 7.4) and afterwards mounted and counterstained with 4',6-diamidino-2'-phenylindole dihydrochloride (DAPI, 1 mg/ml) in Vectashield (Vector Laboratories). To determine the number and type of Bs, FISH probes directed against the pericentromeric repeat Sc11 and a subtelomeric repeat (E3900 or D1100) were used in parallel. In case of standard rye B chromosomes, the detected number of both repeats is equal. Plants containing standard Bs were cultivated further under greenhouse conditions (22° C, 16 h light /8 h dark cycle) and subsequently used in this study.

1.3.4 Characterization of the NDJ-deficient B isoform by FISH

For prophase I preparations, rye anthers were fixed in ethanol/glacial acid (3:1; Carl Roth, cat. no. 9165; Merck, cat. no. 100066, respectively) for at least 48 h at room temperature (RT), washed 3×5 min in 0.01 M citrate buffer (0.01 M tri-sodium citrate dihydrate (Carl Roth, cat. no. 4088) and 0.01 M citric acid (Carl Roth, cat. no. 6490); pH 4.5–4.8) and digested for 20 min at 37° C in an enzyme cocktail (0.1% cellulose (Calbiochem, cat. no. 219466), 0.1% pectolyase Y-23 (Sigma-Aldrich, cat. no. P3026), 0.1% cytohelicase (Sigma-Aldrich, cat. no. C8274) in 0.01 M citrate buffer). Afterwards, the anthers were washed 3×5 min in ice-cold 0.01 M citrate buffer. Single anthers were placed on slides and homogenized with a dissection needle in 8 µl of 60% acetic acid. Additional 8 µl of 60% acetic acid were added and incubated for 2 min at RT. Another 8 µl of 60% acetic acid were added and the slides were put on a 42° C hot plate for 2 min. On the hot plate, the material was spread by hovering the dissection needle over the meiocyte suspension drop without touching the slides, using only the surface tension. Subsequently, the acetic acid drop was surrounded by 200 µl of 4° C cold ethanol/glacial acid (3:1) and incubated for 30 sec at RT to precipitate the nuclei on the slide. More ethanol/glacial acid (3:1) was added to rinse the whole slide. Afterwards, slides were incubated for 10 min in 60% acetic acid at RT and finally washed by dipping 10× in a glass cuvette containing ice-cold 100% ethanol. After air-drying, slides were directly used for FISH or kept at 4° C in 100% ethanol until hybridization.

Mitotic chromosome spreads were prepared according to Aliyeva-Schnorr *et al.* (Aliyeva-Schnorr *et al.* 2015). Root tips of rye carrying Bs were cut, mitotic metaphases were accumulated by overnight treatment in ice-cold water and then fixed in ethanol/glacial acid (3:1). Root tips were washed 3× in ice-cold water and digested (50–60 min, 37° C) in an enzyme cocktail (1% cellulose (Calbiochem, cat. no. 219466), 1% pectolyase Y-23 (Sigma-Aldrich, cat. no. P3026), 1% cytohelicase (Sigma-Aldrich, cat. no. C8274) in 0.01 M citrate buffer). Afterwards, root tips were consecutively washed in ice-cold 0.01 M citrate buffer and 100% ethanol. Subsequently, root tips were transferred to glacial acid/ethanol (3:1; 200 µl/25 root tips) in a 1.5 ml tube and disrupted with a dissection needle. 8 µl of

this mitotic cell suspension was dropped on glass slides placed on ice, air-dried and stored in 100% ethanol at 4° C.

For FISH, the probe-containing hybridization mix (FISH probe diluted in 20% dextran sulphate (Sigma-Aldrich, cat. no. D 8906), 50% deionized formamide, 300 mM NaCl, 30 mM tri-sodium citrate dehydrate, 50 mM phosphate buffer, pH 7.0) was applied to the air-dried slides. Then, the slides were incubated for denaturation for 2 min on a hot plate at 80° C in darkness. FISH was performed overnight (37° C, in darkness). Slides were washed 3×5 min in 1× PBS and afterwards mounted and counterstained with DAPI (1 mg/ml) in Vectashield (Vector Laboratories).

1.3.5 Immunostaining followed by FISH on meiotic chromosomes

Rye anthers with meiocytes at prophase I were fixed 25 min under vacuum in 4% ice-cold paraformaldehyde in 1× PBS (pH 7.4), washed 3×5 min in ice-cold 1× PBS and 20 min digested at 37° C in an enzyme cocktail (0.1% cellulose (Calbiochem, cat. no. 219466), 0.1% pectolyase Y-23 (Sigma-Aldrich, cat. no. P3026), 0.1% cytohelicase (Sigma-Aldrich, cat. no. C8274) in 1× PBS. After washing 3×5 min in ice-cold 1× PBS, single anthers were transferred to slides and squashed in 1× PBS + 0.001% Tween-20 using coverslips. After coverslip removal using liquid nitrogen, the slides were stored in 1× PBS. For longer storage, they were transferred to 100% glycerol (Carl Roth, cat. no. 3783) and kept at 4° C. The following primary antibodies were applied at 37° C for 90 min: rabbit anti-*Zea mays* ASY1 (1:200), guinea pig anti-*Zea mays* ZYP1 (1:200; (Golubovskaya et al. 2011)), rabbit anti-*A. thaliana* NSE4A (1:200; (Zelkowski et al. 2019)), mouse anti-*Oryza sativa* HEI10 (1:200; (Wang et al. 2012)) and rabbit anti-grass CENH3 (1:1000; (Sanei et al. 2011)). For detection, the following secondary antibodies were applied at 37° C for 60 min: goat anti-rabbit Dylight488 (1:200; Dianova, cat. no. 111-485-144), goat anti-guinea pig Alexa Fluor594 (1:400; Molecular Probes, cat. no. A11076), goat anti-mouse Cy3 (1:400; Dianova, cat. no. 115-166-146) and donkey anti-guinea pig Alexa Fluor647 (1:200; Dianova, cat. no. 706-605-148). Afterwards, the slides were washed in 3× 5 min 1× PBS, dehydrated (2 min each step; 70%, 90% and 100% ethanol), air-dried and fixed in ethanol/acetic acid (3:1; 24–48 h in darkness at RT). Subsequently, the slides were air-dried and incubated with the FISH probe-free hybridization mix (see above) for 12 h at 37°C. After short washing for 5 min in 2× SSC containing 0.1% Triton X100, the slides were dehydrated and air-dried. For DNA denaturation, slides were incubated in 0.2 M NaOH (in 70% ethanol; 10 min at RT), dehydrated and air-dried. Then, the FISH probes were diluted and denatured for 5 min at 95° C in the hybridization mix prior to application on slides. FISH was performed in darkness at 37° C overnight using Bilby or the B-specific probes. Slides were washed 3× 5 min in 1× PBS and afterwards mounted and counterstained with DAPI (1 mg/ml) in Vectashield (Vector Laboratories).

1.3.6 Characterization of the SC of B chromosomes

Immunostaining using the primary antibodies directed against *Z. mays* ASY1 and *Z. mays* ZYP1, and subsequent FISH using the rye B chromosome-specific probes Sc11, Sc55c1, Sc63c34, D1100, E3900 and Sc36c82, were performed on meiocytes as described above. The determination of the pairing configurations was done using a BX61 microscope (Olympus) equipped with an ORCA ER-CCD camera (Hamamatsu) or by super-resolution microscopy. For quantification only meiocytes with completed synapsis were considered.

1.3.7 NSE4A antibody specificity test

To test the specificity of anti-NSE4A, recombinant NSE4A was added to the NSE4A antibody at a concentration of 800 nM, and immunostaining was performed as described above. Recombinant NSE4A was kindly provided by Dr. Udo Conrad (IPK Gatersleben).

1.3.8 Super-resolution microscopy

To analyse the ultrastructure of immunosignals and chromatin beyond the classical Abbe/Raleigh limit at a lateral resolution of ~120 nm (super-resolution, achieved with a 488 nm laser), spatial structured illumination microscopy (3D-SIM) was applied using a 63×/1.4 Oil Plan-Apochromat objective of an Elyra PS.1 microscope system and the software ZENblack (Carl Zeiss GmbH). Images were captured separately for each fluorochrome using the 642, 561, 488, and 405 nm laser lines for excitation and appropriate emission filters (Weisshart et al. 2016). Maximum intensity projections of whole meiocytes were calculated *via* the ZEN software. Zoom in sections were presented as single slices to indicate the subnuclear chromatin and protein structures at the super-resolution level. 3D rendering and CENH3 volume measurements based on SIM image stacks were done using the Imaris 8.0 (Bitplane) software.

1.4 Results

1.4.1 Characterization of a rye NDJ-deficient B chromosome

For *S. cereale*, various isoforms of B chromosomes are described. Besides the standard B, isochromosomes of the long or short arm and Bs deficient in parts of specific chromosome arm regions occur in natural rye population or were synthesized under laboratory conditions (Müntzing 1944, Jones et al. 1993, Endo et al. 2008). One of these isoforms is a so called NDJ-deficient (deletion) B chromosome (delB) characterized by a deletion of the terminal segment of the long arm. This isoform is especially interesting, as the deletion includes the nondisjunction control region, essential for the 'drive' mechanism of rye Bs. B chromosomes lacking the NDJ separate at anaphase I of pollen mitosis do not accumulate in the generative nucleus (Hasegawa 1934, Müntzing 1945, Müntzing 1946, Müntzing 1948). To analyse the extent of the deletion, we performed FISH using rye B-specific high-copy sequences as markers (Figure 4). Due to the high compaction of fully condensed chromosomes, some of the marker probes (Kulla, D1100, Sc55, and Sc63) were applied on prophase I (zygotene/pachytene) meiocytes for better resolution of the hybridization signals. Comparison between the standard B and the delB revealed that the deletion breaking point occurred in the Sc55-positive region and resulted in a rearrangement of Sc55- and Sc63-positive regions (Figure 4A-C). Whereas the standard B harbours a distinct cluster of Sc63 flanked by two clusters of Sc55, the delB chromosome showed a reversed orientation of multiple Sc63 cluster flanking one Sc55 cluster. Moreover, D1100, a NDJ marker and the subtelomeric repeat Kulla were not detected on delBs, indicating a complete rather than a partial loss of the terminal segment. The detection of *Arabidopsis*-type telomeres was possible on both isoforms, which implies either a *de novo* synthesis of telomeres on the delB isoform, or a deletion of only an acrocentric subterminal fragment occurred keeping the original telomeres at the shortened chromosome arm. Notably, the two high-copy sequences Sc380 and Sc250 which can be found in the (sub-) terminal regions of all rye A chromosomes, were detected neither on the standard B, nor on the delB.

A Standard rye B chromosome **B** Deletion rye B chromosome

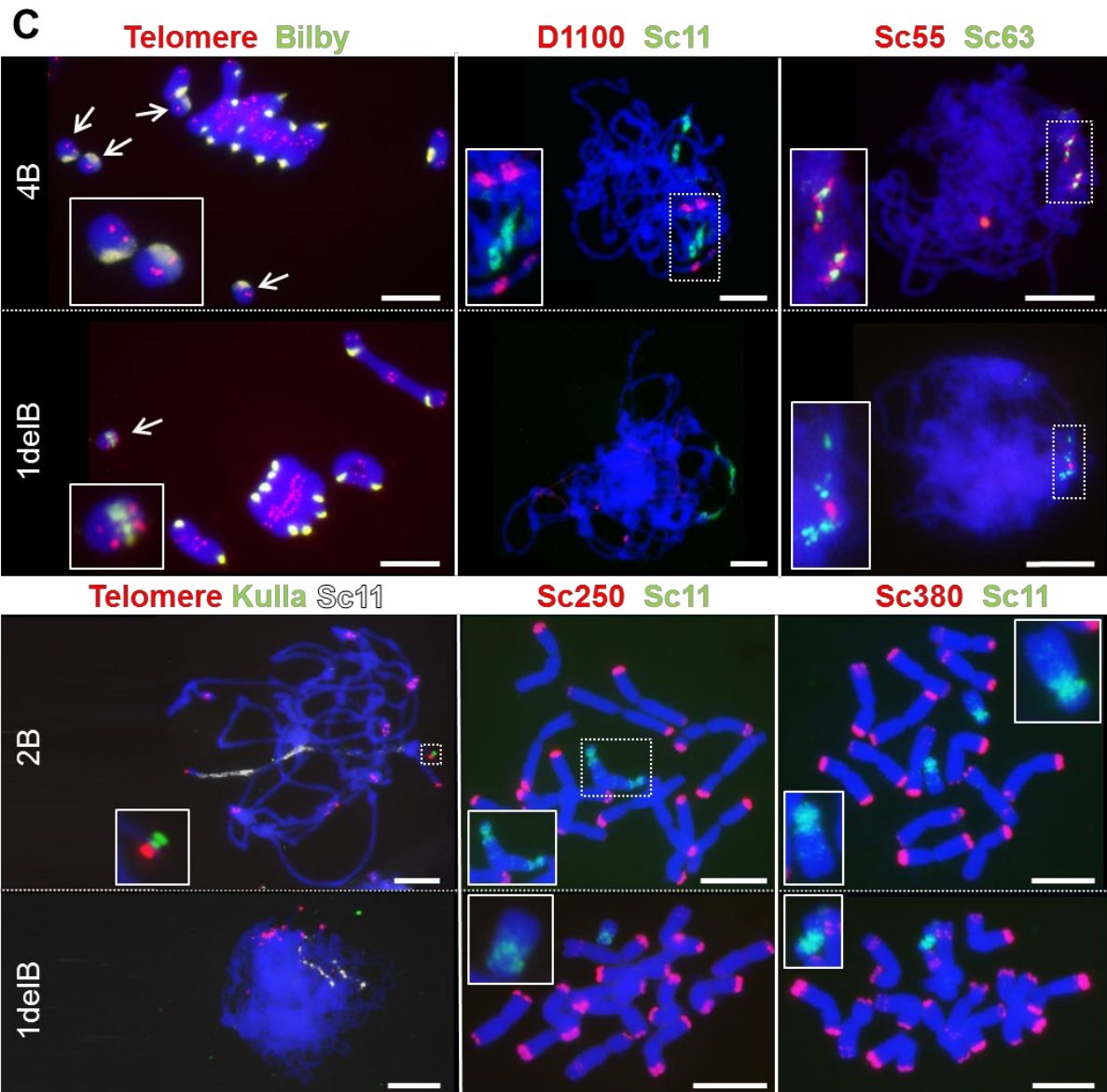
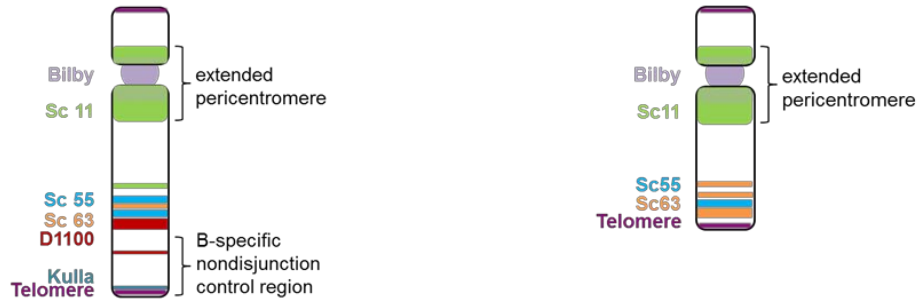


Figure 4 | Characterization of a rye B chromosome isoform harbouring a deletion of the nondisjunction control region (NDJ). To detect the indicated marker repeats, FISH was performed on meiocytes (*Arabidopsis*-type telomere, Kulla, D1100, Sc55, Sc63) or metaphase chromosomes (Sc250, Sc380) using the corresponding FISH probes. Each sequence is represented by a colour as indicated. Chromatin was counterstained by DAPI (blue). **(A)** Model of the distribution of marker repeats on a standard rye B chromosome. The centromere is marked by the rye centromere-specific repeat Bilby and its extended pericentromeric sequence Sc11. The repeats Sc55, Sc63 and D1100 mark the long arm and the beginning of the NDJ. The subtelomeric region of the long arm is characterized by the repeat Kulla. *Arabidopsis*-type telomeres are detectable on both B

chromosome ends. Adapted from (Klemme et al. 2013). **(B)** Model of the marker repeats distribution on the NDJ-deficient rye B chromosome. At the breaking point region, rearrangements (loss and/or amplification of the repeats Sc55 and Sc63) occurred. Telomeres are detected at both ends. **(C)** FISH of different marker repeats on rye material carrying either standard or NDJ-deficient Bs (delB). On both B isoforms telomeres are detectable on all chromosomes ends (arrows). D1100 and Kulla are not detectable on delB chromosomes suggesting a complete deletion of the long arm end. The deletion of the NDJ occurred at the position of the Sc55 sequence and caused structural changes in the sequence composition of this region. Interestingly, the repeats Sc250 and Sc380 are only detectable on rye A chromosomes. Bars = 10µm.

1.4.2 Rye B chromosomes participate in the 'bouquet' formation

In most species of plants, animals and fungi, meiotic chromosome pairing before synapsis is accompanied, and possibly facilitated, by the clustering of telomeres at a small region of the nuclear envelope, called the 'bouquet' (Harper et al. 2004, Scherthan 2007).

To investigate whether the B chromosomes also participate in the 'bouquet' formation as the A chromosomes do, we performed FISH analysis using three types of probes on rye plants carrying 1B, 2B or 4B chromosomes. The telomere 'bouquet' was visualized with by an *Arabidopsis*-type telomere probe, the B chromosome ends were specifically identified by the subtelomeric high-copy sequence Kulla, and the B centromere by the pericentromeric repeat Sc11 (Figure 5). Only nuclei including all detectable A chromosome telomere signals in a 'bouquet' formation were considered for analysis to ascertain the right stage of the meiocytes. Due to the low occurrence of 1B individuals, only one plant (meiocytes n=100), whereas in case of 2B and 4B three plants (meiocytes per plant n=100) were analysed. In all rye plants investigated, the Kulla FISH signals were always closely associated with the telomere cluster, thus indicating the participation of the B chromosomes in this formation. In contrast, the corresponding anther tissue nuclei show a broad distribution of telomeric and Kulla FISH signals, and thus allow the clear distinction of meiotic and somatic cell (Figure 5).

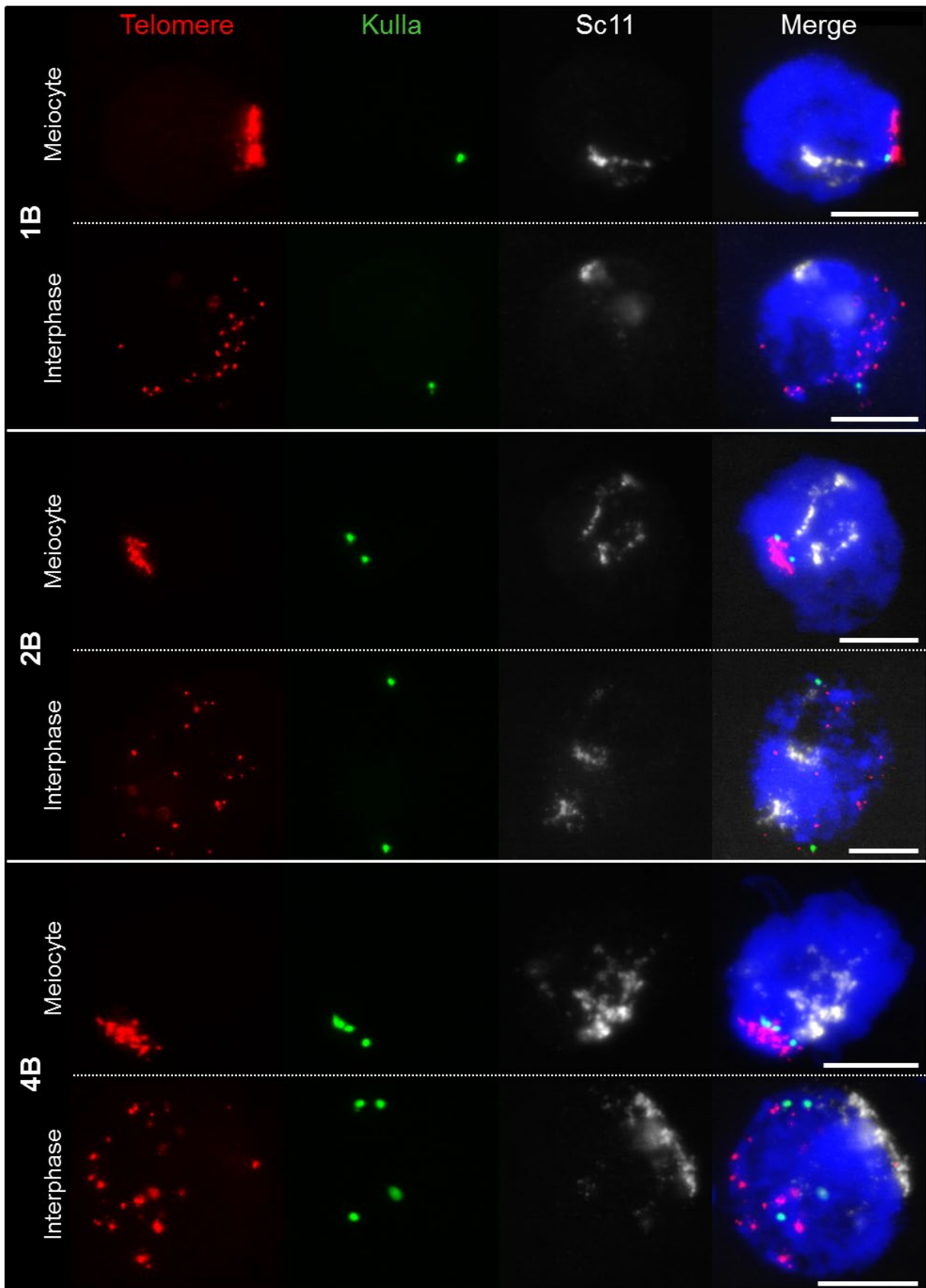


Figure 5 | Bouquet formation of rye carrying 1B, 2B and 4B chromosomes. FISH performed to detect telomeres by an *Arabidopsis*-type telomere- specific probe (red), B chromosome ends by the B-specific subtelomeric repeat Kulla (green), and B chromosome centromeres by the pericentromeric repeat Sc11 (white). Chromatin was counterstained by DAPI (blue). The meiocytes show a clear bouquet formation of all telomeres. The subtelomeric signals of the Kulla repeat locate in close proximity to the telomere bouquet,

indicating that also B chromosomes participate in this formation. In contrast, interphase nuclei of the corresponding anther tissue show a distant distribution of telomeric and Kulla signals within the nucleus. Bars = 10µm.

1.4.3 The use of structured illumination microscopy (SIM) for meiotic studies in rye

Compared to widefield microscopy, super-resolution microscopy enables a significantly increased resolution, thus offering the analysis of plant chromatin at the nanoscopic level (Baroux and Schubert 2018). Here, we applied fluorescence-based microscopy and 3D-SIM to investigate chromatin and protein substructures in more detail to obtain new insights in the structure of paired homologous chromosomes in prophase I meiocytes of rye (Figures 6-14). Indeed, a clearly increased resolution and the removal of out-of-focus blur have been achieved by SIM as compared to widefield microscopy (Figure 6).

The localization and dynamics of the specifically stained SC components ASY1 and ZYP1, as well as the associated proteins NSE4A and HEI10, were monitored during prophase I at rye A and B chromosomes (Figures 6-14).

To identify centromeres and to conclude on the orientation of uni- and bivalents the A and B centromeres were subsequently labelled by the centromere-specific FISH probe Bilby (Francki 2001) and CENH3-specific antibodies (Figure 8B, Figure 9B-B₂, Figure 10B, E, Figure 12, Figure 13D).

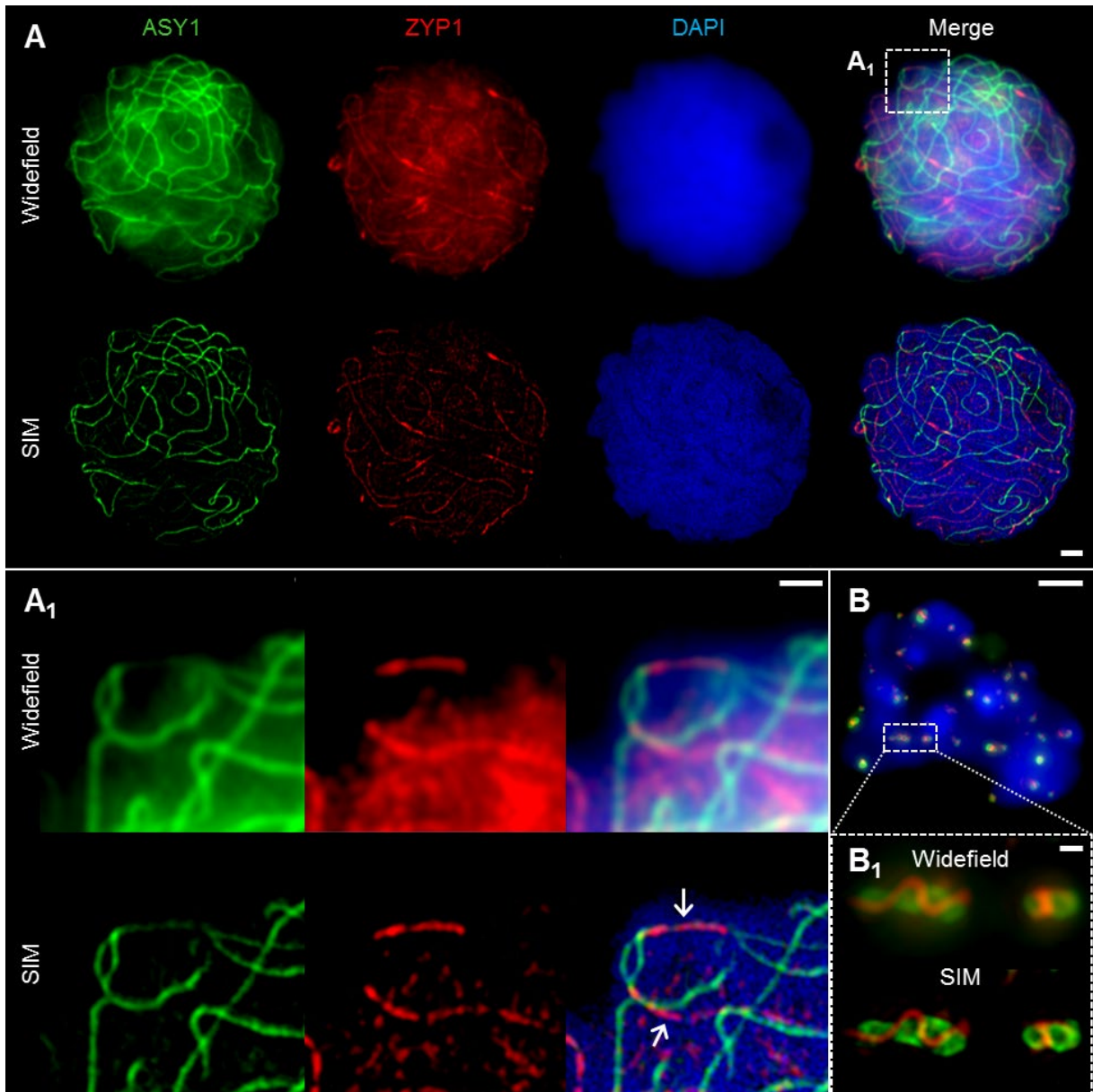


Figure 6 | SIM improves the resolution and thus the identification of SC nanostructures significantly. Chromatin was stained with DAPI. **(A)** Comparison of ASY1 and ZYP1 immunosignals at zygotene acquired by conventional widefield microscopy and SIM. The increased resolution of SIM reveals more nanostructures and improves the colocalization analysis by higher precision. Bar= 2 μ m. **(A₁)** Enlarged region, showing clearly the interstitial synapsis (arrow) by SIM. Bar= 1 μ m. **(B)** Widefield imaging of the ball-like ASY1 and ZYP1 structures at late diakinesis. Bar= 5 μ m. **(B₁)** SIM provides clearly increased substructural information compared to widefield microscopy. ZYP1 is embedded in a ball of ASY1. Bar= 0.5 μ m.

1.4.4 ASY1 and ZYP1 form typical structures during SC assembly and disassembly

The dynamics of the synaptonemal complex during prophase I was monitored by immunolocalization of ASY1 and ZYP1 (Figure 6, Figure 7, Figure 9, Figure 10, Figure 11, Figure 13, Figure 14)). At zygotene, synapsis is initiated at several sites along both homologues. During the SC assembly, ASY1 is partially released from synapsed chromosomes resulting in substantially lower fluorescence intensity and diffuse ASY1 signals in the nucleoplasm at pachytene. Notably, apart from linear tracts disperse ZYP1 signals can also be detected, likely indicating yet unassembled protein (Figure 7A₁). At the beginning of pachytene, synapsis completes and the SC tripartite structure is clearly visible (Figure 7A₃). ASY1 signals appear as discontinuous stretches and spots with varying intensities. At pachytene, the ongoing chromatin condensation is accompanied by SC convolution, showing the most compact coiled structure at diplotene. The compaction of chromosomes also results in a more contiguous staining of ASY1. The first initiation of SC disassembly can be detected at late pachytene by the re-organization of ASY1 at single SC sites to form transient loop-like structures. At positions where both ASY1 strands dissociate from the SC, ZYP1 signals are no longer detectable, indicating the local release of synapsis (Figure 7A₂₋₄, Figure 10D). During progression of the SC disassembly at diplotene, ASY1 undergoes partial degradation that results in the emergence of fragmented ASY1 threads (Figure 7A₄, Figure 10D, Figure 11A₃, Figure 11C-C₁). At early diakinesis, the SC fragments continue condensing, at which ASY1 winds up around residual ZYP1 fragments. Further shortening of these fragmented SCs progresses until 2-3 compact ball-like structures per bivalent remain at late diakinesis (Figure 6B₁, Figure 7A₅, Figure 10E, Figure 13E). The SC structures marked by ASY1 and ZYP1 disappear completely at the end of diakinesis.

In summary, we conclude that the SC structures composed by ASY1 and ZYP1 are essential not only during the establishment of synapsis. Obviously, they are also required to organize and stabilize the paired homologues during chromatin condensation until prophase I terminates.

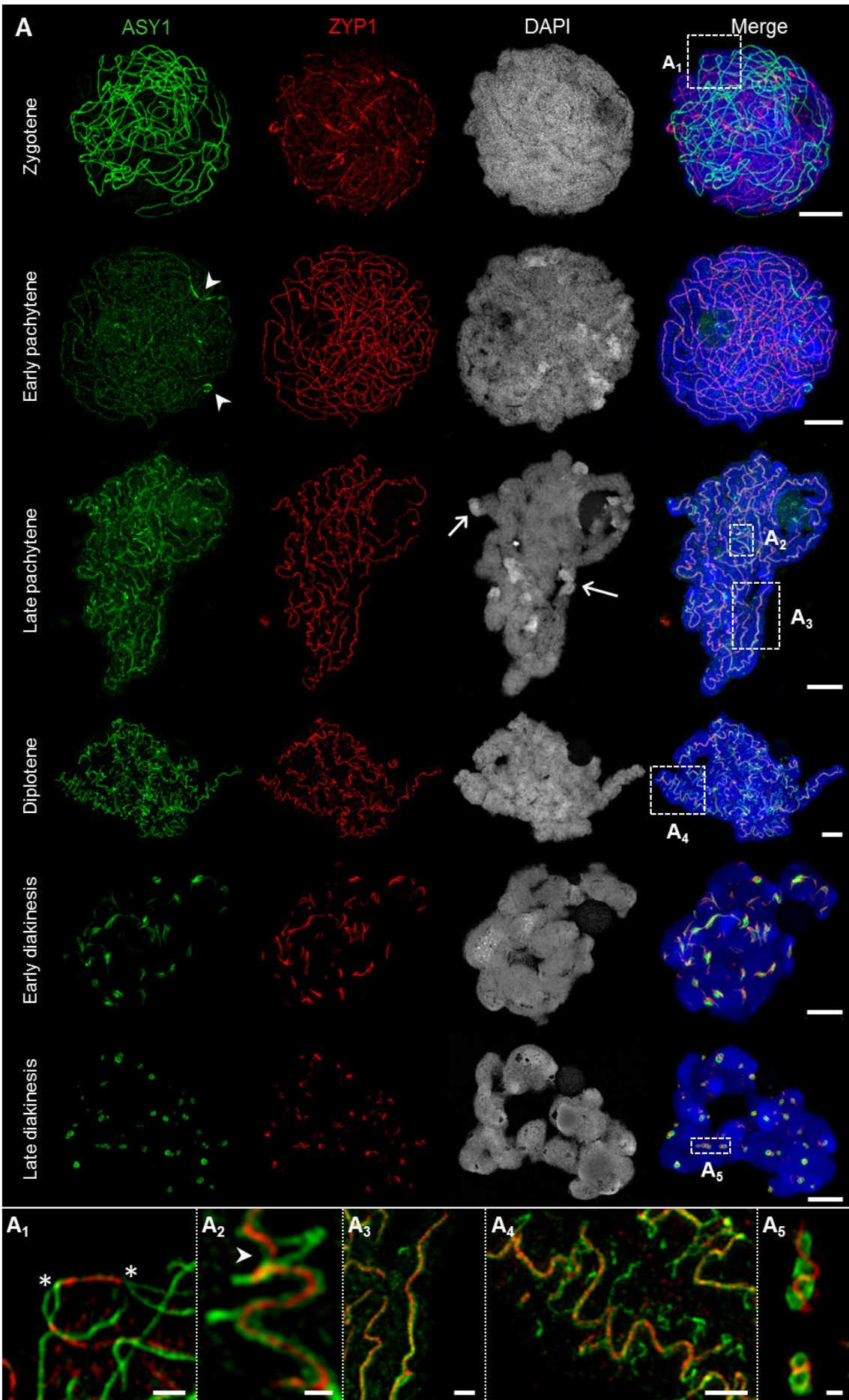


Figure 7 | The behaviour of ASY1 and ZYP1 during prophase I. The images A₁-A₅ show enlarged regions delimited by dashed boxes. Chromatin was stained with DAPI. **(A)** Representative examples of immunostaining of ASY1, a marker for chromosome axis, and ZYP1, a SC transverse filament protein. At zygotene, intense ASY1 signals are visible along not yet synapsed chromatin axes. When synapsis proceeds at early pachytene, the SCs assemble at multiple sites of the chromatin and the ZYP1 signals become more prominent. The ASY1 signal intensity strongly decreases at synapsed regions, but never vanishes completely. At early pachytene, all homologues are synapsed. The last separated regions can be identified by brighter ASY1 signals (arrowheads). At late pachytene, the ongoing chromatin condensation causes a convoluted SC structure. ASY1 starts separating from ZYP1, reflecting the initiation of SC disintegration (**A₂**, **A₃**). Note the regions with a substantially higher DAPI staining intensity at the telomeric heterochromatin (arrows) corresponding to increased chromatin condensation. At diplotene, the SCs form spiral-like structures with ASY1 strands retracting from the SC at multiple positions (**A₄**), which reflects proceeding SC disassembly and further chromatin condensation. At early diakinesis, ZYP1 staining detects only short SC fragments enwrapped by ASY1. At late diakinesis, only compact ball-like ASY1 structures with embedded ZYP1 remain (**A₅**). They disappear completely until the end of diakinesis (Figure 11A₄, E). Bars = 5µm. **(A₁)** An interstitial synapsis initiation site showing ZYP1 signals flanked by still separated ASY1 strands (asterisks). Bar = 1µm. **(A₂)** Initiation of SC disintegration at late pachytene. ASY1 strands dissociate from single SC sites *via* loop formation. At positions where both ASY1 strands become retracted from the SC, ZYP1 disappears (arrowhead). Bar = 0.5µm. **(A₃)** ZYP1 enwind in two ASY1 strands during late pachytene. Bar = 1µm. **(A₄)** At diplotene, the ASY1 structures dissociate from the SC and start to dissolve at various positions indicating multiple sites of SC disassembly. Bar = 2µm. **(A₅)** At late diakinesis, short ZYP1 fragments are embedded in ball-like ASY1 structures. Bar = 0.5µm.

1.4.5 The SMC5/6 complex δ -kleisin NSE4 colocalizes to ZYP1 within the SC during synapsis

The SMC5/6 complex has been implicated to have versatile functions in meiotic processes, i.e. in recombination as well as in SC assembly and stability (Verver et al. 2016). To investigate the role of SMC5/6 complex subunits during prophase I, we analysed the distribution and dynamics of δ -kleisin NSE4 in rye. To confirm the specificity of the *A. thaliana* NSE4A antibodies (Zelkowski et al. 2019) we performed a competition assay. Therefore, the NSE4A antibodies were pre-incubated before immunolabelling with recombinant NSE4A to block all binding sites and prevent a specific staining on rye meiocytes. In contrast to the unblocked antibody, the pre-incubated antibodies show beside dot-like background staining only a very weak spiral-like NSE4A detection, suggesting that most of the antibodies were blocked by recombinant NSE4A and that the *A. thaliana* NSE4A antibodies are suitable to detect the rye NSE4 homologs. To exclude unspecific signal detection, which could potentially be induced by fluorescence crosstalk of ZYP1, rye meiocytes were labelled with NSE4A antibodies only (Figure 8A). The detected twisted NSE4A immunosignal corresponds to the typical SC labelling visible at synapsed homologues during diplotene (Figure 7A, A₄, Figure 8B, Figure 9B-B₂, Figure 10B). Concurrently, the chromosomes were labelled by the centromere-specific FISH probe Bilby to identify centromeres and paired homologues (Figure 8B, Figure 9B-B₂, Figure 10B, E, Figure 12, Figure 13E).

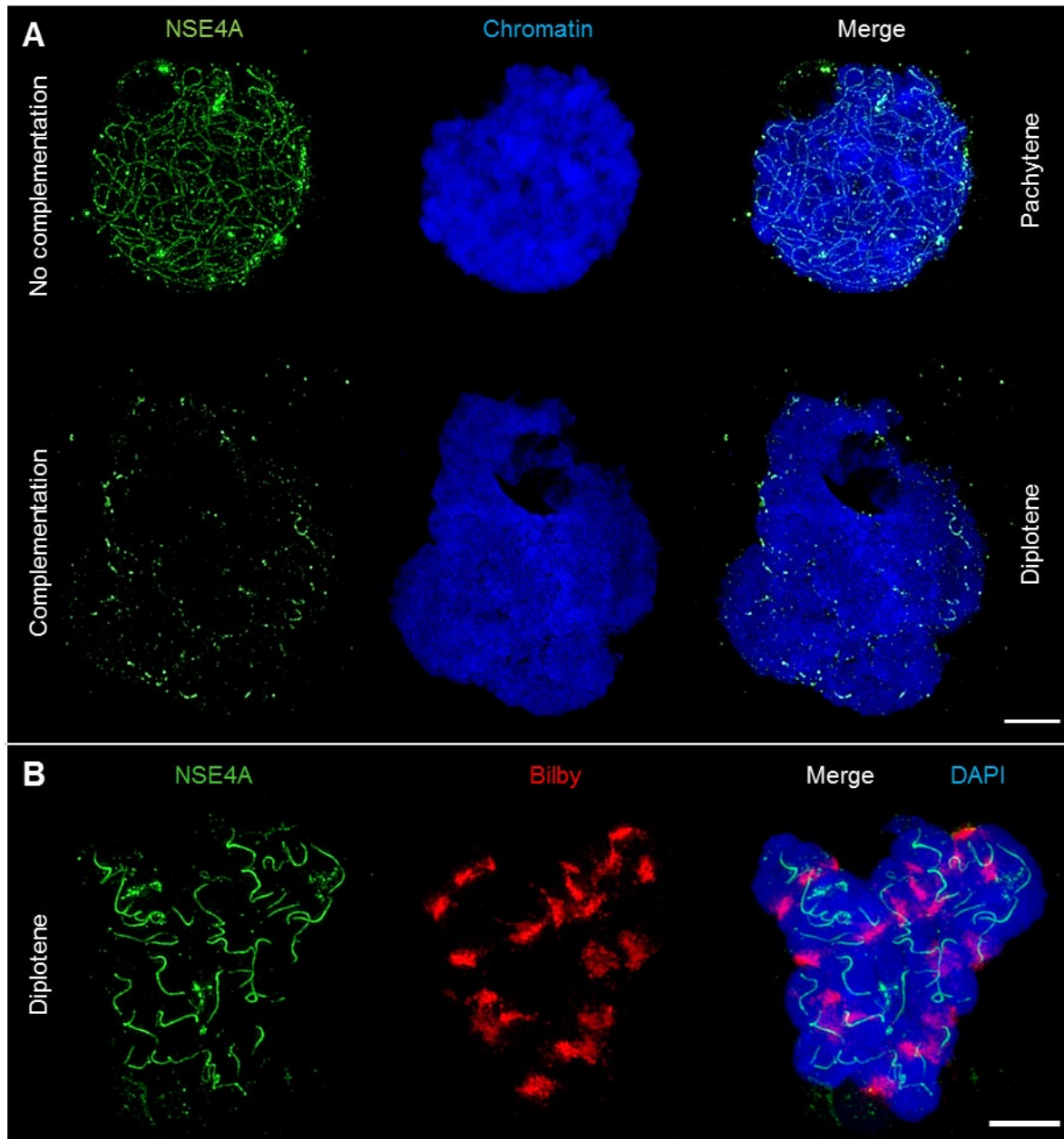


Figure 8 | Characterization of the Nse4A antibody in rye. (A) NSE4A labelling of the synaptonemal complexes in rye ($2n=14+2Bs$) meiocytes without and after antibody complementation. The competed antibodies show only weak spiral-like NSE4A staining in contrast to the unblocked antibodies and therefore indicate the specificity of the detected signals in rye. (B) The NSE4A antibodies, without a ZYP1 co-labelling, show the typical convoluted NSE4A signals during diplotene, thus excluding a fluorescent crosstalk possible *via* double labelling. (Peri)centromeric regions of the homologues are marked by Bilby FISH probes. Chromatin was stained with DAPI. Bars= 5 μ m.

The simultaneous labelling of NSE4A and ZYP1 revealed a strong colocalization of both proteins at the central region of the SC (Figure 9A). At zygotene, NSE4A is present only along the synapsed homologues. As the chromatin condensation progresses, the twisted structure of NSE4A follows the SC structure typical visible at diplotene. During SC disassembly at early diakinesis, the NSE4A signals match to the spatial distribution of ZYP1 and can be detected exclusively on the remaining ZYP1-

positive SC fragments (Figure 9A₁). At late diakinesis, typical colocalized ball-like structures of NSE4A and ZYP1 are evident (Figure 9A₂-A₃, Figure 10C).

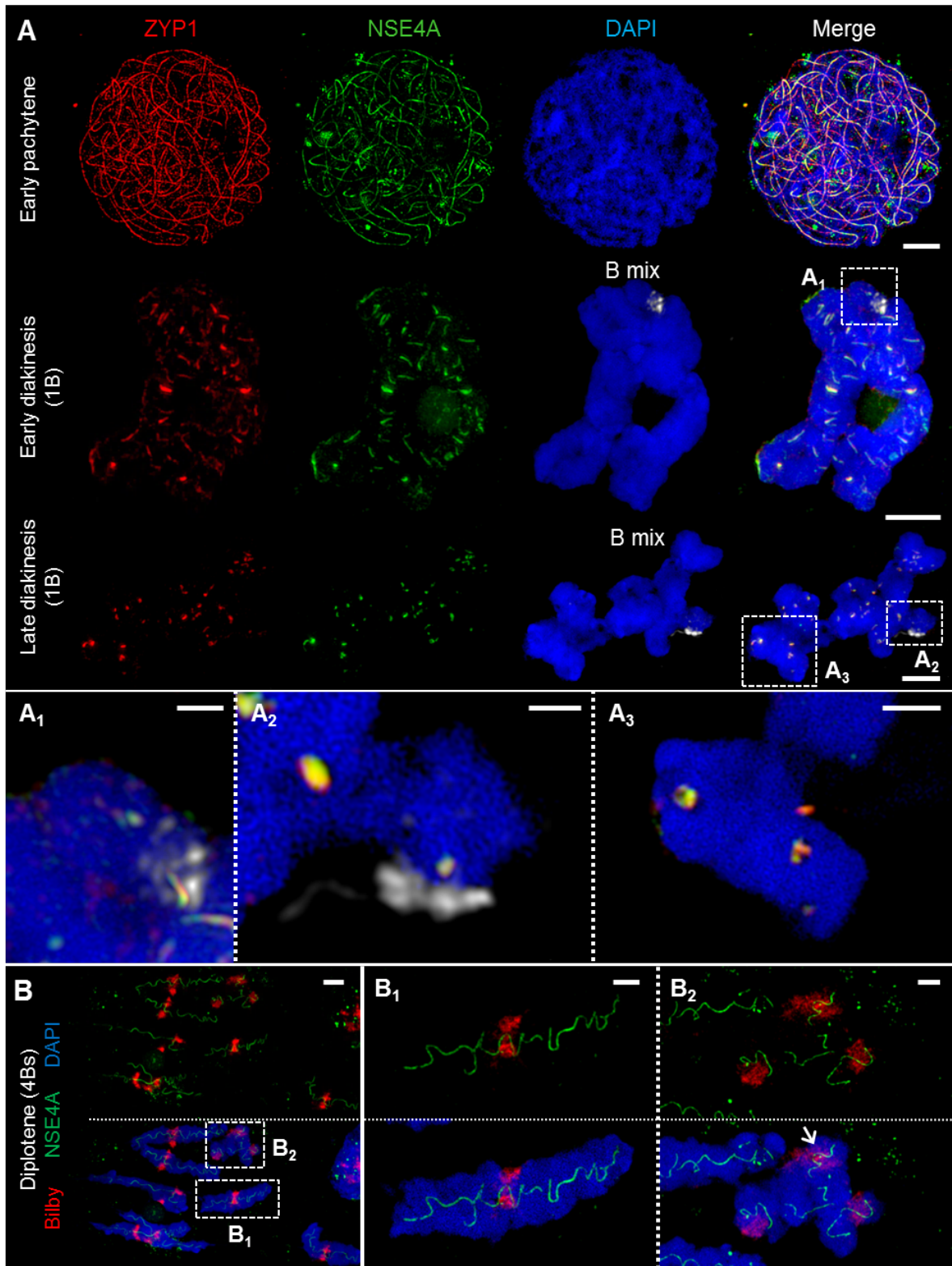


Figure 9 | ZYP1 and NSE4A colocalize at the SCs of rye A and B chromosomes. The images A1-A3, B1 and B2 show enlarged regions delimited by dashed boxes. The B chromosomes were detected by a B-specific FISH probe mix, centromeres by the specific repeat Bilby. The chromatin was stained with DAPI. **(A)** The simultaneous immunolocalization of NSE4A and ZYP1 shows clearly their colocalization at the central region of the SC throughout prophase I. At zygotene, the NSE4A signals are present along the synapsed homologues.

When degradation proceeds during diakinesis, NSE4A can be detected only at ZYP1-positive SC fragments. A and B chromosomes behave similar **(A1-A3)**. Bars = 5 μ m. **(A1)** A self-pairing rye B chromosome shows the colocalization of NSE4A and ZYP1 at early diakinesis. Bar = 1 μ m. **(A2)** At late diakinesis, a self-paired rye B chromosome displays typical ball-like residual structures of the SC complex identical to those present on A chromosomes. NSE4A and ZYP1 colocalize. Bar = 2 μ m. **(A3)** An A chromosome bivalent showing ball-like structures of the remaining SC at late diakinesis. Note the colocalization of NSE4A and ZYP1. Bar = 2 μ m. **(B)** A meiocyte with seven A homologues and four B chromosomes (4Bs) at diplotene. The convoluted NSE4A signals follow the SC structure typically present at diplotene. Bilby identifies the centromeres of the bivalents. The NSE4A structures are identical at A and B chromosomes **(B1, B2)**. Bars = 5 μ m. **(B1)** Typical convoluted NSE4A structure of an A bivalent. Bar = 2 μ m. **(B2)** Convoluted NSE4A structures indicate the SCs at four B chromosomes forming a multivalent. The Bs can be distinguished from As by their smaller size and the increased Bilby signal dispersion. Two of the B centromeres are associated (arrow). Bar = 2 μ m.

Our findings suggest that NSE4, together with ZYP1, is involved in the organization and stabilization of synapsis during prophase I in rye.

1.4.6 The SC is a protein structure embedded in chromatin

The immunolocalization of ASY1, ZYP1 and NSE4A at the SCs and the absence of DNA-specific DAPI staining indicate that the inner SC is mainly a chromatin-poor protein structure during prophase I (Figure 10A-C). This structure becomes visible at zygotene (Figure 7A) and is present until late diakinesis (Figure 10C).

The resolution achieved by SIM allows assessment of the relative width of the ASY1 and ZYP1 structures at different prophase I stages (Figure 10D, E). At diplotene the width of single ASY1 loops is approximately half of that of synapsed regions. This reflects the retraction of individual chromosome axes regions during the SC disintegration at diplotene. At diakinesis, ASY1 signal measurements indicate that the ball-like structures are established by accumulation of separate ASY1 threads around a ZYP1 core.

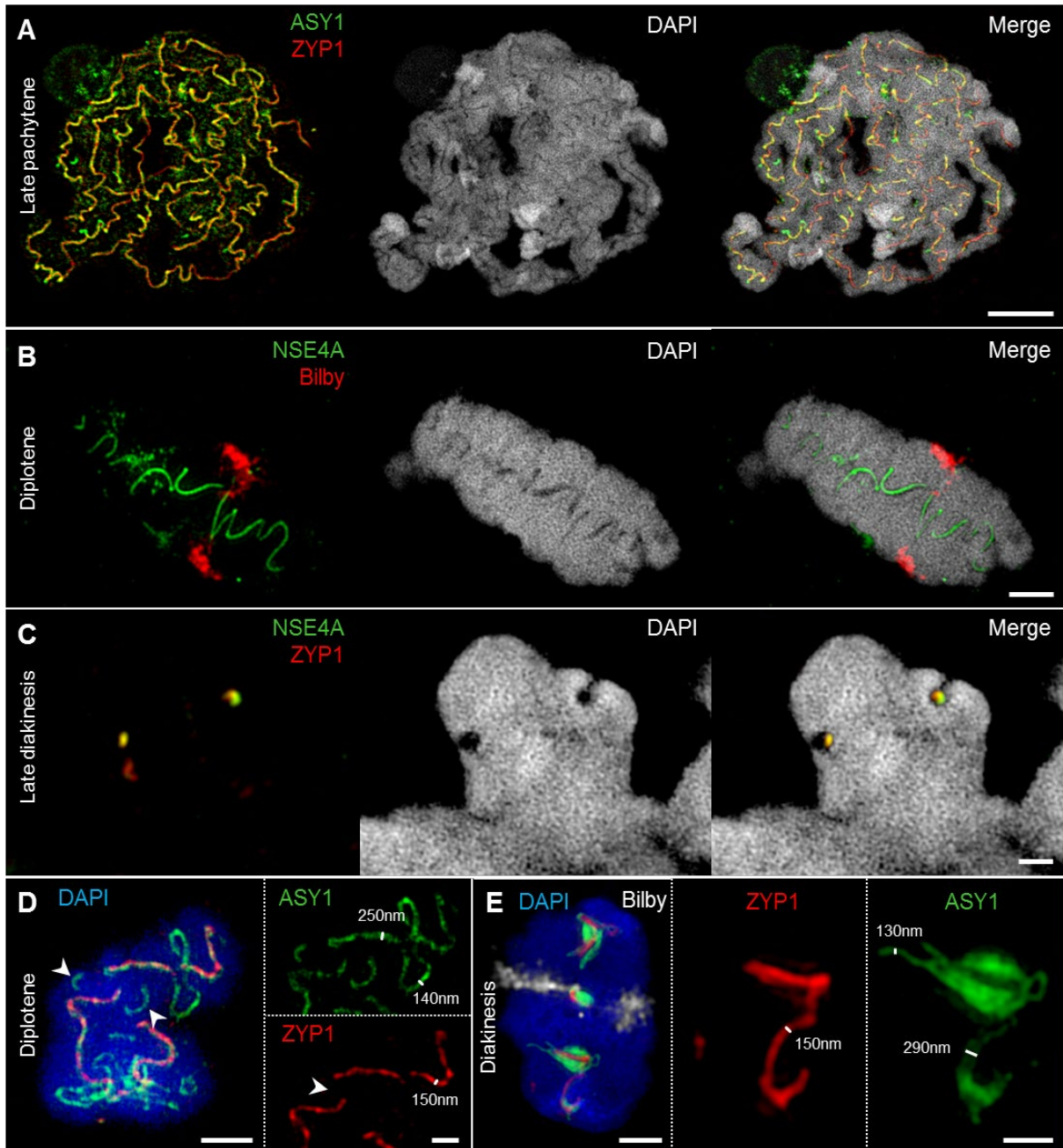


Figure 10 | SIM identifies the SC as a complex protein structure embedded in chromatin. Chromatin was stained with DAPI. **(A-C)** At different stages of prophase I, chromatin-poor structures can be visualized within paired homologues. They comprise colocalized ASY1, ZYP1 and NSE4A proteins indicating the inner SC as chromatin-poor. Bars = 5 μ m **(A)**, 2 μ m **(B)**, 1 μ m **(C)**. **(D)** An A chromosome bivalent at diplotene showing SC disintegration accompanied by the retraction of ASY1 from the SC. While ASY1 forms loop structures at early Sc disassembly, ZYP1 disappears at positions where pairing is already resolved (arrowheads). Bars = 2 μ m (bivalent), 1 μ m (enlarged region). **(E)** At diakinesis ASY1 winds up around the short residual ZYP1 strands at few positions suggesting a special role of these emerging ball-like structures. The centromeres were labelled by Bilby. Bars = 2 μ m (bivalent), 1 μ m (enlarged region). The SIM resolution allows to measure the relative width of the ASY1 and ZYP1 structures at different prophase I stages **(D, E)**.

1.4.7 HEI10 localizes to the SC during synapsis and indicates the location of recombination sites at late diakinesis

Recently it has been shown, that the ZMM protein family member HEI10 is involved in homologous recombination, and that it marks class I crossover loci in a number of organisms such as rice, *Arabidopsis* and mouse (Ward et al. 2007, Chelysheva et al. 2012, Wang et al. 2012, Qiao et al. 2014). To examine whether HEI10 is characterized by the same localization pattern in rye, we labelled different stages of prophase I with ASY1, ZYP1 and HEI10 antibodies simultaneously (Figure 11). At zygotene, many distinct HEI10 signals were detected exclusively at the central region of the SC marked by ZYP1 (Figure 11A₁). When synapsis is completed at pachytene, a reduced number of HEI10 foci become clearly distinguishable (Figure 11A₂). At diplotene, when the progression of the SC disassembly results in SC fragmentation, HEI10 can be detected as numerous low-intensity foci located along the central element of the SC. Additionally, a few prominent foci slightly apart from ZYP1 were present. The preferential localization of such foci towards the bivalent termini suggests a staining of potential crossover sites present in chromatin regions looped out from the SC (Figure 11C, D). At late diakinesis, ASY1 and ZYP1 signals disappear almost completely, but distinct HEI10 puncta remain at potential class I crossover loci. The quantification of HEI10 signals in 50 meiocytes at this stage resulted in a mean of 13.1 signals per cell (SD=1.57). This value corresponds to the expected number of chiasmata observed in diploid rye by Jones and strongly suggests the detection of class I crossover sites by anti-HEI10 (Jones 1967).

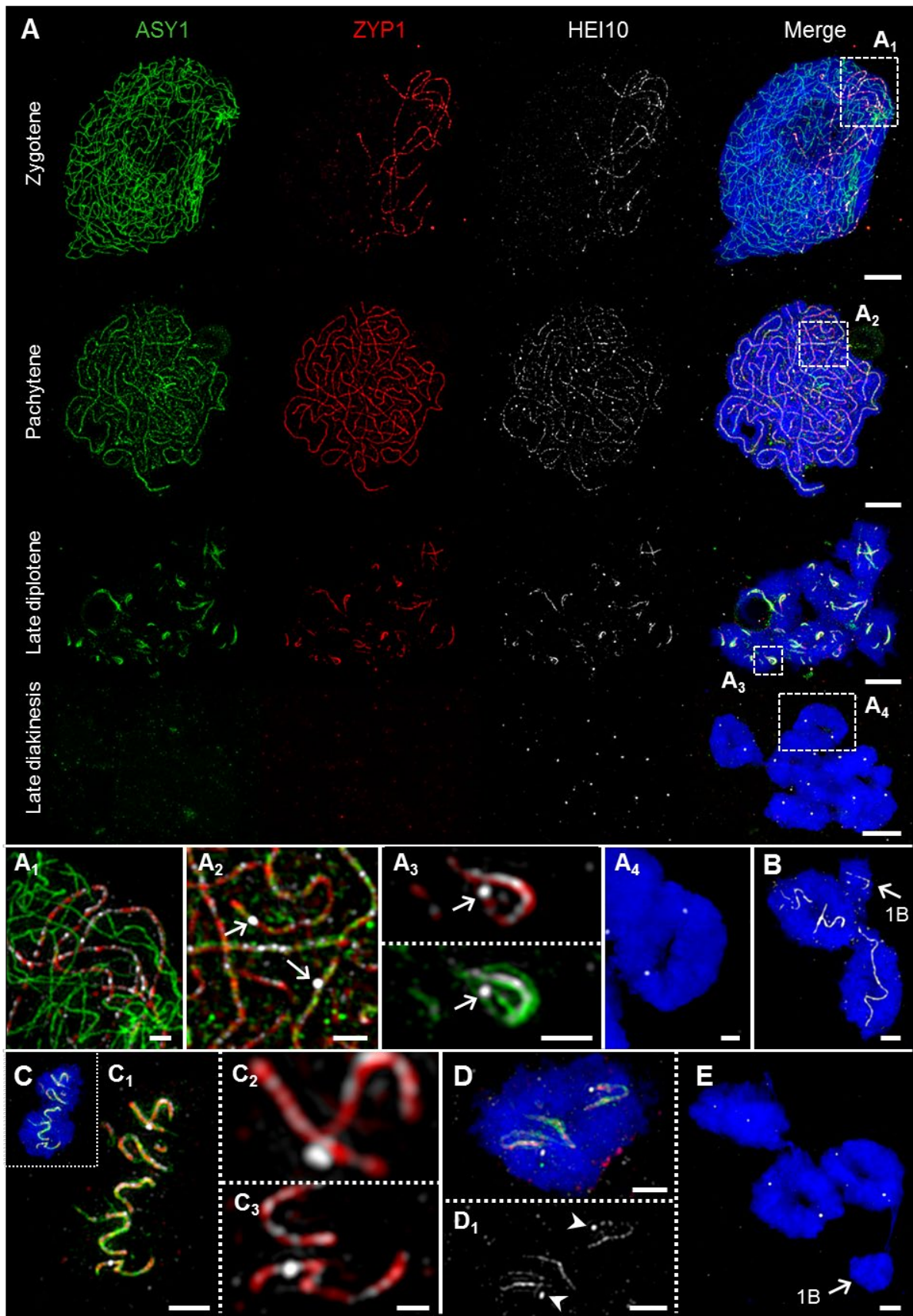


Figure 11 | HEI10 behaviour in comparison to ASY1 and ZYP1 dynamics during prophase I. The images A₁-A₄ show enlarged regions delimited by dashed boxes. Chromatin was counterstained with DAPI. **(A)** Throughout prophase I until late diplotene, HEI10 foci follow the dynamics of ZYP1. At zygotene, HEI10 foci are present at the central region of the SC marked by ZYP1. At the end of synapsis during pachytene single HEI10 foci become more prominent. At diplotene, the progression of SC disassembly causes the fragmentation of the SC, and

HEI10 can be detected either as numerous low-intensity foci organized along the central element, or as a few prominent foci most likely corresponding to crossover- fated recombination sites. At late diakinesis, ASY1 and ZYP1 disappear, but HEI10 proteins remain as distinct spots at the potential recombination sites. Bars = 5µm. **(A₁)** At zygotene, HEI10 foci occur exclusively in SCs marked by ZYP1. Bar = 1µm. **(A₂)** At pachytene, individual HEI10 foci become more pronounced and clearly distinguishable (arrows). Bar = 1µm. **(A₃)** Low-intensity HEI10 foci along the residual central region of the SC exist in parallel to a pronounced HEI10 focus (arrow) indicating a recombination site at late diplotene. ASY1 threads coil up at this position. Bar = 1µm. **(A₄)** An A chromosome ring bivalent at late diakinesis with two HEI10 spots marking the potential sites of crossovers. ASY1 and ZYP1 signals are no longer detectable. Bar = 1µm. **(B)** Two A chromosome ring bivalents accompanied by a single B chromosome (arrow) at diplotene. Similar to the A chromosomes, HEI10 threads are evident on the self-paired B chromosome. Bar = 2µm. **(C)** Typical convoluted SC structures marked by ASY1, ZYP1 and HEI10 on an A bivalent at diplotene. **(C₁)** The enlarged view of (C) shows the colocalization of the three proteins at the fragmented SC, and indicates the ongoing SC disassembly. Bar = 2µm. **(C₂, C₃)** Besides weak HEI10 foci along ZYP1, two pronounced HEI10 spots are visible at higher magnification. The localization of such foci towards the bivalent connection sites at late diakinesis (A₄, D) suggests the staining of crossovers. Note, the HEI10 spot in (C₂) is localized slightly apart from the central element of the SC marked by ZYP1. Bar = 2µm. **(D, D₁)** Distinct HEI10 spots (arrowheads) on an A chromosome ring bivalent at late diplotene. Both spots are not located on SC residues and likely correspond to the HEI10 signals exclusively evident at late diakinesis (A₄). Bar = 2µm. **(E)** Three A bivalents at late diakinesis show two HEI10 foci each. Instead, the single B chromosome (arrow) does not contain any HEI10 spots. Bar = 2µm.

1.4.8 Centromeres and the SC structure of rye A and B chromosomes do not differ

The proper function of centromeres and the SC are crucial for the correct segregation of chromosomes at meiosis and pollen mitoses. As rye A and B chromosomes show different segregation behaviour during the first pollen mitosis, the centromeres and the SC structure of both type of chromosomes were compared. An earlier study by Banaei-Moghaddam et al. (2012) showed that all A centromere sequences can be found in the centromeres of Bs, but the higher sequence organization of both types of centromeres differs. FISH using the centromere-specific probe Bilby showed, as previously described, that the meiotic B centromeres exhibit an extended and diffuse Bilby signal distribution compared to those of As (Banaei-Moghaddam et al. 2012). Taking the signal size of an antibody recognising the centromere-specific histone H3 variant CENH3 as a parameter to determine centromere activity (Wang et al. 2018), the simultaneous labelling of meiocytes by Bilby and anti-CENH3 revealed that the actual size of active centromeres does not differ between A and B chromosomes (Figure 12).

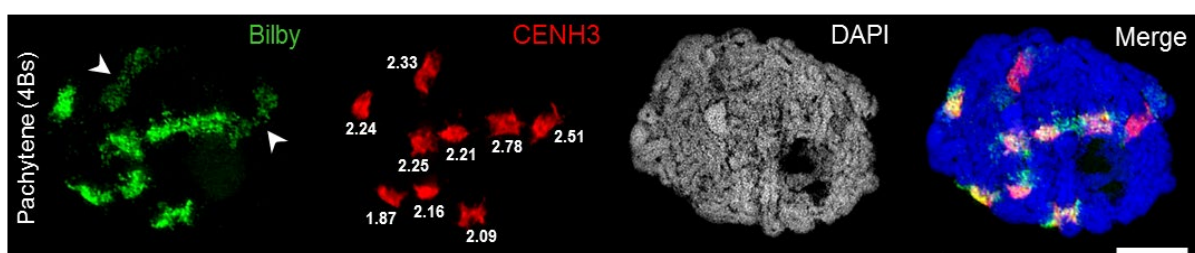


Figure 12 | Bilby repeats and CENH3 identify the centromeres of A and B chromosomes. A rye meiocyte containing four Bs at zygotene shows the pairing of all centromeres labelled with Bilby and CENH3 at the centromeric regions. The brighter Bilby signals reflect the seven (peri)centromeric regions of the A bivalents. In contrast, the Bilby signals of the Bs (arrowheads) appear darker and less condensed. Interestingly, this difference is not reflected by the CENH3 labelling implying that the actual size of active centromeres does not

differ between A and B chromosomes. The global chromatin staining with DAPI reveals the chromatin-free SC structures. Bar = 5 μ m.

Rye Bs may occur in even or odd numbers ranging from 1 to 8 (Jones et al. 1982). Analysis of the SC structure revealed that ASY1 becomes loaded onto the B chromosome axis at early prophase I irrespective of the presence of a homologous pairing partner (Figure 13A, Figure 14). In case of 2Bs, a normal SC assembly accompanied by the incorporation of ZYP1, occurs at pachytene. However, the SC formation of Bs present in odd numbers may be impaired. Beside the absence of ZYP1 and/or ASY1 loading (Figure 14A₁, Figure 14B₁), the intrachromosomal SC formation ranging from small clusters (Figure 14D₁) to long SC stretches (Figure 13C, Figure 14C₁) was observed on univalent Bs. When prophase I progresses, B chromosome SCs show the same twisted structure evident on As (Figure 9B, B₂, Figure 13C, D). No differences between inter- and intrachromosomal SCs were observed. At diplotene, the SC disintegration, indicated by the retraction of ASY1, results in transient ASY1 threads, SC fragmentation and the subsequent formation of residual ball-like SC structures (Figure 9A₁₋₂, Figure 13D, Figure 13E). The immunolocalization of NSE4A and HEI10 on Bs showed the colocalization of both proteins with ZYP1, and followed the above-mentioned SC dynamics (Figure 9, Figure 10). Nevertheless, on univalent Bs HEI10 disappeared completely at the end of diakinesis, indicating the absence of class I crossovers at synapsed Bs (Figure 11E).

Taken together, these results showed that Bs form similar SCs as As. In addition, the SC formation of Bs may be impaired depending on the B chromosome number per meiocyte.

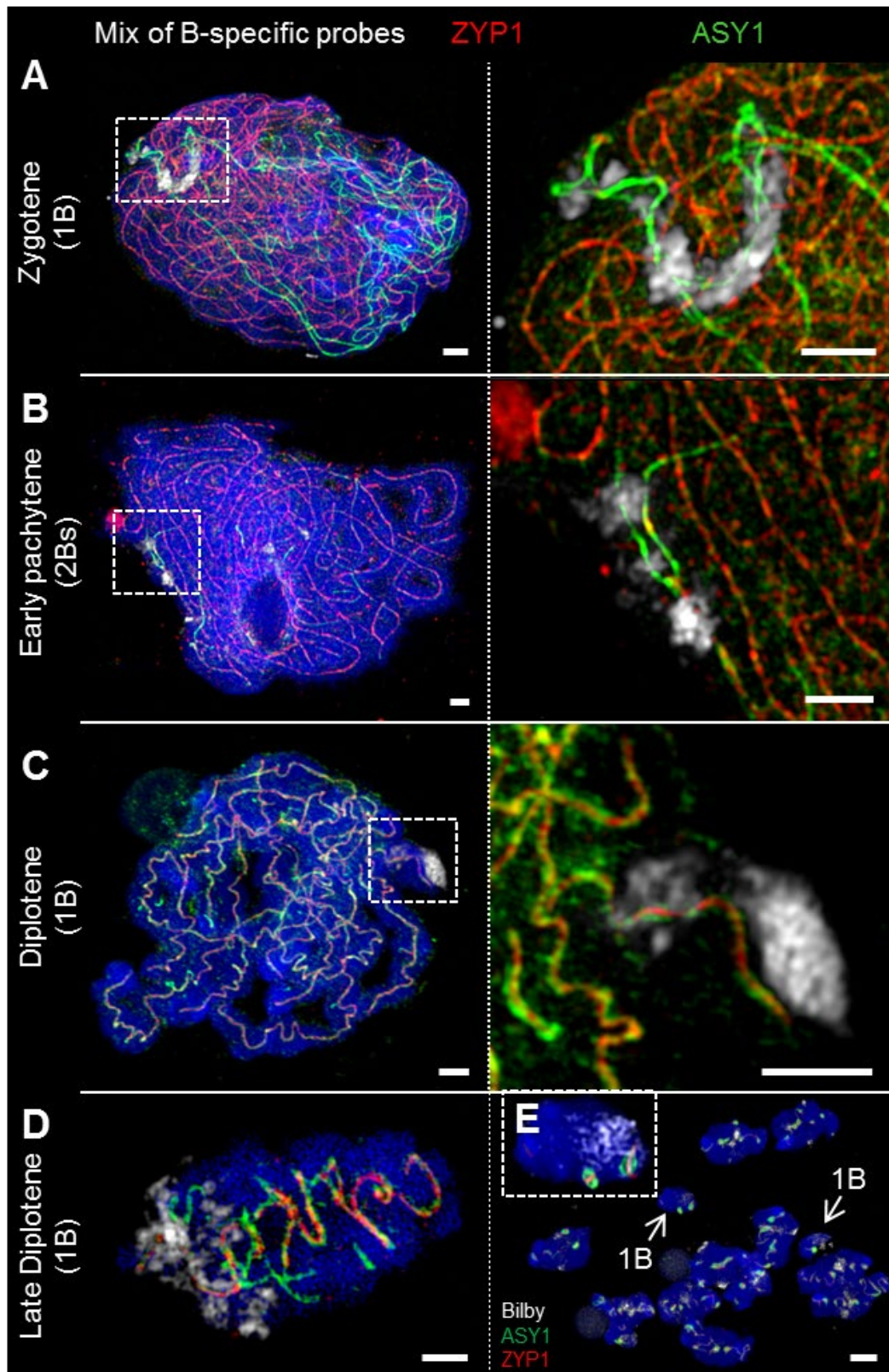


Figure 13 | The SC structure of B chromosomes does not differ from that of As. Bs were detected by means of a B-specific FISH probe mix. The chromatin was counterstained with DAPI. **(A)** At zygotene, ASY1 is associated with the B chromosome axis similar as on As. The loading of ASY1 is independent of the B chromosome number, thus also occurring at single Bs performing intrachromosomal synapsis. Bars = 2 μ m. **(B)** In case of 2 Bs, normal synapsis of both chromosomes occurs. The enlargement shows a not yet synapsed B chromosome region indicated by two separate ASY1 strands with brighter fluorescence at early pachytene. Bars = 5 μ m. **(C)** In absence of a homologous pairing partner, intrachromosomal synapsis of single B chromosomes takes place. The ASY1 and ZYP1 staining is identical to that of A bivalents during diplotene. Bars = 2 μ m. **(D)** Similar to that of

A bivalents at late diplotene (Figure 7A₄), B bivalents show the retraction of ASY1 strands from the SC during desynapsis. Bar = 2µm. **(E)** Two meiocytes (mixed by squashing) of rye carrying 1B chromosome each at diakinesis. Both Bs (arrows) can be distinguished from As by smaller size. The inset shows one of the B chromosomes with two typical ball-like residual structures of the SC complex. Bar = 5µm.

1.4.9 Prophase I pairing configurations of B chromosomes depend on their number

The quantification of the meiotic pairing within PMCs of rye plants containing different numbers of Bs made it possible to distinguish various types of B chromosomes' behaviour. In case of one B chromosome, ASY1/ZYP1-positive SC fragments reflecting self-synapsis were detected on all examined univalents (n=10). Plants with 2Bs (n=12) showed regular SC assembly and bivalent formation. Only in one case, two univalents were formed and fragmented SCs were observed. Plants carrying 3Bs (n=94) revealed three modes of SC formation during prophase I. Namely, 84.0% of the analysed meiocytes formed one bivalent and one univalent (Figure 14A-C), in 12.8% a clusters of all 3Bs was formed, and only 3.2% of the cells contained three univalents (Figure 14D). In case of plants carrying 4Bs (n=121), the following configurations were observed: 64.5% of meiocytes contained only bivalents, in 29.7% multivalents joining up all Bs were formed, and 5.8% had one bivalent plus two univalents.

Altogether, the data demonstrate that the number of B chromosomes strongly affects their pairing configurations.

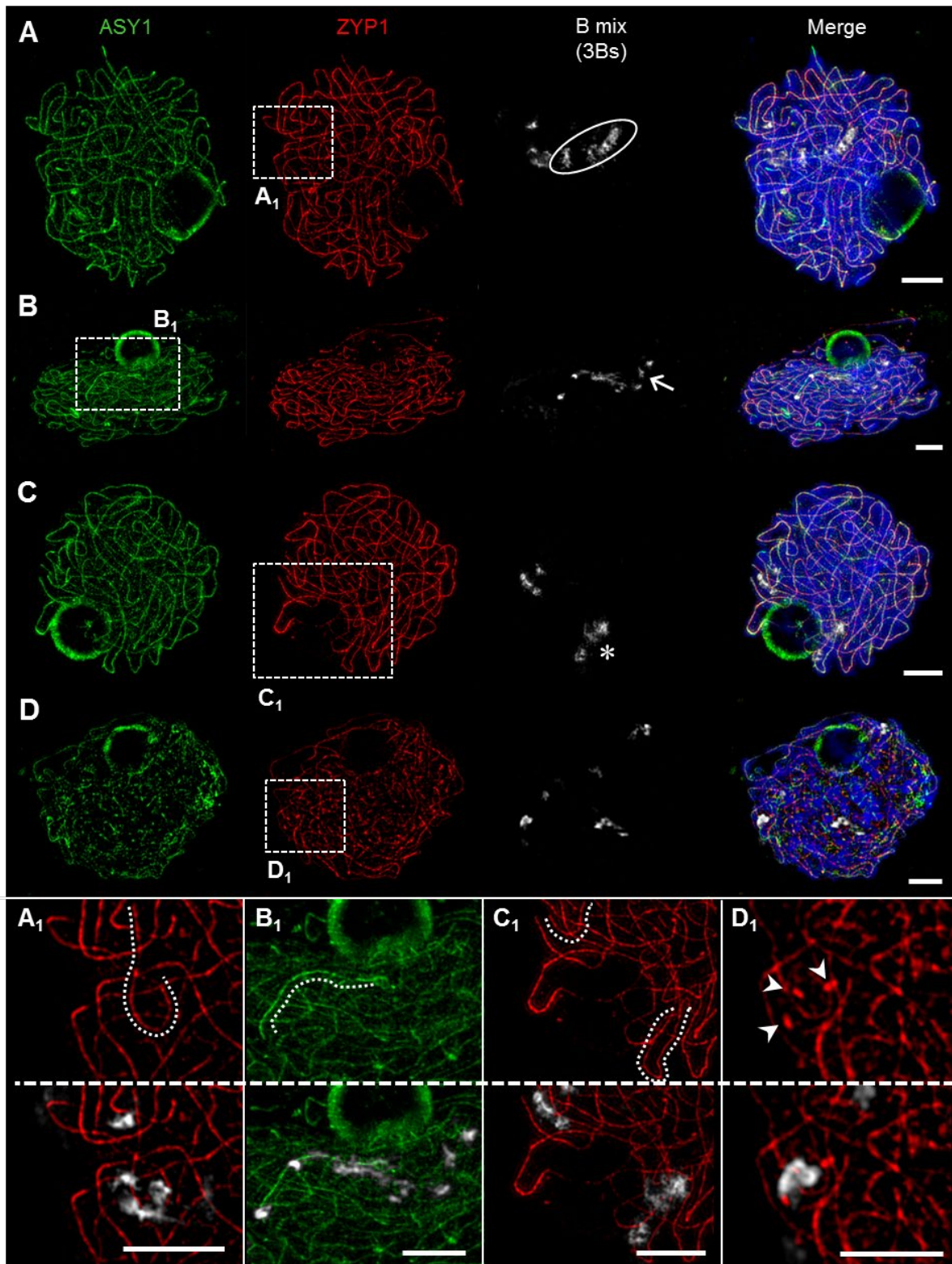


Figure 14 | Pairing configurations of B chromosomes at pachytene. 3Bs were detected by means of a B-specific FISH probe mix, SCs with ASY1- and ZYP1-specific antibodies. Three different types of B chromosome arrangement were observed. Chromatin was counterstained with DAPI. **(A)** The Bs form one bivalent and one univalent. The bivalent (**A₁**) shows normal synapsis, whereas the univalent B (circle) did not show any labelling by ASY1 or ZYP1 indicating the absence of a SC. **(B)** One B univalent and one B bivalent associate. While the bivalent (arrow) performs normal synapsis indicated by ZYP1, the univalent (**B₁**) was exclusively loaded with ASY1. **(C)** Formation of one B bivalent and one B univalent. The bivalent (asterisk) performs normal synapsis, while the univalent B shows intrachromosomal synapsis reflected by ZYP1 labelling (**C₁**). **(D)** Three B univalents show a fragmented SC formation (**D₁**, arrow heads). Bars = 5 μ m.

1.5 Discussion

1.5.1 The dynamics of ASY1 and ZYP1 indicates the SC assembly and disassembly during prophase I

Previous studies demonstrated that antibodies raised against the two SC proteins ASY1 and ZYP1 of *A. thaliana* are suitable for the detection of orthologous proteins in other plant species, e.g. in barley and rye (Mikhailova et al. 2006, Phillips et al. 2008, Phillips et al. 2010). Here, we employed anti-ASY1 and anti-ZYP1 to investigate homologous pairing events during prophase I in rye utilizing SIM. Synapsis is initiated in rye at telomeres and interstitial sites as previously reported (Abirached-Darmency et al. 1983). Once synapsis occurred, the ASY1 signal intensity decreases severely. It cannot be ruled out that this observation stems from a decreased accessibility of the ASY1 antibodies to the epitopes as a consequence of the SC assembly and chromatin compaction (Golubovskaya et al. 2006). However, a weak ASY1 staining in the nucleoplasm is detectable at early pachytene, suggesting that ASY1 is partially removed from the AEs/LEs during synapsis. Similar observations were reported for various other species. In rice, maize and yeast the signal intensity for the orthologues PAIR2, ASY1 and HOP1, respectively, also significantly decreases during synapsis (Smith et al. 1997, Nonomura et al. 2006). However, in contrast to these species, in rye ASY1 is not removed from the axes during pachytene. It remains at the SC until its disintegration, resembling the dynamics described for the orthologous proteins of barley and *Arabidopsis* (Armstrong et al. 2002, Phillips et al. 2012). Previous studies, using rye synaptic mutants as experimental material, reported that ASY1 and ZYP1 can undergo pre-assembly. It was hypothesized that these double layer tracts could be formed in wild-type rye well before synapsis and later could interact to form the SC (Mikhailova et al. 2006, Phillips et al. 2008). In our study, we did not observe such a pre-alignment of SC fragments in wild-type rye meiocytes carrying accessory B chromosomes, but ASY1 located exclusively to the AE/LE elements in As and Bs. At zygotene, ZYP1 was incorporated at the CR of the SC in a zipper-like manner. Moreover, a diffuse staining of yet unassembled ZYP1 within the nucleoplasm was found, which decreased when synapsis has finished. These deviating observations could be partially due to the different rye genotypes studied, as well as to different specificity of ASY1 and ZYP1 antibodies used in present (anti-maize) and previous (anti-*Arabidopsis*) studies. Certain inconsistency in results could also arise due to different slide preparation techniques (e.g., the fixation in 4% vs. 2% paraformaldehyde), as well as due to substantially higher resolution and detection sensitivity achieved by SIM, which enables more precise observations compared to confocal laser scanning microscopy. Indeed, during the progression of prophase I, we observed remarkable structural chromatin changes. At the end of pachytene, the SC adopts a twisted structure, consistent with previous studies (Fedotova et al. 1989, Mikhailova et al. 2006, Simanovsky et al. 2014). This coiling was not the result of helical winding of the chromosomes, because the SC structures did not form

symmetrical spirals, but instead was a result of contracting chromatin. According to the 'dynamic matrix model', coiled solenoids bind to interconnected matrix fibres. During condensation, the matrix fibres may act in an actin/myosin-like manner, whereby the parallel arrangement of the matrix favours shortening and thickening of the chromosomes. We propose that a similar mechanism could occur in meiotic chromosomes. But in contrast to mitosis, meiotic chromosomes need to condense and separate two paired homologues. Therefore it is plausible, that the SC does not only provide the platform for recombination but it may also link both homologues to synchronize the condensation process. By tethering chromomeres of all chromatids to a common axis, a random chromatin organization may be prohibited. Given that chromosomes condense during complete prophase I, a successive compaction of the chromomeres is reached. As a consequence of the sterical restrictions, the tension along the paired homologues increases and, thus, causes the bending of the SC at pachytene. At late pachytene/diplotene, when the tension increases further, a local repulsion of single LE occurs, apparent by the retraction of ASY1 threads that form transient loops. Similar dynamic structures of ASY1 were recently described in meiotic chromosomes of wheat and barley (Colas et al. 2017). During these processes, ZYP1 disappears from the CR and disintegration of the SCs takes place. Through disassembly of the SC, both homologues become separated piecewise. Possibly, the ball-like SC structures of ZYP1 and ASY1 that are being formed at this stage serve the purpose of counteracting the tension throughout diakinesis. Hence, a stabilization of the bivalents is achieved and the premature separation of recombination site and centromeres may be prevented. Last traces of the SC are lost at the end of diakinesis, when chiasmata and centromere formation are fully accomplished.

The persistence of SC components at centromeres, additionally to the recombination sites during their disassembly in late prophase I, has also been described in yeast and *Drosophila*, mouse and human (Qiao, Chen et al. 2012, Kurdzo and Dawson 2015). The finding that the SC components accumulate also at plant centromeres during the SC disassembly indicates a conserved phenomenon, which is needed to ensure proper meiotic chromosome segregation.

In many organisms, including protists, fungi, animals and plants, the aggregation of SC-related material to form so-called polycomplexes was reported (Zickler et al. 1999). Given our finding that the formation of ball-like structures directly follows SC disassembly, we conclude that they are not SC-independent aggregations of SC-related proteins as present in polycomplexes (Zickler et al. 1999). Despite intense studies, polycomplexes have never been reported in prophase I stages of rye. Therefore, we exclude this option.

1.5.2 The SMC5/6 complex δ -kleisin NSE4 seems to be required for synapsis and recombination

NSE4 is the crucial non-SMC δ -kleisin component of the SMC5/6 complex, and therefore can be considered as a reliable marker for its localization (Palecek et al. 2006). In *A. thaliana*, two orthologues, *Nse4A* and *Nse4B*, were identified. Both genes are expressed in different tissues and are required to realize complete fertility. However, *Nse4A* is the more essential gene (Watanabe et al. 2009, Zelkowski et al. 2019). Despite the increasing knowledge about SMC5/6 of non-plant eukaryotes (Verver et al. 2016), the immunohistochemical analysis of the NSE4 distribution and its dynamics during meiosis in plants was challenging so far due to the lack of specific antibodies. In the present study, we localized for the first time the SMC5/6 complex subunit NSE4 in the prophase I of rye, using antibodies raised against NSE4A of *A. thaliana* (Zelkowski et al. 2019). The detection of NSE4 from early zygotene until late diakinesis is similar to the localization pattern found in mammalian meiosis (Verver et al. 2016). In rye, NSE4 co-localizes with the TF protein ZYP1, indicating the restriction of NSE4 to synapsed chromosomes. Consistent observations were described in mice, where a SYCP1-dependent loading of SMC6 occurs (Gomez et al. 2013), and in human, where SMC5/6 localizes to synapsed chromosome axes (Verver et al. 2014). By its recruitment to synapsed axes, the SMC5/6 complexes might facilitate the formation and/or stabilization of synapsis in rye. Moreover, in *C. elegans*, fission and budding yeasts the SMC5/6 complexes are involved in homologous recombination and proper chromosome segregation (Pebernard et al. 2004, Bickel et al. 2010, Wehrkamp-Richter et al. 2012, Copsey et al. 2013, Lilienthal et al. 2013, Xaver et al. 2013). Our observed localization pattern of NSE4, especially at the late ball-like SC structures during diakinesis, might also indicate a function of SMC5/6 complexes in homologous recombination of rye.

The involvement in synapsis has also been proven for the meiotic α -kleisin of the SMC family complex cohesin. Its presence in prophase I was shown in plants such as *A. thaliana* (Cai et al. 2003), tomato (Qiao et al. 2011), rice (Zhang et al. 2006, Shao et al. 2011) and, in addition, its localization with ZYP1 was proven in *Luzula* (Ma et al. 2016). These findings support the importance of SMC complex proteins for proper meiosis.

1.5.3 HEI10, a marker for class I crossovers in rye?

In mice, the two RING-family E3 ligases HEI10 and RNF212 were shown to be essential for recombination (Reynolds et al. 2013, Qiao et al. 2014). In contrast to mammals, plants possess only one member of the broad RNF212/HEI10 protein family (Toby et al. 2003, Ward et al. 2007, Chelysheva et al. 2012, Wang et al. 2012, Rao et al. 2017). During meiosis of *A. thaliana* and rice, HEI10 proteins label the sites of class I crossovers (Chelysheva et al. 2012, Wang et al. 2012, Ziolkowski et al. 2017).

Our study provides evidence that antibodies raised against HEI10 of *O. sativa* (Wang et al. 2012) detect the corresponding proteins in rye. In rice, a punctate pattern of HEI10 occurs in early leptotene. Importantly, a linear distribution of signals alongside of ZEP1 (ZYP1 orthologue of rice) can be observed during synapsis, but disappears at diplotene. From late pachytene to diakinesis, additional prominent HEI10 foci were localized at the chromosomes, presumably marking class I crossover sites (Wang et al. 2012). Similar results were obtained in *A. thaliana* (Chelysheva et al. 2012). The localization of the orthologous rye protein found in our study differs from those reports, as HEI10 foci were not detectable before the onset of ZYP1 installation/loading. Thus, a crucial role of HEI10 at pre-synaptic events of recombination seems to be unlikely in rye.

Recent studies in *Sordaria* and mice revealed a similar localization pattern of HEI10 as seen in rye, by being associated only with SCs, although HEI10 is not a SC component. In both species, it was shown that HEI10 becomes engaged after the Mer3/MLH- and/or DMC1-mediated homologue pairing, and seems to regulate post-synapsis steps of meiotic recombination, e.g. the formation and turnover/disappearance of recombination complexes, *via* a SUMO-ubiquitin switch (Storlazzi et al. 2010, Qiao et al. 2011, De Muyt et al. 2014). In *Sordaria*, HEI10/MSH4 foci were classified by morphology and dynamics, and proposed to mark three different types of recombination complexes: early and late SC-associated nodules, as well as non-nodule associated interactions (De Muyt et al. 2014). Previous electron microscopy studies characterized two morphologically different types of recombination nodules: one at early and the second at late pachytene of rye (Abirached-Darmency et al. 1983). Given the lower resolution of SIM as compared to electron microscopy, the differentiation of these nodule types during pachytene of rye is not feasible. Nevertheless, it is tempting to assume that our observation of high fluorescence intensity HEI10 foci from pachytene on corresponds to such recombination nodules, whereas the weak foci represent axis-associated HEI10 involved in the SUMO-ubiquitin switch. This assumption is supported by the distinct HEI10 foci present at late prophase I. During SC disassembly at diplotene, both types of HEI10 foci are clearly distinguishable, i.e. weak signals associated with the remaining SC fragments, as well as prominent foci located towards the end of the bivalents either directly on, or in close proximity to the SC. After the complete disintegration of the SC at the end of diakinesis, only one prominent HEI10 spot per chromosome arm still persists. The mean number of those foci (13.1; SD=1.57; n=50 cells) matches the observed number of chiasmata in rye (Jones 1967, Kalyuzhnaya et al. 2005). Therefore, we assume that HEI10 may be the first recombination marker identified in rye, most likely labelling class I crossovers.

1.5.4 A model for the behaviour of rye chromosomes during prophase I

Despite extensive studies on the mechanisms of SC establishment and disassembly in various organisms, it is still challenging to decipher the complex events underlying the SC formation and recombination.

Based on our findings, we propose a model for the homologous chromosome behaviour during prophase I based on the observed dynamics of ASY1, ZYP1, NSE4A and HEI10 (Figure 15). At leptotene, the AE/LE-associated protein ASY1 is loaded onto the chromosome axes prior to SC formation. As synapsis occurs, ZYP1, NSE4A and HEI10 become incorporated at the central region of the SC. Further, the ongoing condensation of the chromatin throughout prophase I leads to the coiling of the SC at late pachytene. The following disintegration of the SC is accompanied by the retraction of ASY1 from the central region, most likely as a result of the increasing tension on chromatin caused by condensation. At positions where both ASY1 threads are retracted, the CR is dissolved and ZYP1, NSE4A and HEI10 are no longer detectable (Figure 15, enlarged). As a consequence, SC fragmentation and the formation of ball-like structures can be observed at early diakinesis. Additionally to weak HEI10 signals on the remaining SC, distinct foci at both ends of the bivalent reflecting the sites of crossover are detectable. Colocalizing ASY1, ZYP1 and NSE4A proteins are also present in between the homologous centromeres. However, HEI10 is missing here, indicating the absence of crossovers. The presence of ASY1, ZYP1 and NSE4A in between of the centromeres seems to be required to keep tension between the centromeres, when spindle fibres attach to separate both homologues. At late diakinesis, the SC disassembly is completed as indicated by the disappearance of ASY1, ZYP1 and NSE4A at the crossover sites as well as at the centromeres. Only the class I crossovers remain marked by HEI10.

In the proposed model, we show that ASY1, ZYP1 and NSE4A and HEI10 seem to be involved not only in the formation of structures important for synapsis and recombination. They are also required for SC disassembly during chromatin condensation and for proper homologue separation.

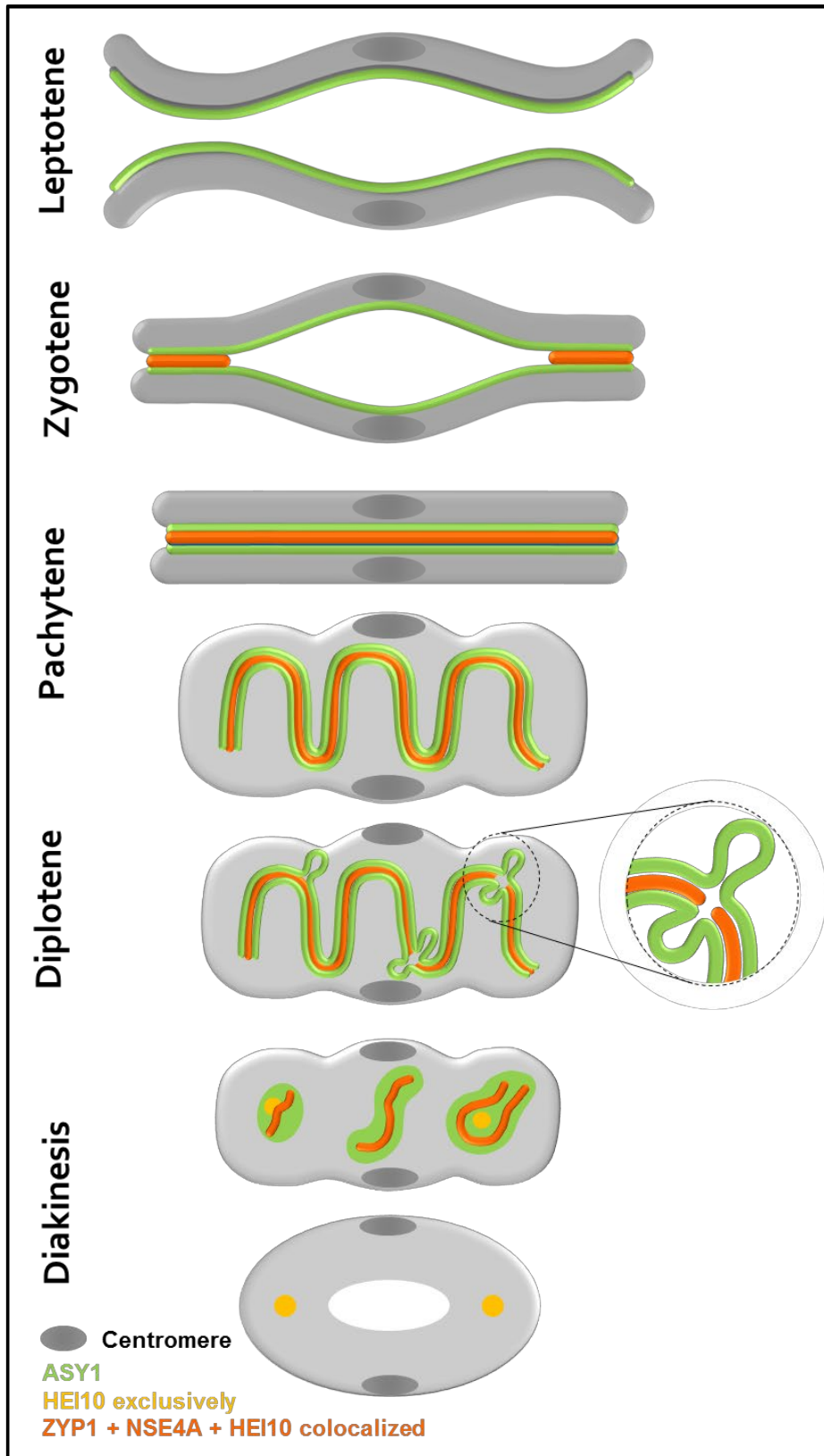


Figure 15 | Scheme showing the behaviour of two homologous chromosomes, together with the localization of the SC proteins ASY1, ZYP1, NSE4A and HEI10 during prophase I. Before synapsis, ASY1 is loaded along each chromosome axis at leptotene. During zygotene, the assembly of the SC occurs at multiple sites of the homologues. Thereby, ZYP1, NSE4A and HEI10 are incorporated at the central region. Synapsis completes at the beginning of pachytene visible by the tripartite structure consisting of two lateral elements enclosing the central region. The proceeding degree of condensation observed throughout prophase I, is accompanied by a convolution of the SC at late pachytene. At diplotene, the onset of SC disintegration is accompanied by the

retraction of ASY1 forming transient loops. At positions, where both ASY1 threads are retracted from the SC, ZYP1 disappears (enlarged). The progression of the SC degradation results in fragmented ball-like SC structures at diakinesis in both chromosome arm regions, but also in between both homologous centromeres. In addition to the CR-associated HEI10 labelling, distinct HEI10 foci marking crossover sites are evident at the arms but missing in between the centromeres. At the end of diakinesis, the SC disassembly is completed, and ASY1, ZYP1 and NSE4A disappeared completely. Only the sites of crossovers remain clearly marked by HEI10.

1.5.5 B chromosomes behave like A chromosomes during prophase I

For decades, the origin of rye B chromosomes remained enigmatic. The application of next generation sequencing revealed that Bs originate from several A chromosome fragments and contain an accumulation of various repeats and insertions of organelle DNA (Martis et al. 2012). Moreover, it was shown that Bs possess their own evolutionary pathways and that they accumulate high copy sequences, allowing identifying rye Bs during prophase I by FISH (Klemme et al. 2013). In our study, we aimed to investigate two different B isoforms, the standard B and a NDJ-deficient B variant lacking the subtelomeric region of the long arm. Recent study by Klemme *et al.* (2013) identified the high-copy sequence composition of the standard rye B chromosomes and revealed that the B-specific sequences can be found primarily in the subtelomeric region of the long arm including the nondisjunction control region. Our comparative analysis of various B-specific repeats using FISH showed that most of this region was lost in the NDJ-deficient B isoform of our material. In this context, two processes could have caused such a loss of the NDJ region. First, a deletion of only the subtelomeric fragment including the NDJ occurred. Second, the complete NDJ-containing distal part of the long arm of the B chromosome was deleted, and subsequently the resulting acentric fragments were lost. At the breaking point of the (sub-)terminal deletion, we observed a rearrangement of two repeat clusters (Sc55, Sc63). The observation that the subtelomeric high-copy sequence Kulla of the standard B was missing on the NDJ-deficient B strongly suggests that the complete terminal segment of the long arm was lost. As Sc55 and Sc63 are still detectable, the NDJ region of standard Bs is composed only of DNA located distal from these two repeat clusters. Nevertheless, *Arabidopsis*-type telomeric FISH signals were detectable. Since the pioneering work in maize of Barbara McClintock in the late 1930s, it is known that broken chromosomes lacking their natural ends are highly unstable in gametophytes and endosperm and cycle through repeated breakage-fusion bridge events (McClintock 1931, McClintock 1938, McClintock 1941). However, in the embryo occasionally a repair process, termed by her 'chromosome healing', occurs to stabilize such chromosomes (McClintock 1939, McClintock 1941). It is very likely that the telomeres detected on the broken arm of the NDJ-deficient B are a result of such a *de novo* telomere formation and thus stabilize the B to prevent its elimination. Unfortunately, the density of the remaining FISH-detectable repeats was insufficient to allow a reliable tracking of the NDJ-deficient B during prophase I.

Therefore, we excluded this material from further meiotic studies and continued our study only with standard B chromosome material.

The B-specific subtelomeric repeat Kulla allowed for the first time to investigate *via* FISH whether B chromosomes participate in one of the early events of meiosis, which is the formation of the 'bouquet' at the leptotene/zygotene transition during prophase I. Despite the diverse details of meiosis, nearly all organisms studied so far retained the telomere 'bouquet' in their meiotic program, implying an important role of this clustering (Harper et al. 2004, Scherthan 2007, Zickler et al. 2016). Only *C. elegans* and *A. thaliana* are known to not form a *bona-fide* 'bouquet'. However, telomere attachment to the nuclear envelop and loose clustering are still present (Armstrong et al. 2001, Roberts et al. 2009, Rog et al. 2013). From studies of haploid rye and trihaploid wheat it is known, that the 'bouquet' formation does not require interactions between homologous chromosomes (Wang 1988, Jong et al. 1991, Santos, Jiménez et al. 1994). Moreover, only telomeric or subtelomeric sequences are shown to be responsible for the formation of the 'bouquet' cluster, independent from their localization within the chromosomes, i.e. interstitial or at the physical end (Carlton et al. 2002, Sadaie et al. 2003, Voet et al. 2003). Since Bs harbour the same *Arabidopsis*-type telomeres as the A chromosomes, it is not surprising that our analysis revealed that rye Bs, despite their different number of occurrence, are able to participate in the 'bouquet'.

By combining antibodies against ASY1, ZYP1, NSE4A and HEI10 with B-specific FISH probes, we analysed the SC composition of Bs. Previous EM studies of the SC formation in various species revealed substantial differences between the meiotic pairing of As and Bs, dependent on their number (Jenkins 1985, Świtoński et al. 1987, Kolomiets et al. 1988, Shi et al. 1988, Santos et al. 1993). Moreover, studies of the Chinese racoon dog demonstrated diverging SC structures of As and Bs. Here, during pachytene the SC axes of the Bs are significantly denser than those of the As. Depending on the number of Bs, bivalents and multivalents may be formed. When three Bs are present in parallel, the alignment of all three SC axes may occur (Shi et al. 1988). For single rye Bs it was shown, that in contrast to 2Bs, univalents and higher B chromosome numbers induce either intrachromosomal SCs or possess segmental pairing resulting in multivalents. In contrast to the Chinese racoon dog, SCs of rye Bs formed by more than two AEs/LEs have never been observed (Santos et al. 1993). In rye with increasing B numbers, altered SC formation occurs unrelated to the mean number of A-located chiasmata (Diez et al. 1993), while in *Crepis capillaris* SC irregularities of As correlate with defective A chromosome pairing when 4 Bs are present (Demidov et al. 2009). Our study revealed that in general the SC composition of Bs does not differ from that of As, as proven on meiocytes containing 2Bs. All four investigated proteins localize to the SCs of Bs and undergo the same dynamics as described for As. Despite their different nature compared to As, rye Bs apparently

utilize the same protein structures to ensure meiotic pairing and proper chromosome condensation. Rye plants comprising either less, or more than 2Bs also show a similar SC composition independent of segmental or intrachromosomal pairing. Obviously, by producing the same SC structures the Bs try to fulfil the pairing requirements. Similar observations were described also for univalent A chromosomes, e.g. in barley, lily, wheat and maize (Gillies 1974, Holm 1977, Gillies 1981, Hobolth 1981). Only in very rare cases, the formation of SCs failed and either ASY1 only, or none of the proteins were detectable. Previous studies suggested that the intrachromosomal pairing is a non-homologous process and has no genetic consequences due to the lack of recombination (Santos et al. 1993).

The prophase I meiotic pairing configurations of rye Bs were found to be genotype-dependent, and are linked to the efficiency of B chromosome transmission to the next generation. While bivalent formation secures the successful transmission of Bs, the uni- and multivalents have much lower transmission rate (Jimenez et al. 2000). The rye variety 'Paldang' we analysed in present study has a B transmission rate of about 20% (Romera et al. 1989).

In summary, we conclude that A and B chromosomes share the same processes and establish similar SC structures to perform pairing in prophase I.

1.6 Summary

During prophase I, large-scale reorganization of the nucleus occurs to enable homologous pairing, recombination and correct segregation of the chromosomes. In many organisms, homologous pairing is accompanied by the formation of a telomere ‘bouquet’ and followed by the assembly of the synaptonemal complex (SC), a scaffold to connect homologous chromosomes along their lengths. Recent studies in various organisms ranging from yeast to mammals identified several proteins involved in SC formation. However, the process of SC disassembly remains largely enigmatic. In this study, we determined the structural changes during SC formation and disassembly in rye meiocytes containing accessory (B) chromosomes. During this study, we focused on two different B isoforms, namely the standard B and a NDJ-deficient B variant lacking the subtelomeric region of the long arm. Our FISH analyses revealed a rearrangement of the two repeat clusters Sc55 and Sc63 at the breaking point of the (sub-)terminal deletion. As the density of the remaining FISH-detectable repeats was insufficient for a reliable tracking of the NDJ-deficient B during prophase I, we excluded such material and continued with standard B chromosome material only. The use of super-resolution microscopy (3D-SIM) combined with immunohistochemistry and FISH allowed us to monitor the ultrastructural changes during prophase I. Visualization of the proteins ASY1 and ZYP1 revealed an extensive SC remodelling during prophase I. For the first time, we detected NSE4A and HEI10 in the central region of the rye SC. The analysis of the dynamics of these four proteins demonstrated that the SC disassembly is accompanied by the retraction of the lateral and axial elements from the central region of the SC. In addition, late diakinesis was characterized by SC fragmentation and the formation of ball-like SC structures. We show here that rye B chromosomes participate in the ‘bouquet’ formation and that their SC composition does not differ from that of the A chromosome complement. Our investigation indicates that the dynamic behaviour of the studied proteins is essential for SC formation, synapsis and SC degradation. Our data demonstrate that these proteins are functionally engaged during SC disassembly and chromosome condensation to ensure proper recombination and homologue separation.

1.7 Outlook

The data derived from this study imply subsequent questions and topics to be addressed in future:

1. The approach used in the present study needs to be applied in other model organisms, e.g. *A. thaliana*, *Caenorhabditis elegans*, *Drosophila melanogaster*, for a cross-species (cross-taxa) comparison and deciphering of common mechanisms.
2. Investigation of the chromosome axis dynamics in holocentric species.
3. Further characterization of NSE4a and Hei10 function(s) in rye with a special emphasis on meiotic mutants and plants carrying different numbers of B chromosomes.

2. Fluorescent labelling of *in situ* hybridization probes through the copper-catalysed azide-alkyne cycloaddition reaction

2.1 Introduction

2.1.1 Fluorescence *in situ* hybridization (FISH)

In situ hybridization (ISH) is a fundamental method in modern molecular cytogenetics for the detection of DNA and RNA. In 1969, Pardue and Gall, as well as John *et al.* independently developed this technique to detect nucleic acid sequences on morphologically preserved chromosomes (John *et al.* 1969, Pardue *et al.* 1969). At this time, radioisotopes were the only available labels for the detection of hybridized sequences. Importantly, only sequences purified and isolated *via* conventional methods, e.g. gradient centrifugation, could be used as probes (Lavanaia 1998). Aside from safety problems regarding the use of radioisotopes, ISH was characterized by limited spatial resolution, poor stability of probes and the time-consuming autoradiography. In 1975, Timmis *et al.* applied isotopic ISH in plants for the first time to detect satellite DNA in *Vicia faba* and *Scilla sibirica* (Timmis *et al.* 1975). At the beginning of 1980s, non-radioactive ISH was introduced by several groups (Langer-Safer *et al.* 1982, Manuelidis *et al.* 1982, Rayburn *et al.* 1985). Subsequent improvements on molecular techniques, such as cloning of nucleic acids and availability of better non-radioactive labels (e.g. fluorophores), allowed a tremendous progress in development and applicability of the ISH. Starting from early 1990s, *in situ* hybridization using fluorescence-based detection (FISH) became a powerful tool to investigate not only the genome and chromosome architecture, but also the gene activity at DNA/RNA level (Lavanaia 1998). Currently, all *in situ* hybridization techniques follow a basic principle that is essentially the same as that of Southern hybridization, i.e. the detection of specific sequences on cytological target like metaphase chromosomes, interphase nuclei or extended chromatin fibres by fluorescently labelled short DNA probes (Lavanaia 1998, Speicher *et al.* 2005).

The FISH procedure involves several sequential steps. The first step is the labelling of the DNA probe with either fluorescently-labelled nucleotides (direct labelling) or with modified nucleotides that are rendered fluorescent later on (indirect labelling). Next, probe and target DNA must be denatured to break hydrogen bonds and allow the following hybridization of probe and target. Such denaturation is typically carried out using chemicals and/or heat. Subsequently, target DNA and probes are mixed together to enable access of the probe to anneal to the complementary sequences of the target. In case of indirect labelling, an additional step that uses an immunological detection system to visualize the probe is needed. After several washing steps, fluorescent signals can be detected and acquired using fluorescence microscopy for further analysis (Figure 16).

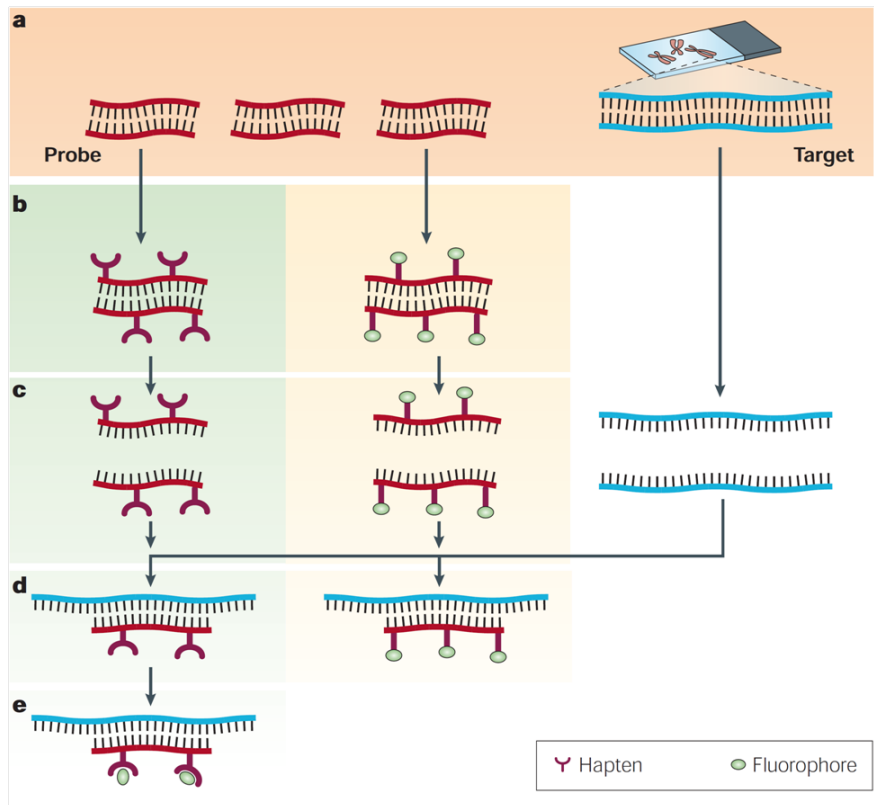


Figure 16 | The principles of fluorescence *in situ* hybridization (FISH). (a) For FISH, a cytological target sequence (blue) and a complementary DNA probe (red) are the basic requirements. (b) Prior to hybridization, the probe has to be labelled with modified nucleotides. Indirect labelling uses nucleotides containing a hapten (green background), whereas direct labelling makes use of modified nucleotides containing a fluorophore (yellow background). (c) Probe and target get denatured, which results in the emergence of single-stranded DNA. (d) Probe and target are combined to allow the annealing of complementary sequences. (e) In case of indirect labelling, a subsequent step visualizing the non-fluorescent haptens *via* an immunological detection system is required. Adapted from (Speicher et al. 2005).

The labelling of DNA probes is commonly performed using nick translation (NT), random-primed labelling and polymerase chain reaction (PCR). While the direct labelling of target nucleic acids is faster, the indirect labelling offers the advantage of signal amplification if multiple antibody layers are used (Speicher et al. 2005). The most important advantage of fluorescence-based ISH over other techniques is the possibility of simultaneous detection of several sequences (Lavania 1998). By the choice of probes, FISH can be categorized into three groups of applications, namely whole chromosome/genome detection, detection of repetitive sequences and single copy sequence detection (Jiang et al. 1994). Especially, the single copy FISH is characterized by poor signal-to-noise ratio and a limited spatial resolution, which necessitates a constant search and development of better labelled and more sensitive probes. Particularly for generation of more sensitive probes, novel alternative methods of labelling the probe DNA are of great interest.

2.1.2 General introduction to click chemistry

In 2001, the Nobel prize winner K. Barry Sharpless introduced a new concept in the field of organic synthesis that is nowadays called 'click-chemistry' (Kolb et al. 2001). Driven by the need to develop new ways of organic synthesis that are not associated with substantial synthetic challenges (e.g. in pharmaceutical industry), Sharpless formulated a number of characteristics that define his concept. Chemical interactions are considered as 'click-chemistry' reactions, if they are (1) modular, (2) wide in scope, (3) give very high yields, (4) generate only easily removable inoffensive by-products and are (4) stereospecific (Kolb et al. 2001). The synthesis itself should ideally require rather simple reaction conditions, involve readily available starting materials and reagents, the use of no or benign solvents that are easy to remove and be characterized by simple product isolation (Kolb et al. 2001). Until now, several reactions have been identified that meet these criteria, e.g. cycloadditions underlying hetero-Diels-Alder reaction, the Staudinger ligation and Thiol-ene click-chemistry (Kolb et al. 2001, Mamat et al. 2009, Hoyle et al. 2010, Wiessler et al. 2010) .

Another click-chemistry reaction, which became more and more relevant in the past years, is the Cu (I)-catalysed azide-alkyne cycloaddition (CuAAC). Described independently in 2001 by the groups of K. Barry Sharpless and Morten Meldal, CuAAC is applicable to a wide range of applications including surface engineering, bioconjugation, and synthesis and modification of polymers, proteins, natural products and biomolecules (Rostovtsev et al. 2002, Tornoe et al. 2002, Lahann 2009). The CuAAC is based on the classical Huisgen 1, 3-dipolar cycloaddition. Thereby, the reaction of azides and alkynes takes place at high temperature and gives 1,2,3-triazoles as a mixture of 1,4- and 1,5-substituted regioisomers (Tornoe et al. 2002). By using a copper(I) ion source as catalyst, the Huisgen cycloaddition has been optimized to be dramatically (7 to 8 magnitudes) faster, to undergo at room temperature and yield only 1,4-distributed 1,2,3-triazoles (91% yield, Figure 17) (Rostovtsev et al. 2002). However, the accessibility of only terminal alkynes substantially limits the range of potential applications of the CuAAC reaction.

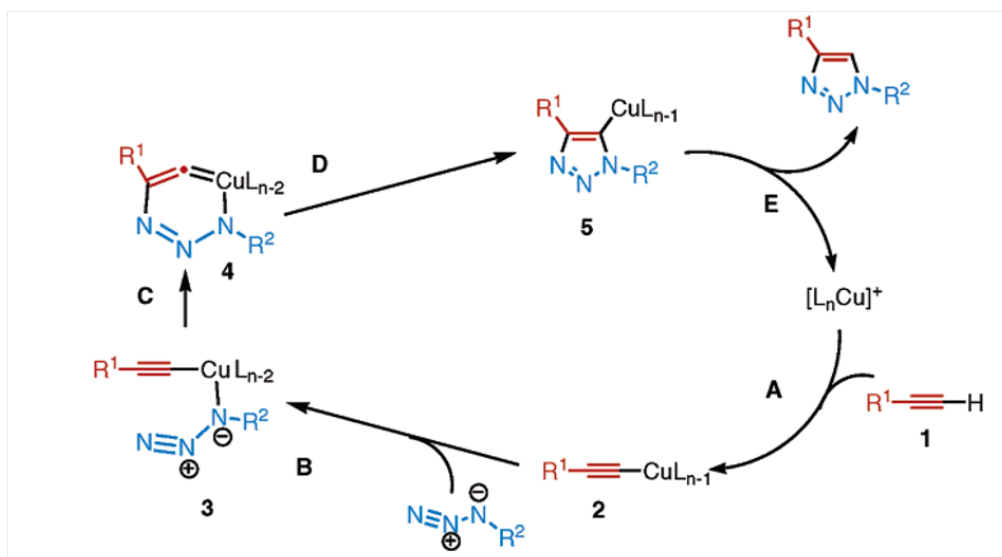


Figure 17 | Proposed reaction mechanism of the copper (I)-catalysed azide-alkyne cycloaddition (CuAAC). (A) The reaction starts with the coordination of the alkyne to the copper(I) species (**1**) causing a displacement of one acetonitrile ligands. This results in conversion of the alkyne to the acetylide (**2**). (B) In the next step, the azide replaces one of the ligands and binds to the copper atom *via* the nitrogen proximal to carbon, thus forming an intermediate (**3**). (C) Now, the distal nitrogen of the azide (**3**) attacks the C-2 carbon of the acetylide to form the six-membered copper (III) metallacycle (**4**). (D) At this point, the barrier for the ring contraction, which forms the triazolyl- copper derivative, is very low (**5**). (E) The last step is the proteolysis of (**5**) resulting in the triazole product. Adapted from (Himo et al. 2005).

2.1.3 Application of click-chemistry to nucleic acids

The application of the copper(I)- catalysed azide-alkyne cycloaddition (CuAAC) to nucleic acids was hindered by the fact that copper ions damage DNA *via* strand scission (Burrows et al. 1998, Thyagarajan et al. 2006). However, with the discovery of polytriazoles like 1-(1-benzyltriazol-4-yl)-N,N-bis[[1-benzyltriazol-4-yl)methyl]methanamine (TBTA) as powerful copper(I)- stabilizing ligands, the application of CuAAC to DNA has become possible (Chan et al. 2004). Already in 2006, the CuAAC was successfully used to modify DNA (Burley et al. 2006, Gierlich et al. 2006, Seela et al. 2006). For this purpose, alkyne- or azide-bearing DNA modifiers are incorporated into the DNA strand *via*, for instance, chemical solid phase synthesis or enzymatic synthesis (Geci et al. 2007, Rozkiewicz et al. 2007, Gramlich et al. 2008). However, the choice of DNA modifiers is limited regardless of the method of synthesis. In case of solid phase synthesis, the use of azide-bearing phosphoramidites is intrinsically difficult because the phosphorus (III) atom reduces the azide group (Gramlich et al. 2008). Similarly, the enzymatic synthesis using DNA polymerases is restricted to those DNA modifiers that are accepted as a substrate. In striking contrast, DNA can be modified using CuAAC with a wide variety of different available labels, such as fluorophores, biotin, polyethylene glycols, amino acids and Ferrocens. Moreover, this technique allows the labelling of DNA probes with multiple modifications (Gramlich et al. 2008). Given these advantages of CuAAC over other alternative

techniques, this approach to label DNA probes gained increasing attention in the field of applied click-chemistry.

2.1.4 Click-chemistry-labelled oligonucleotides as probes for FISH

The development and validation of novel synthetic methods to construct chemically modified DNA oligonucleotides is particularly important for nanotechnological and biological applications. In the field of nucleic acid research, it quickly became apparent that the CuAAC reaction has great potential, as azides and alkynes are attachable to nucleic acids without significant disturbance of their biophysical properties. Furthermore, azides and unactivated/inactive alkynes are nearly inert towards functional groups normally found in nature and react only with each other. Likewise, triazole is non-toxic and extremely stable (El-Sagheer et al. 2010). This makes CuAAC also interesting as an alternative method to label DNA probes for fluorescence *in situ* hybridization. Therefore, a fraction of the normal dNTPs is substituted by alkyne-bearing dNTPs *via* solid phase synthesis or PCR. Using fluorophore-coupled azides, the DNA probes can be easily labelled *via* the CuAAC reaction (Figure 18).

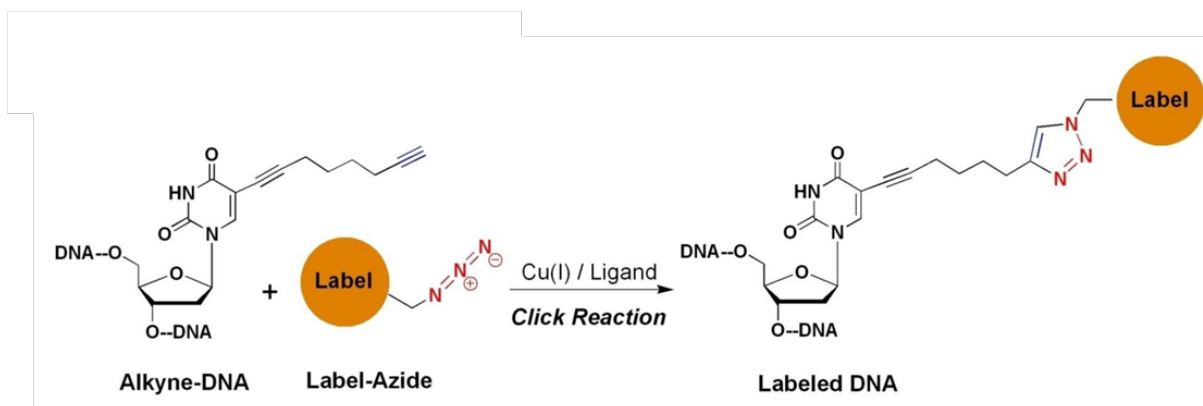


Figure 18 | The CuAAC reaction can be used to functionalise alkyne-modified DNA nucleobases. The CuAAC is a Huisgen 1, 3-dipolar cycloaddition, where alkyne-labelled DNA (blue) and azide-coupled dyes (red) react to provide labelled DNA fluorescence *in situ* hybridization (FISH) probes. This reaction is catalysed by copper (I) ions, which are stabilised by polytriazole ligands, e.g. TBTA. (Courtesy of A. Manetto)

Click-chemistry-based probe synthesis offers some advantages as compared to conventional probe labelling, e.g. nick translation. Through solid phase synthesis, DNA probes can be stepwise labelled at any desired position, leading to a range of potential outcomes from mono-labelled to multiple (colour) labelled oligonucleotides (Figure 19). Moreover, varying linkers at the C8 position of the modified dNTP offer the advantage of avoiding steric hindrances between the dye molecules that could enable substantially higher labelling rates. Therefore, one could speculate that click-chemistry-

based DNA probes can be considered as suitable and promising for further development of FISH to increase its sensitivity and spatial resolution.

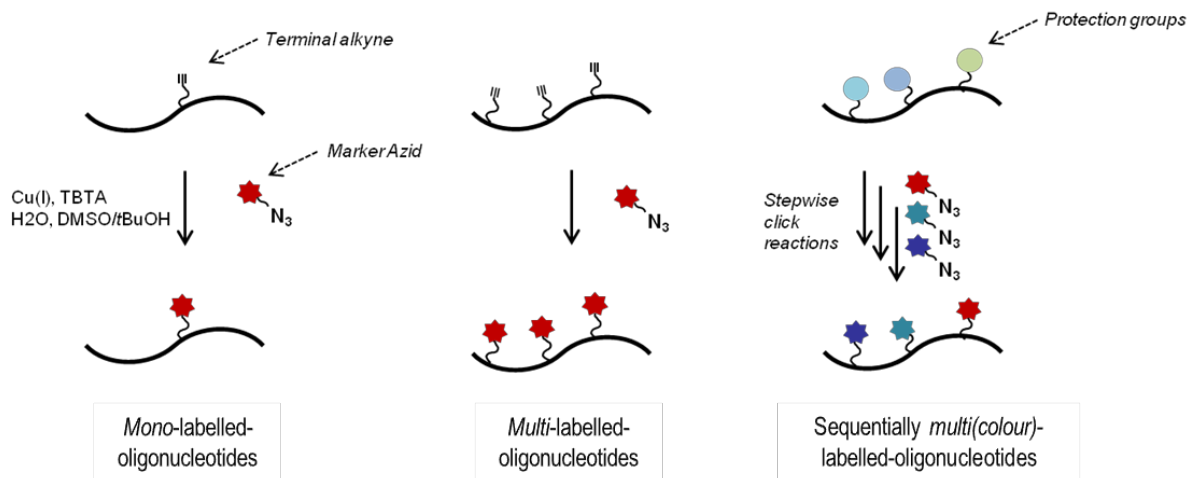


Figure 19 | Different DNA labelling strategies based on CuAAC. Solid phase synthesis allows for precise positioning of modified dNTPs within the DNA probe ranging from *mono*-labelled to multiple labelled oligonucleotides. With the help of different protection groups, the stepwise implementation of CuAAC allows production of *multicolour*-labelled probes. (Courtesy of A. Manetto)

2.2 Aims of the PhD work

In situ hybridization using fluorescence-based detection is a powerful tool to investigate the genome and chromosome architecture, as well as the gene activity at DNA and RNA levels. To improve the sensitivity and resolution of fluorescence *in situ* hybridization (FISH), we investigated an alternative technique of probe labelling based on the copper (I)-catalysed azide-alkyne cycloaddition (CuAAC). Thereby, we aimed to address following questions:

1. Is it possible to detect repetitive and single copy sequences using CuAAC-labelled FISH probes?

For the detection of repetitive sequences, oligonucleotide probes carrying different amounts of modifications should be compared to conventionally labelled FISH probes. For single copy FISH, a mix of 95 CuAAC-labelled oligonucleotides is to be tested.

2. Is it possible to combine FISH using CuAAC-labelled probes with other cytological methods, primarily the 5-Ethynyl-deoxyuridine (EdU) labelling and immunohistochemistry?

The possibility to combine FISH (at higher sensitivity and spatial resolution) with other conventionally accepted methods in a single preparation will facilitate deeper understanding of the genome and chromosome architecture.

2.3 Materials and methods

2.3.1 Plant materials

Rye (*S. cereale* L. cv. Petkuser Sommerroggen), barley (*Hordeum vulgare* L. cv. Morex and Emir) and hexaploid wheat (*Triticum aestivum* L. cv. Kanzler) were grown at greenhouse conditions (16 h light, 22° C day/ 16° C night). *A. thaliana* ecotypes Pro-0 (Proaza, Asturias) (ID no. 8213 (Fulcher et al. 2015) and Hov1-10 (ID no. 6035) were grown until rosette stage at short day (8 h light, 21° C) afterwards at long day conditions (16 h light, 21° C) at greenhouses.

2.3.2 Preparation of mitotic chromosomes for non-single copy FISH

Rye, wheat and barley seeds were etiolated for 2–3 days at RT. Root tips were cut, mitotic metaphases were accumulated by overnight treatment in ice-cold water, fixed in 3:1 ethanol/glacial acid (Carl Roth, cat. no. 9165; Merck, cat. no. 100066, respectively) and kept at –20° C until use. For mitotic chromosome preparation, root tips were washed in ice-cold water and digested (50–60 min, 37° C) in an enzyme cocktail (1% cellulase (Calbichem, cat. no. 219466), 1% pectolyase Y-23 (Sigma-Aldrich, cat. no. P3026), 1% cytohelicase (Sigma-Aldrich, cat. no. C8274) in citrate buffer (0.01 M tri-sodium citrate dihydrate (Carl Roth, cat. no. 4088) and 0.01 M citric acid (Carl Roth, cat. no. 6490); pH 4.5–4.8)). Afterwards, root tips were washed in 0.01 M citrate buffer and ice-cold ethanol consecutively. For preparation of mitotic chromosome spreads, root tips were transferred to glacial acid/ethanol 3:1 (200 µl/ 25 root tips) and disrupted with a dissection needle. Eight microliters of this mitotic cell suspension were dropped onto glass slides placed on ice, air-dried and stored in 100% ethanol at 4° C (Aliyeva-Schnorr et al. 2015). *A. thaliana* slide preparation was performed according to Armstrong *et al.* with minor modifications (Armstrong et al. 1998). Flower buds were fixed in ethanol/glacial acid (3:1), washed and digested in an enzyme cocktail (0.1% cellulase, 0.1% pectolyase, 0.1% cytohelicase in 0.01 M citric buffer). After washing, flower buds were disrupted on a slide in 10 µl of 60% acetic acid and placed on a hot plate (1 min, 43° C). The cell suspension was covered with fixative and air-dried. For FISH, *A. thaliana* slides were treated with pepsin (2 min, 38° C; 0.05 mg/ml; Sigma-Aldrich, cat. no. 10108057001), washed and fixed (10 min, RT, 4% formaldehyde (Carl Roth, cat. no. 4979). After washing and dehydration in ethanol, the slides were used for FISH.

2.3.3 Preparation of mitotic chromosomes for single copy FISH (standard method)

Seeds of *H. vulgare* were etiolated for 2–3 days at room temperature; root tips were cut and incubated overnight in ice-cold water to arrest mitotic metaphases. Afterwards, they were fixed in

3:1 ethanol/glacial acid (Carl Roth, cat. no. 9165; Merck, cat. no. 100066, respectively) for two days at room temperature and stored at -20° C until use. Preparation of mitotic metaphases was performed using the dropping technique by Kato *et al.* and post-fixation of slides was carried out according to Ma *et al.* 2010 (Kato *et al.* 2004, Ma *et al.* 2010).

2.3.4 Preparation of mitotic chromosomes for single copy FISH (alternative method)

Seeds of *H. vulgare* and *S. cereale* were etiolated for 2–3 days at room temperature. To synchronize cell division, the seedlings were incubated at least 24 hours at 4° C followed by 24 hours at room temperature. Root tips were cut and incubated overnight in ice-cold water to arrest mitotic metaphases. Afterwards, they were fixed in 3:1 ethanol/glacial acid (Carl Roth, cat. no. 9165; Merck, cat. no. 100066, respectively) for at least 5 days at room temperature. Fixed root tips were washed first in distilled water and then in citrate buffer (0.01 M tri-sodium citrate dihydrate (Carl Roth, cat. no. 4088) and 0.01 M citric acid (Carl Roth, cat. no. 6490); pH 4.5–4.8). To digest the cell walls, the root tips were digested (50 min, 37° C) in an enzyme cocktail (1% cellulase (Calbichem, cat. no. 219466), 1% pectolyase Y-23 (Sigma-Aldrich, cat. no. P3026), 1% cytohelicase (Sigma-Aldrich, cat. no. C8274) in citrate buffer). After washing in citrate buffer, single root tips were macerated in 45% acidic acid (Merck, cat. no. 100066) on slide, covered with a coverslip and carefully squashed. The slide was heated briefly in an open flame before the coverslip was removed using liquid nitrogen. Subsequently, slides were air-dried.

2.3.5 Preparation and sorting of isolated nuclei

Isolation of nuclei was performed according to Dolezel *et al.* with slight modifications (Dolezel *et al.* 1989). Approximately 0.1 g of leaf material was fixed in 4% formaldehyde in Tris buffer (10 mM Tris (Carl Roth, cat. no. 5429); 10 mM Na₂EDTA (Carl Roth, cat. no. 8043); 100 mM NaCl (Carl Roth, cat. no. 9265); 0.1% TritonX-100 (AppliChem, cat. no. A 1388); pH 7.5) on ice for 20 min in a centrifugal vacuum concentrator (Eppendorf, model 5301). After washing twice in ice-cold Tris buffer, leaves were chopped in 1 ml nuclei isolation buffer (15 mM Tris; 2 mM Na₂EDTA; 0.5 mM Spermine tetrahydrochloride (Serva); 80 mM KCl (Carl Roth, cat. no. 6781); 20 mM NaCl; 15 mM β-mercaptoethanol (Carl Roth, cat. no. 4227); 0.1 % Triton X-100; pH 7.5). The resulting suspension was filtered in a 5-ml polystyrene round-bottom tube with 35 μm cell strainer snap cap (Falcon, product # 352235). Nuclei were stained with 1.5 μg/ml 4', 6-diamidino-2-phenylindole (DAPI; Thermo Fischer, cat. no. 1306) and flow-sorted into Eppendorf tubes using a BD FACSAria IIu (BD Biosciences). For barley 2C nuclei and for *A. thaliana* ecotype Pro-0 and Hov1-10 endopolyploid 4C nuclei were collected. Equal amounts (12–15 μl) of sucrose solution (40% sucrose (Carl Roth, cat. no. 4621) in Tris

buffer; pH 7.5) and flow-sorted nuclei suspension (approx. 450 nuclei/ μ l) were pipetted on glass slides, gently mixed, air-dried overnight and kept at -20° C.

2.3.6 FISH probe preparation

Arabidopsis-type telomeric and CTT, as well as the 95 barley single copy gene specific alkyne-bearing oligonucleotides (Table 1, Appendix) were synthesized using an ABI 394 DNA/RNA Synthesiser (Applied Biosystems) and C8-Alkyne-dU phosphoramidites at baseclick GmbH (Neuried, Germany). The subsequent click reaction was performed using 5-TAMRA-azide (cat. no. BCFA-008, baseclick GmbH) or 6-FAM-azide (cat. no. BCFA-001, baseclick GmbH) and the OligoClick labelling Kit (cat. no. BCK-FISH, baseclick GmbH) according to the provided manual. At baseclick GmbH (Neuried, Germany), alkyne-bearing oligonucleotides and fluorescent-labelled oligonucleotides were analysed using RP-HPLC (Waters) equipped with a photodiode array detector (Waters) and a reversed phase column (XBridge OST C18, 4.6 mm \times 50 mm, Waters) using a gradient method (from 45 to 85% acetonitrile buffer). Correct masses were measured with an Auto-Flex II MALDI-TOF (Brucker Daltonics). If indicated, probes were purified using the QIAquick nucleotide removal Kit (Qiagen, cat. no. 28115) provided by baseclick GmbH (Neuried, Germany).

Probes for detection of the rye centromeric retrotransposon Bilby (Francki 2001) were generated from a vector containing the repeat-specific sequences kindly provided by Dr. Sonja Klemme (Klemme et al. 2013) and labelling was done by nick translation using an Atto647N NT Labelling Kit (Jena Bioscience GmbH, Jena Germany).

The 5'-end-labelled *Arabidopsis*-type telomere probe (CCCTAAA)₄ was synthesized by Eurofins Genomics (Ebersberg, Germany). Nick translation-labelled telomere probes were produced *via* PCR according to Ijdo *et al.* with minor changes (Ijdo et al. 1991). PCR was accomplished using primers (CCCTAA)₃ and (TTAGGG)₃ without template (Eurofins Genomics) and Taq DNA polymerase (Qiagen, cat. no. 201207). The annealing temperature was 60° C. Nick translation was performed using a NT Labelling Kit (Jena Bioscience GmbH, Jena Germany) according to the manual with the following triphosphates: 0.5 mM dATP, 0.5 mM dCTP, 0.5 mM dGTP, 0.25 mM dTTP and 0.25 mM aminoallyl-dUTP-5/6-TAMRA (Jena Bioscience GmbH).

The NT-labelled probe to detect the 7670 bp-long barley single copy gene (ID 43694) was produced according to Aliyeva-Schnorr *et al.* and consisted of 5 fragments labelled by nick translation using a NT Labelling Kit (Jena Bioscience GmbH, Jena Germany) according to the manual with the following triphosphates: 0.5 mM dATP, 0.5 mM dCTP, 0.5 mM dGTP, 0.25 mM dTTP and 0.25 mM aminoallyl-dUTP-5/6-TAMRA (Jena Bioscience GmbH) (Aliyeva-Schnorr et al. 2015).

The 5S ribosomal DNA probe was generated by PCR from genomic DNA of barley as described by Fukui *et al.*, purified (QIAquick PCR Purification Kit, Qiagen) and labelled by nick translation using an Atto488 NT Labelling Kit (Jena Bioscience GmbH, Jena Germany) (Fukui et al. 1994).

Table 1 Synthesized FISH probes

Name	Sequence (label position underlined)
4PTel4	CCC <u>I</u> AA ACC C <u>T</u> AAAC CC <u>I</u> AAA CCC <u>I</u> AA A
4PTel2	CCC <u>I</u> AA ACC CTAAAC CC <u>I</u> AAA CCC TAA A
3PTel3	CCC <u>I</u> AA ACC C <u>T</u> AAAC CC <u>I</u> AAA
3PTel2	CCC <u>I</u> AA ACC CTAAAC CC <u>I</u> AAA
CTT	CTT C <u>T</u> T CTT CTT C <u>T</u> T CTT CTT C <u>T</u> T CTT CTT

2.3.7 Treatment of oligonucleotide FISH probes by ammonia for pH change

To each 50 µl of the *pre*-hybridization-labelled 95 oligonucleotide FISH probe mix (baseclick GmbH, Neuried), a drop of concentrated ammonia (32%) was added using a glass Pasteur pipette (Carl Roth, cat. no. 4518). After short vortexing and brief centrifugation, the ammonia was evaporated in a thermomixer (at 45° C in darkness, until the ammonia-typical smell could no longer be detected). The treated probe mix was used for FISH as usual.

2.3.8 Fluorescence *in situ* hybridization using *pre*- or *post*-hybridization click probes

Selected preparations of mitotic chromosomes were post-fixed (4% formaldehyde in 2× SSC (300 mM NaCl; 30 mM tri-sodium citrate dehydrate, pH 7.0); 10 min, RT) and washed in 2× SSC. After dehydration (stepwise in 70, 90 and 100% ethanol) slides were air-dried. Alkyne-labelled or fluorochrome-labelled probes in hybridization mix (20% dextran sulphate (Sigma-Aldrich, cat. no. D 8906), 50% deionized formamide (Sigma-Aldrich, cat. no. 4767), 300 mM NaCl, 30 mM trisodium citrate dehydrate, 50 mM phosphate buffer, pH 7.0) were used for *post*- and *pre*-hybridization, respectively. The hybridization mix containing the probes was applied to slides, which were subsequently covered with coverslips and sealed with rubber gum. The denaturation was performed on a heating plate (2 min, 80° C). Hybridization was carried out in a moisture chamber (overnight, 37° C). Washed slides were mounted in Vectashield (Vector Laboratories, cat. no. H1000) containing DAPI (10 ng/µl; Thermo Fischer, cat. no. D1306). Images were acquired with an epifluorescence microscope BX61 (Olympus, <http://www.olympus.fi/medical/en/microscopy>) using an Orca ER CCD camera (Hamamatsu).

2.3.9 Single-copy fluorescence *in situ* hybridization

Single-copy FISH was performed as described in (Aliyeva-Schnorr et al. 2015) with minor modifications. For post-fixation directly before FISH, the slides were fixed for 10 min with 4% PFA in 2x SSC (0.3 M NaCl (Carl Roth, cat. no. 3957); 0.03 M tris-sodium citrate dihydrate (Carl Roth, cat. no. 4088, pH 7.0), washed in 2x SSC , dehydrated (70, 90, 100% ethanol) and air-dried for 1 hour. Then, the hybridization mix (10 µl deionized formamide, 5 µl 4x buffer (8x SSC; 0.04 M Tris-HCL pH 8.0 (Carl Roth, cat. no. 9090); 0.004 M EDTA; 0.63 µg herring sperm DNA in ddH₂O)) containing the probes (Control: 810 ng/slide; oligonucleotides as indicated) was applied to slides, covered with coverslips, sealed with rubber gum and denatured on a hot plate (80° C, 2 min). If indicated, probes with hybridization mix were denatured (96° C, 6 min) and quickly cooled down on ice before hybridization. For hybridization, slides were incubated overnight at 37° C in a moisture chamber. Subsequently, slides were washed (2x SSC, 20 min, 58° C), dehydrated (stepwise in 70, 90 and 100% ethanol) and mounted after drying at RT in Vectashield (Vector Laboratories, cat. no. H1000) containing DAPI (10 ng/µl; Thermo Fischer, cat. no. D1306). Images were acquired with an epifluorescence microscope BX61 (Olympus, <http://www.olympus.fi/medical/en/microscopy>) using an Orca ER CCD camera (Hamamatsu).

2.3.10 Combined 5-Ethynyl-deoxyuridine (EdU)-based DNA replication analysis and FISH using *pre*-clicked probes

Germinated seeds were grown for 2 h in darkness on filter paper (Macherey Nagel, cat. no. MN616) soaked with 15 µM 5-ethynyl-deoxyuridine (BCK-EdU555, baseclick GmbH, Neuried) and afterwards placed for 2.5 h on deionized water only. Root tips were cut and mitotic metaphases were accumulated by treatment with ice-cold water overnight. Mitotic slides were prepared as described above. To detect 5-ethynyl-deoxyuridine, the CuAAC reaction using 5-TAMRA-azide was performed according to manufacturer's protocol (BCKEdU555, baseclick GmbH). After washing, slides were dehydrated in ethanol and used for FISH with *pre*-hybridization CuAAC probes as described above.

2.3.11 Combined immunohistochemistry and hybridization of *pre*-hybridization CuAAC-labelled FISH probes

Root tips were fixed (4 % paraformaldehyde in 1x PBS (137 mM NaCl, 2.7 mM KCl; 10 mM Na₂HPO₄) (Carl Roth, cat. no. 4984); 1.8 mM KH₂PO₄ (Carl Roth, cat. no. 3904; pH 7.4)), washed in ice-cold 1x PBS and digested in an enzyme cocktail (see above). After washing in ice-cold 1x PBS, single root tips were transferred to glass slides and squashed in 1x PBS + 0.001% Tween-20 using cover slips (Th. Geyer, cat. no. 7695024). After freezing in liquid nitrogen, the cover slips were removed and slides

were stored in 1× PBS. Incubation with primary (rabbit anti-grass CENH3 (1:1000; (Sanei et al. 2011)); 90 min, 37° C) and secondary antibodies (donkey anti-rabbit coupled to Alexa 647 (Dianova, cat. no. 711-606- 152); 60 min, 37° C) was performed. Slides were washed, dehydrated (70, 90 and 100% ethanol), air-dried and fixed in ethanol/glacial acid (3:1; 24–48 h in darkness). Subsequently, the slides were air-dried and incubated with hybridization mix (see above) without FISH probes (12 h; 37° C). After short washing (2× SSC containing 0.1% Triton X100), slides were dehydrated and air-dried. For denaturation, slides were incubated in 0.2 M NaOH (in 70 % ethanol; 10 min at RT), dehydrated and air-dried. Alkyne-modified probes were heated up (5 min; 95° C) in hybridization mix (see above) before application on slides. FISH was performed at 37° C overnight using *pre*-hybridization-labelled CTT and 4PTel4 probes. Slides were washed and afterwards mounted in Vectashield containing DAPI (10 ng/μl). Acquisition of FISH signal was carried out using an Olympus BX61 microscope equipped with an Orca ER CCD camera (Hamamatsu).

2.3.12 Quantification of telomeric FISH signals

Acquisition of FISH signal was carried out using an Olympus BX61 microscope equipped with an Orca ER CCD camera (Hamamatsu). For quantification of telomeric FISH signals, flow-sorted endopolyploid nuclei (4C) of *A. thaliana* were used. For each FISH probe, 300 nuclei were analysed. Statistical analysis was done using Kruskal-Wallis ANOVA followed by median test in STATISTICA data analysis software system (Statsoft, USA). Factorial effects and differences between groups were considered as significant at $P < 0.05$.

2.4 Results

2.4.1 Characterization of *Arabidopsis*-type telomere-specific CuAAC-labelled oligonucleotide probes

To examine whether the Cu (I)-catalysed azide-alkyne cycloaddition (CuAAC) is suitable for the synthesis of FISH probes, we designed oligonucleotides recognizing the *Arabidopsis*-type telomeric sequence ((TTTAGGG)_n). The solid phase-synthesised alkyne-modified oligonucleotides were labelled before hybridization with TAMRA fluorochrome at defined positions using the CuAAC technique (Tab.1). FISH of mitotic barley and *A. thaliana* chromosomes resulted in telomere repeat-typical signals as distinct puncta in distal position of the chromosomes, thus demonstrating that CuAAC-labelled probes are indeed suitable for the *in situ* detection of telomeric sequences by FISH (Figure 20A).

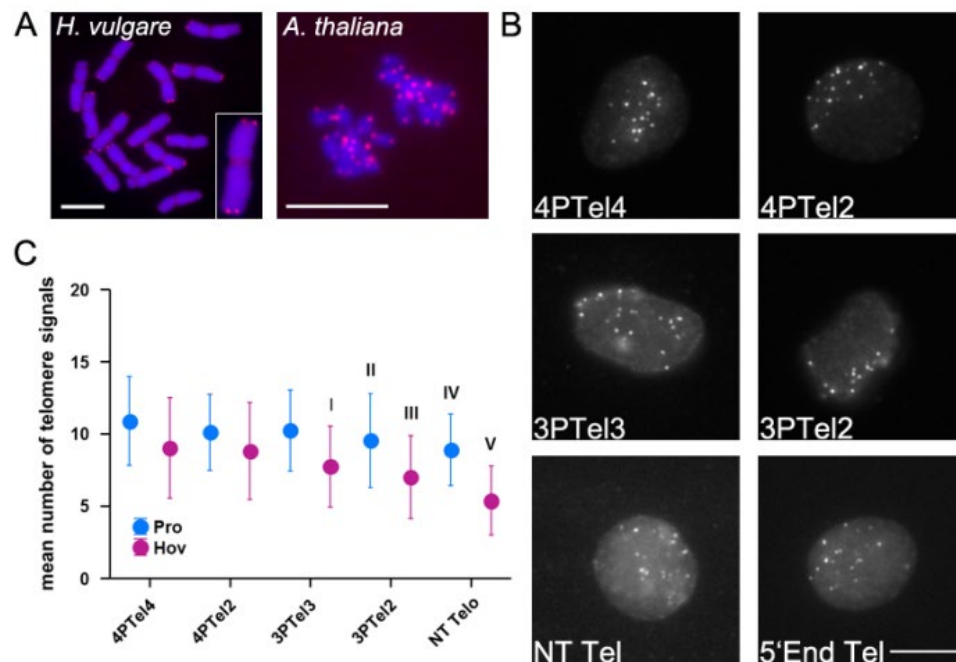


Figure 20 | CuAAC-labelled DNA probes are suitable for FISH. (A) Representative images of CuAAC-labelled *Arabidopsis*-type telomere ((TTTAGGG)_n) probes (in red) hybridized on mitotic chromosomes of barley and *A. thaliana*. The inset shows a further enlarged chromosome (exemplary images). **(B)** CuAAC labelled probes (4PTel4, 4PTel2, 3PTel3, 3PTel2, nick translation labelled telomere probe and 5'-end labelled probe) hybridized on sorted 2C barley nuclei. All scale bars represent 10 μ m **(A; B)**. **(C)** Quantification of detected telomeric FISH signals on sorted 4C nuclei of *Arabidopsis* ecotypes possessing long (Pro ~9.3 kb) and short (Hov ~1 kb) telomeres by CuAAC labelled telomere probes and nick translation labelled telomere probe. Statistical analysis revealed that performance of all probes was markedly better in the Pro ecotype, as compared with the Hov ecotype. Significant differences within each ecotype ($P < 0.05$; protected two-way ANOVA followed by Bonferroni post hoc test) are labelled with Roman numerals I-V at which (I, III) means significant different to 4PTel4, 4PTel2, nick translated telomere probes, (II) to 4PTel4, (IV) to 4PTel4, 4PTel2, 3PTel3, (V) to 4PTel4, 4PTel2, 3PTel3 3PTel2.

To investigate whether the length of probes and the quantity of fluorochromes conjugated to the probe influences the performance of CuAAC-labelled FISH probes, oligonucleotides consisting of either 3 or 4 5'-CCCTAAA-3' repeats, each of which was labelled with 2 to 4 fluorochromes, were synthesised and compared to conventional nick translation and 5'-end labelled probes. We found that regardless of oligonucleotide length and fluorochrome number, the telomere signals were reliably detected by all probes on sorted barley interphase nuclei (Figure 20B). Unfortunately, quantification of fluorescence intensities of the probes was not feasible using telomeric repetitive sequences. The combination of variability in signal density, the telomere distribution, as well as the 3D structure of sorted nuclei and the telomere size variations of the individual chromosomes (Wang et al. 1991) complicated the precise quantitative assessment of acquired fluorescent signals.

Next, we evaluated whether the CuAAC-labelled telomere probes show differences in their detection properties. For this purpose, we performed quantification of telomeric FISH signals detected on sorted 4C nuclei of *Arabidopsis* ecotypes possessing long (Pro ~9.3 kb) or short (Hov ~1 kb) telomeres (Figure 20C) (Geci et al. 2007). Comparison of the mean numbers of detected fluorescent puncta (i.e., telomere signals) revealed that the detection performance of all analysed probes was generally better in the Pro ecotype having long telomeres, as compared to the detection efficiency in the Hov ecotype.

2.4.2 The use of CuAAC-labelled probes in combination with immuno-histochemistry and EdU labelling

Each approach to probe labelling applied in cytological studies is advantageous for certain aspects of research, thus the possibility to combine several labelling techniques in a single experiment/preparation is of great value for both academic and industrial applications. Therefore, next we addressed the question whether the CuAAC reaction can also be performed after probe hybridization, similarly to indirect labelling approaches. This would be beneficial because alkyne-labelled probes can be labelled after *in situ* hybridization with various fluorochromes depending on specific needs or experimental settings (Figure 21).

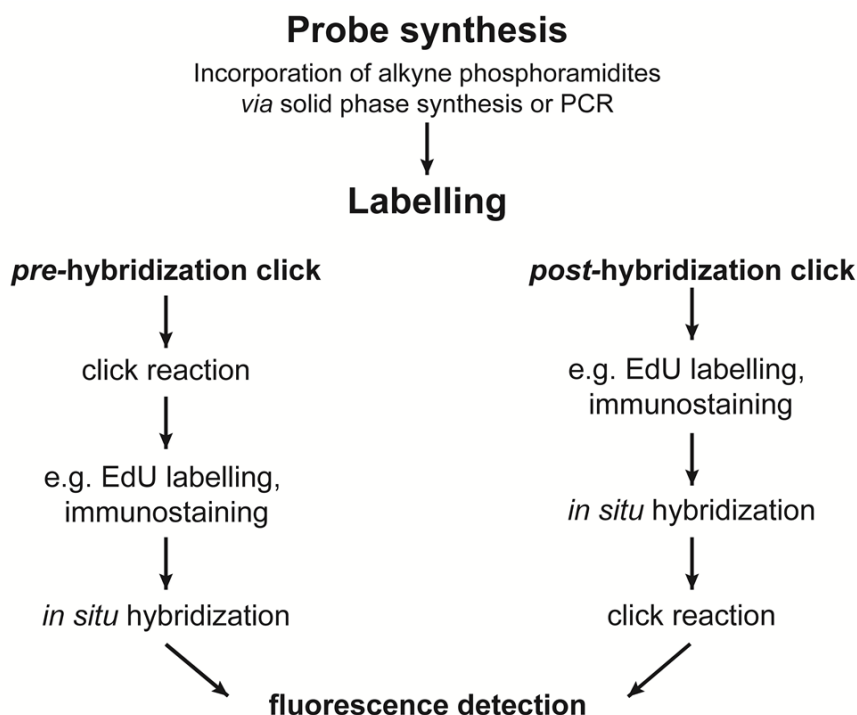


Figure 21 | Workflow of *pre*- and *post*-hybridization CuAAC. The possible application of click chemistry for FISH by *pre*- or *post*-hybridization CuAAC labelling in combination with immunostaining or EdU labelling.

Accordingly, the same set of alkyne-modified telomeric probes used earlier (Table 1) underwent hybridization to mitotic wheat chromosomes, followed by an on-slide CuAAC reaction (*post*-hybridization click). For comparison, a conventional nick translation-labelled telomere probe was co-hybridized. Figure 22A shows that *post*-hybridization labelling of CuAAC oligonucleotide probes indeed resulted in clearly detectable telomeric signals remarkably similar to those obtained using NT-labelled telomere probes. To validate whether the same chromosomal sites were targeted by *pre*- and *post*-hybridization click labelled oligonucleotide probes, we hybridized the *pre*-hybridization fluorescently labelled microsatellite (CTT)₁₀ probes simultaneously with a (CTT)₁₀ probes that were modified with alkyne only. Subsequently, the latter probe was labelled on-slide by a CuAAC reaction (Figure 23). Once again, we found that both types of oligonucleotide probes resulted in comparable hybridization patterns (Figure 22B).

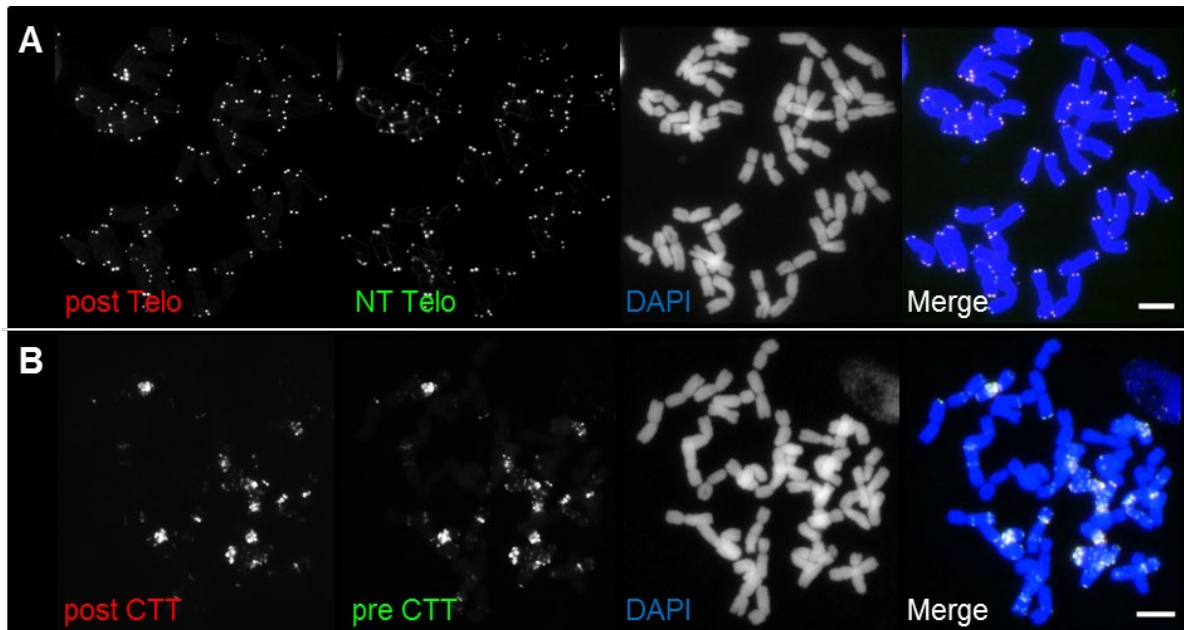


Figure 22 | Combination of *pre*- and *post*-hybridization CuAAC-labelled probes on wheat metaphase chromosomes. Alkyne conjugated oligonucleotides probes were hybridized to the specimen and on-slide labelled *via* CuAAC. **(A)** Detection of post-hybridization labelled 4PTel2 and nick translation labelled *Arabidopsis*-type telomere probes showing co-localized hybridization signals. **(B)** *Pre*- and *post*-hybridization click-labelled microsatellite (CTT)₁₀ probes showed a comparable distribution of hybridization signals. Bars= 10 μm.

To explore a range of potential applications of CuAAC-labelled oligonucleotide probes, in additional experimental set we combined FISH with two conventional cytological techniques, i.e. immunohistochemistry and labelling of DNA replication *via* 5-Ethynyl-deoxyuridine (EdU) uptake (Figure 23). After performing immunohistochemistry, to detect the centromeric variant of histone H3 (CENH3), and click chemistry- based cell proliferation assay using EdU, *pre*-hybridization CuAAC-labelled telomere and microsatellite probes (4PTel4; (CTT)₁₀) were successfully hybridized to barley metaphase chromosomes (Figure 23A, B). Moreover, in our experiments we observed that the *post*-hybridization CuAAC reaction efficiency can be decreased in specimens previously fixed by paraformaldehyde most likely due to penetration problems (data not shown).

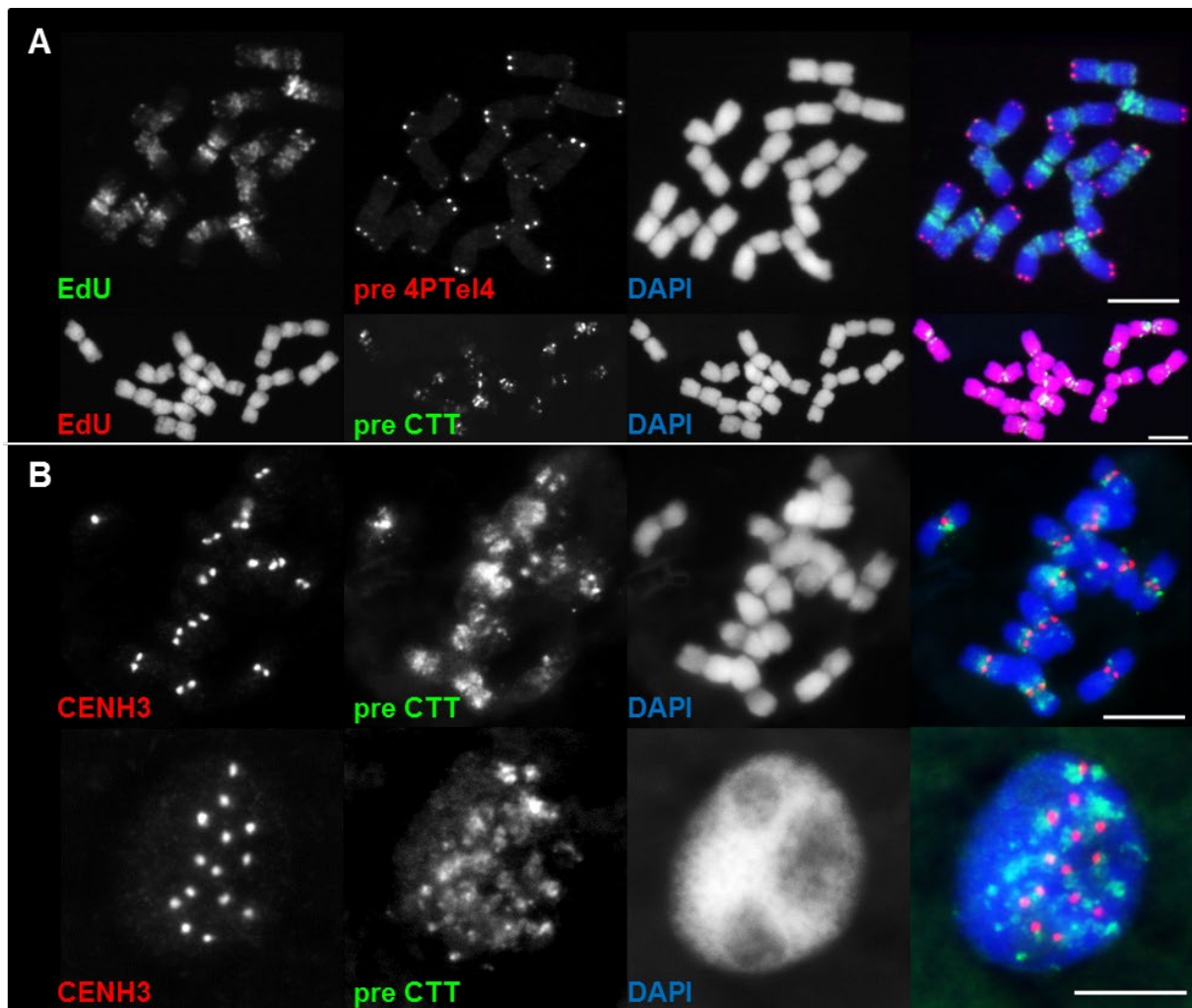


Figure 23 | Combination of CuAAC-labelled microsatellite probes with immunohistochemistry and labelling of replication via 5-Ethynyl-deoxyuridine (EdU). (A) After labelling of early (upper panel, low amount of EdU incorporation) and late DNA replication (lower panel, high amount of EdU incorporation) via click chemistry - based EdU uptake, FISH using *pre*-hybridization click-labelled microsatellite (CTT)₁₀ and telomeric oligonucleotide probes was performed on barley metaphase chromosomes. (B) Immunolabelling of CENH3 was successfully combined with FISH using *pre*-hybridization CuAAC-labelled microsatellite probes ((CTT)₁₀) on metaphase chromosomes and interphase nucleus of barley. Scale bars 10 μ m.

2.4.3 Detection of a single copy sequence of *H. vulgare* chromosome 3H by CuAAC-labelled oligonucleotide probes

Since fluorescence *in situ* hybridization is one of the most powerful tools in cytogenetics, the constant optimization of protocols and probes to improve the resolution of this technique is of highest interest. Single copy FISH is characterized by particularly bad signal-to-noise ratio and a strongly limited resolution, because the standard nick translation approach provides a labelling rate of only 2-10% of the probe nucleotides (Yu et al. 1994, Kato et al. 2006). The CuAAC labelling of oligonucleotides offers the opportunity to increase this labelling rate and thereby improve both signal-to-noise ratio and resolution. Using DNA synthesizers to produce the probes, theoretically any position can be labelled with a modified nucleotide. However, the use of (fluorescent) tags is

restricted by steric hindrance and the limited solubility of probes in aqueous conditions, which are required for FISH applications. To evaluate whether CuAAC-labelled oligonucleotide probes are suitable to detect single copy sequences in plants, we choose barley as a model. In a frame of a cooperative project successfully integrating a physical map into a genetic map of a centromeric 5.5 cM bin of the barley 3H chromosome, Aliyeva-Schnorr *et al.* identified and characterized 70 genomic single copy sequences (Aliyeva-Schnorr *et al.* 2015). This study employed a low copy FISH approach to determine the chromosomal position of these sequences. Therefore, overlapping bacterial artificial chromosome (BAC) clones consisting of 65 fingerprinted contigs, genetically assigned to this chromosomal region (Comadran *et al.* 2012, Ariyadasa *et al.* 2014, Colmsee *et al.* 2015), were screened. For FISH probe generation, the tool Kmasker (Schmutzer *et al.* 2014) was used to predict *in silico* single copy regions. Out of the analysed 70 candidates, we choose a 7670 bp long pericentromeric single copy sequence proven to be reliably detectable by FISH (Aliyeva-Schnorr *et al.* 2015). Five fragments covering the complete sequence were synthesized *via* PCR, pooled, labelled by nick translation, and used as the control probe. Additionally, 95 oligonucleotides with a length of 22 bp each carrying three alkyne-modified dUTPs, were designed to detect the same 7670 bp long sequence. In contrast to the NT-labelled probe, the designed 95 oligonucleotides cover only a region of about 2000 bp of the single copy sequence. After synthesis of the oligonucleotides, the incorporated alkyne-modified dUTPs were labelled with 5-TAMRA-azide (5-Carboxytetramethylrhodamine-azide) *via* the CuAAC click reaction. To exclude an influence of different fluorophores, we performed the nick translation using the same fluorophore (aminoallyl-dUTP-5/6-TAMRA). Assuming a labelling rate of 2-10% (Yu *et al.* 1994, Kato *et al.* 2006), the NT-labelled control probe carries approximately 44-219 fluorophores (2-10% of 2186 thymidine bases found in the 7670 bp long sequence), whereas the 95 oligonucleotides include 285 fluorophores (Figure 24 C). Consequently, the CuAAC-labelled oligonucleotide mix is expected to enable FISH signal detection with much lower sequence coverage.

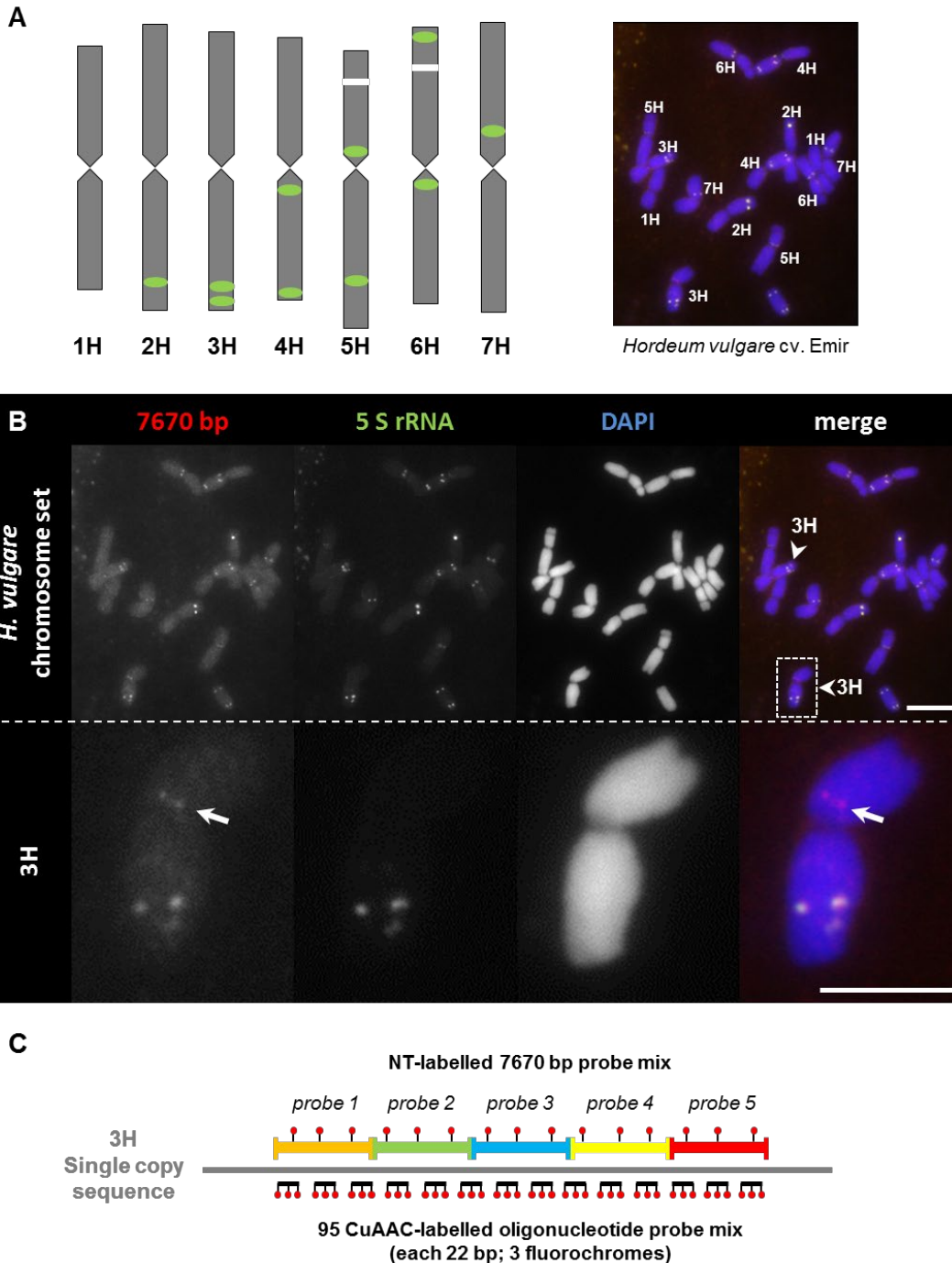


Figure 24 | Detection of a 7670 bp single copy sequence of the barley chromosome 3H by FISH. Chromatin was counterstained with DAPI. **(A)** Scheme of the localization of the 5S rRNA-encoding gene family on *H. vulgare* chromosomes (Fukui et al. 1994). All pairs of barley metaphase chromosome can be identified by the use of 5S rRNA-detecting FISH probes. During preparation of the slides, fragmentation of single chromosomes occasionally occurs. In the lower right corner such chromosome fragment of 4H is visible. **(B)** FISH using NT-labelled probes to detect the 7670 bp long single copy sequence on the chromosome 3H of barley. Probes directed against the 5S rRNA-encoding gene family allowed the identification of both chromosomes 3H (arrow heads). Unspecific channel-to-channel crosstalk of the fluorophore caused the detection of the 5S rRNA probe in parallel to the 7670 bp probe (Scale bar 10 μ m). The enlargement of the 3H (dashed box) shows two distinct signals (arrow) in proximity to the centromere, as reported by Aliyeva-Schnorr *et al.* (2015). A crosstalk signal of the 5S rRNA probe was also detected (Scale bar 5 μ m). **(C)** Model of the two FISH probe types used to detect the single copy sequence of barley chromosomes 3H. The NT-labelled probe mix consists of five probes covering the 7670 bp long region. To detect the same sequence by CuAAC-labelled probes, 95 oligonucleotides with a length of 22 bp each carrying 3 fluorochromes hybridizing along this region were synthesized.

First, we tested the *pre*-hybridization CuAAC-labelled oligonucleotide probe mix at the same concentration (819 ng/slide) as the NT-labelled 7670 bp probe (Figure 25). The single copy FISH using the oligonucleotide probe mix was performed with one minor difference to the FISH employing the NT-labelled probe, namely an additional denaturation step (96° C, 6 min) of the probe-containing hybridization mix was included. By this, potential secondary structures of the oligonucleotides are solved and better hybridization efficiency of the FISH probes is assumed. To identify the barley chromosome 3H, a 5S rDNA-specific probe was used in parallel (Figure 24 A, B). Unfortunately, we observed a channel-to-channel crosstalk of the fluorescent signals. Therefore, the 5S rDNA FISH signals were also visible on all images acquired in the single copy sequence-specific channel (Figure 24 B). Identical settings of the microscope for picture acquisition of both single copy probe types ensured a comparability of the fluorescent signals. The single copy sequence was clearly detected by the NT-labelled probes as being located at the pericentromere in line with previous report by Aliyeva-Schnorr *et al.* (2015) (Figure 25). Surprisingly, no distinct fluorescence signals on chromosome 3H were detected by the CuAAC-labelled oligonucleotide probe mix, but instead dispersed hybridization signals along all chromosomes occurred (Figure 25). To exclude that the unspecific staining was caused by the additional denaturation of the probe-containing hybridization mix, this step was omitted. In a second experiment, neither a positive nor a negative influence on the dispersed hybridization signals was observed (data not shown). Therefore, this denaturation step was no longer part of the protocol used.

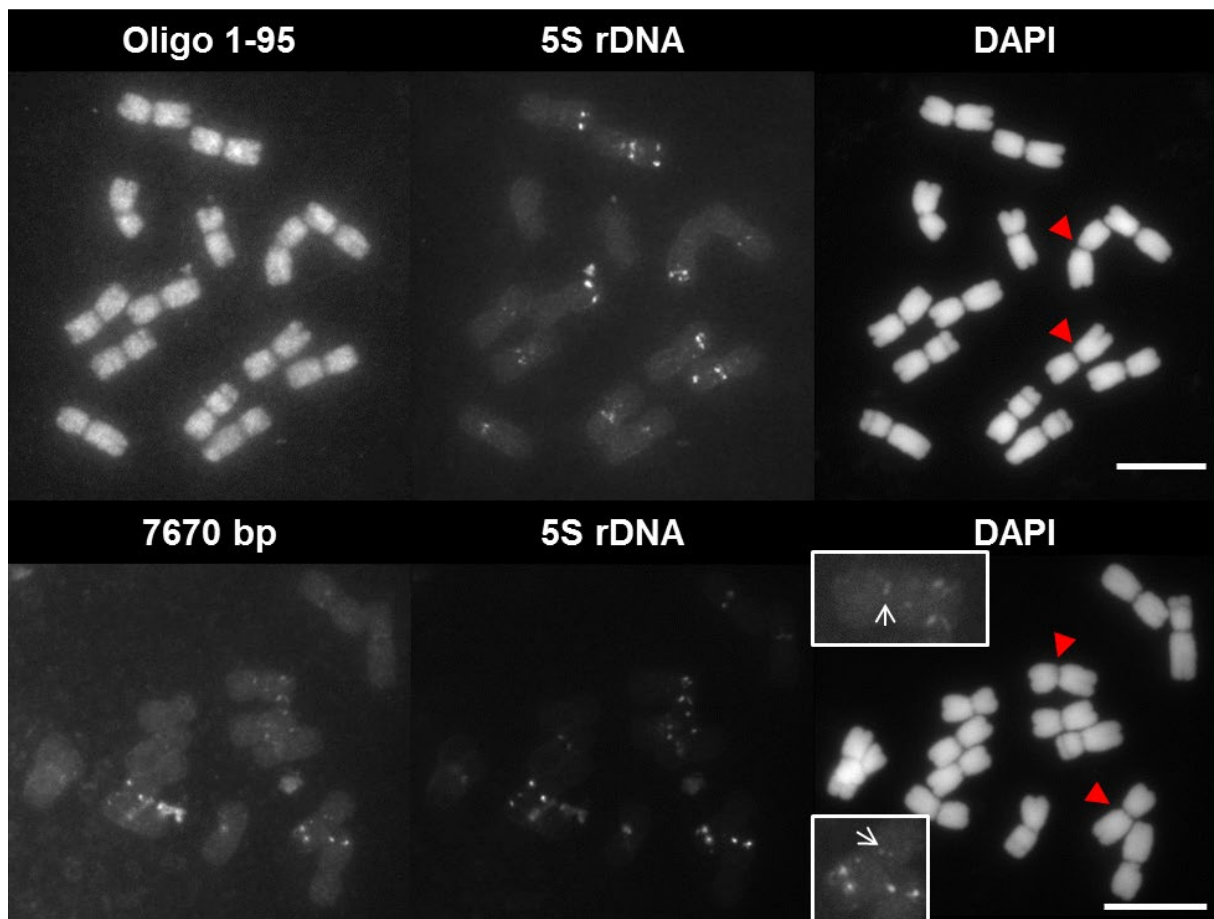


Figure 25| Detection of a single copy sequence on 3H of barley by CuAAC-labelled FISH probes. Representative images of the CuAAC-labelled oligonucleotide probe mix (Oligo 1-95) hybridized to barley metaphase chromosomes. Chromatin was counterstained with DAPI. To identify the chromosome 3H (red arrow heads), probes directed against the 5S rDNA gene family were applied in parallel. As a control, FISH using NT-labelled 7670 probes (7670 bp) to detect the single copy region was performed. Equal amounts of the CuAAC-labelled and the NT-labelled probes were used for FISH and images were acquired with identical microscope settings. In case of the NT-labelled probes, the signals were observed as expected on the chromosomes 3H (white arrows in the inset boxes), whereas the CuAAC-labelled probe showed a uniform staining along all chromosomes. Note that fluorescent crosstalk caused also the detection of the 5S rRNA probe in the channel of the 7670 bp probe, resulting in more than the expected two signals per chromosome. Scale bars 10 μ m.

For a systematic analysis of this unexpected unspecific hybridization signals caused by the *pre*-hybridization CuAAC-labelled oligonucleotide probe mix, we carried out various control experiments.

First, the probe mix was purified using a nucleotide removal Kit (Qiagen) to remove potential leftovers of the click reaction compounds, e.g. copper, that could interfere with the FISH. Moreover, different concentrations (27 ng/slide, 270 ng/slide, and 2.7 μ g/slide) of the oligonucleotide probe mix were tested to examine whether the unspecific hybridization signals occur in a concentration-dependent manner (Figure 26). Despite using different concentrations of the purified *pre*-hybridization CuAAC-labelled oligonucleotide probe mix, we obtained no specific single copy FISH signal. However, a concentration-dependent increase in the uniform hybridization signal was

observed. Notably, already at a concentration of 270 ng/slide the used microscopic settings (exposition time) led to an oversaturation of the signal intensity of the oligo 1-95 image.

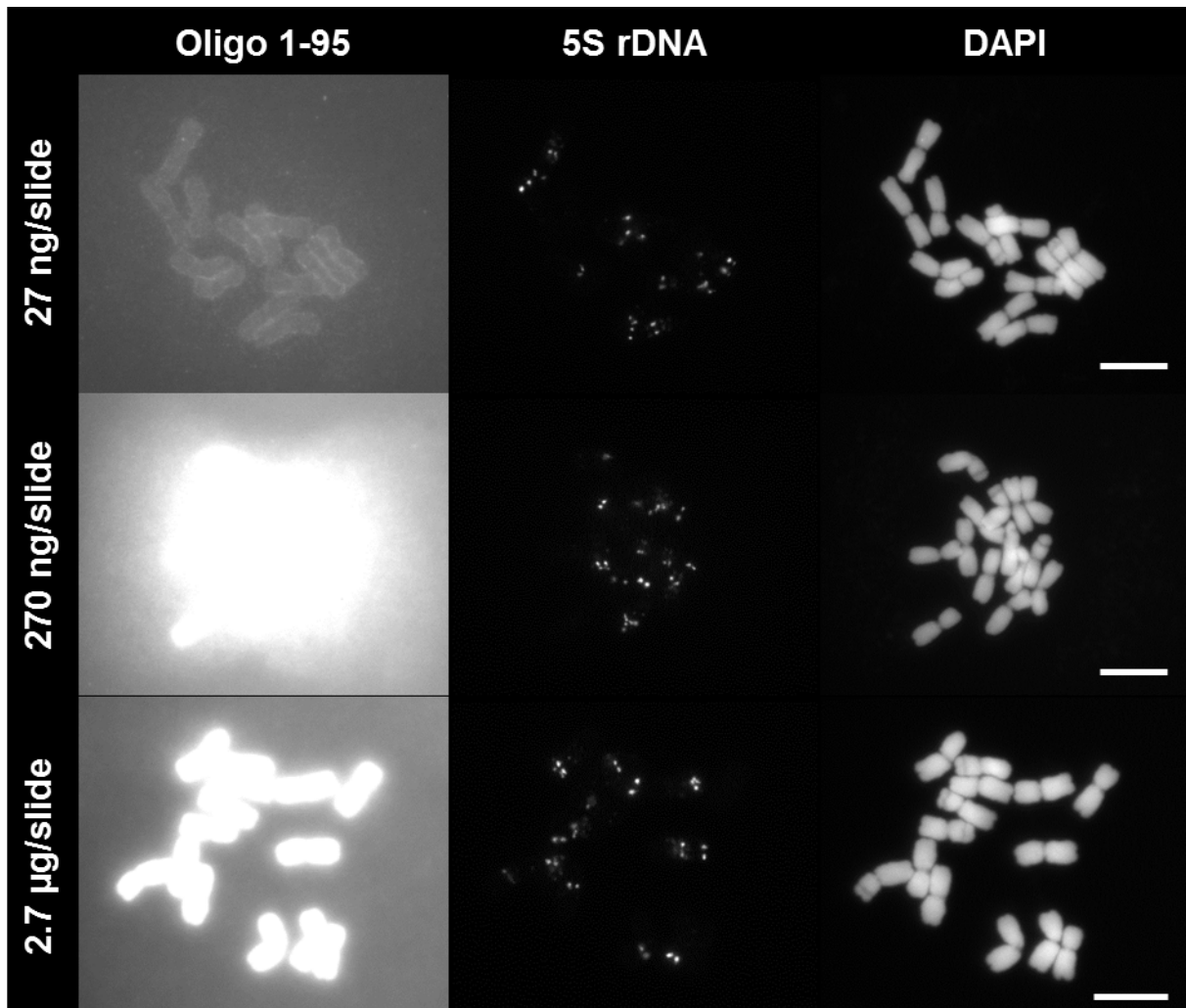


Figure 26 | Purification of the CuAAC-labelled oligonucleotide FISH probe did not result in specific hybridization signals. To remove remaining click reaction compound traces from the CuAAC-labelled probes, the oligonucleotide mix (Oligo 1-95) was purified by a QIAQuick nucleotide removal Kit (Qiagen). In addition, three different concentrations of the probe mix were tested. All pictures of the oligonucleotide mix were taken with identical microscope settings and exposure time (1500 ms). To identify the chromosomes, probes directed against the 5S rDNA gene family were applied and chromatin was counterstained with DAPI. Nevertheless, the unspecific hybridization signal of the oligonucleotide probe mix still occurred in a concentration-dependent manner. Scale bar 10 μm .

Given that the *pre*-hybridization CuAAC-labelled oligonucleotides seemingly hybridize specifically along all chromosomes, we assumed that one or more of the used oligonucleotides bind to disperse sequences of the barley genome. To examine this, we split the probe mix into 5 pools of 20 oligonucleotides each (pool 1: A1-A19, pool 2: A20-A38, pool 3: A39-A57, pool 4: A58- A76, pool 5: A77- A95; Figure 27). If a single oligonucleotide causes the observed all over labelling of the chromosomes, only the probe pool containing this particular oligonucleotide should give a similar

staining, whereas all other probe pools should yield no disperse fluorescent signal. The five oligonucleotide pools were used with a concentration of 800 ng/slide and all microscope settings were identical to allow a comparison to the NT-labelled control. Nonetheless, all 5 probe pools showed the uniform fluorescent staining of the entire chromosome complement in contrast to the control (Figure 27). Pool 2 and 5 were characterized by the weakest staining, which, however, still exceeded that of the NT-labelled 7670 bp probes. These results indicate that either in every pool at least one oligonucleotide binds to an unknown disperse repetitive sequence, or the observed staining pattern is not caused by a sequence-specific binding. In cooperation with Dr. Thomas Schmutzer (IPK, Gatersleben), we analysed all oligonucleotides sequences for their frequency in the *H. vulgare* genome by the program Kmasker (<http://webblast.ipk-gatersleben.de/kmasker> (Schmutzer et al. 2014)). The resulting k-mer values are presented in the appendix table 2. Indeed, none of the oligonucleotides exceeded a value of 5.5, implying that binding to repetitive sequences binding is very unlikely the reason for the observed hybridization signals along the chromosomes.

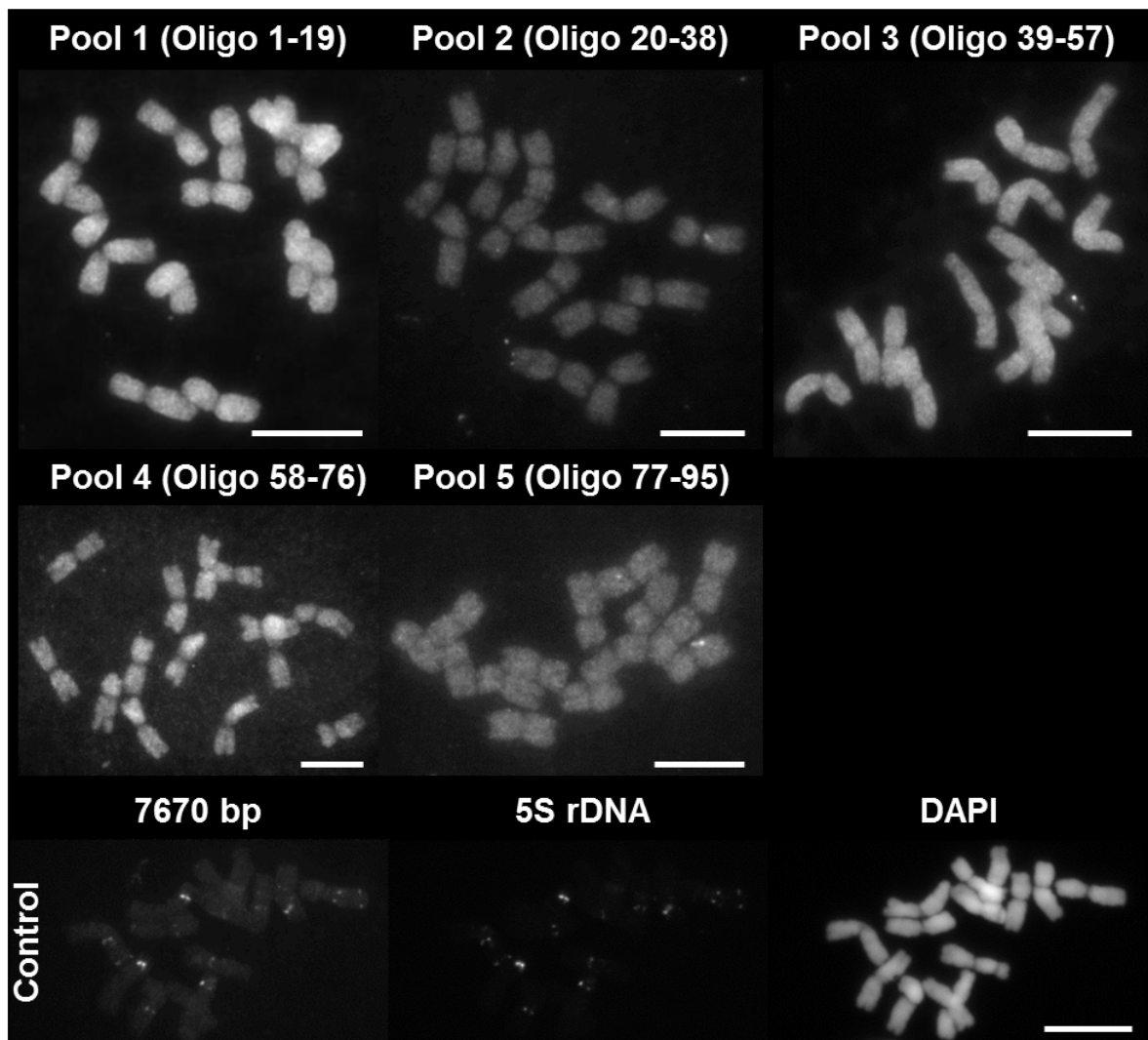


Figure 27 | Characterization of the uniform labelling of the CuAAC-labelled oligonucleotide FISH probes by splitting the mix. To identify whether single oligonucleotides or the general application of the probes caused the uniform staining of chromosomes, the oligonucleotide mix was split into 5 pools of 20 probes each and applied separately on metaphase chromosomes of barley. As a control, hybridization with the NT-labelled 7670 bp probes to detect the single copy region of chromosome 3H was performed. The fluorescence of the CuAAC- and NT-labelled probes was acquired with identical microscope settings and exposure time (1500 ms). All 5 probe pools showed a uniform staining of the entire chromosome complement, suggesting either a general problem of the CuAAC-labelled oligonucleotide probes or an (un)specific binding of multiple oligonucleotides. Note that channel-to-channel crosstalk also caused the detection of the 5S rRNA probe in the channel of the NT-labelled 7670 bp probe. Scale bars 10 μ m.

To rule out the possibility that the observed uniform staining of chromosomes is a result of the *pre*-hybridization click reaction of the oligonucleotides, we also tested the *post*-hybridization click reaction (Figure 28). For this purpose, the alkyne-bearing oligonucleotide probe mix was hybridized to barley metaphase chromosomes. Subsequently, the CuAAC labelling with 5-TAMRA-azide was performed on slides. Unfortunately, also the *post*-hybridization CuAAC labelling led to uniform signals so that no single copy specific FISH signals were detected (Figure 28).

Another reason for our observed uniform staining could be the slide preparation technique. To test this, in additional experiments we used of an alternative technique for slide preparation, which is known to efficiently remove cytoplasm. However, the uniform fluorescence was nonetheless evident

after using the *pre*-hybridization CuAAC-labelled oligonucleotide probe mix (810 ng/slide; Figure 28). To further investigate the potential cause of the dispersed labelling, we also performed a single copy FISH using the same *pre*-hybridization CuAAC-labelled oligonucleotide probe mix (270 ng/slide) on *S. cereale* metaphase chromosomes. A comparable accumulation of signals at the periphery of the chromosomes was found after hybridization. Therefore, we can also exclude a species-dependent reason of the uniformly distributed labelling (Figure 28).

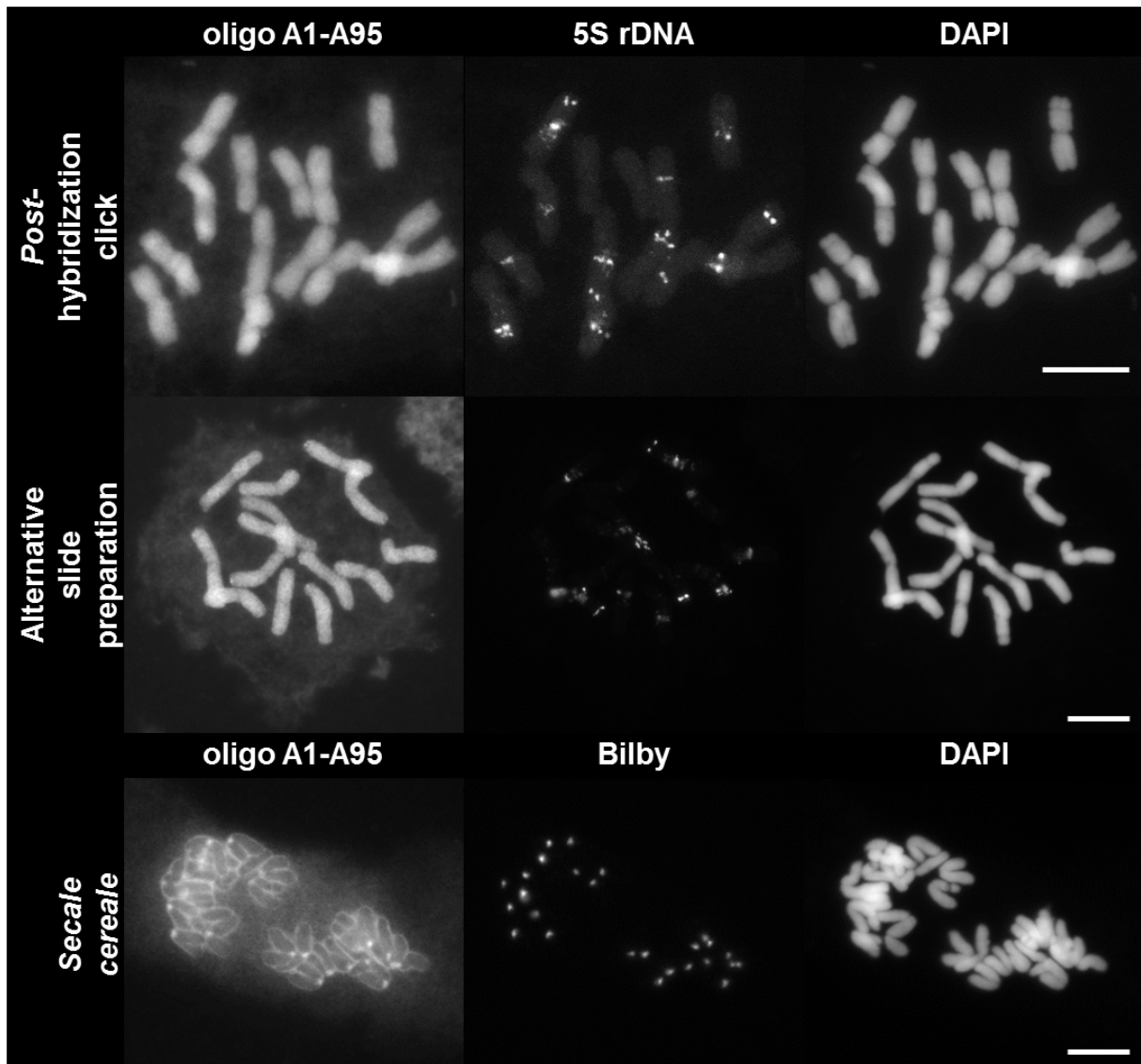


Figure 28 | Alternative strategies to prevent the uniform binding of the CuAAC-labelled oligonucleotide FISH probe mix. Chromatin was counterstained with DAPI. To identify the barley metaphase chromosomes, a 5S rDNA-specific FISH probe was used. Rye chromosomes were marked by a probe directed against the centromere-specific repeat Bilby. FISH using the unlabelled oligonucleotide mix followed by a *post*-hybridization click reaction did not decrease the disperse fluorescent staining. Moreover, the use of an alternative squashing technique to prepare the barley metaphase chromosomes did not reduce this uniform labelling. Application of the mix to *S. cereale* metaphase chromosomes revealed a comparable accumulation of signals at the periphery of all chromosomes and thereby excludes a species-specific phenomenon. Scale bars 10 μ m.

Furthermore, we tested two additional factors that could potentially cause the observed uniform chromosome staining, namely the use of dextran sulphate and high pH. It is known that polymers like dextran sulphate (DS) improve the localization of FISH probes by lowering the viscosity of the hybridization buffer and increase the probe concentration (Kosar et al. 1995, van Gijlswijk et al. 1996, Rocha et al. 2016). To test whether DS has a positive effect on the *pre*-hybridization-labelled oligonucleotides probe mix, the DS-free hybridization buffer was exchanged against a DS-containing one (20% dextran sulphate; 50% deionized formamide; 2x SSC, 0.05M phosphate buffer pH 7.0 (0.5 M Na₂HPO₄ pH 9.0; 0.5M NaH₂PO₄ pH 4.0) solved in ddH₂O) and FISH was performed as described before. The dextran sulphate treatment also did not show any improvement on the uniform probe staining and no specific single copy FISH signals were detected (data not shown).

Finally, we tested the influence of a higher pH of the hybridization solution on our FISH results. The pH of a DNA-containing solution is known to affect the ionization of nucleotides. While a pH in the range between 5 and 9 leaves all bases uncharged and hybridization occurs without interference, a higher pH deprotonates guanine, thymine and uracil bases, thereby hindering the pairing of the single-stranded probes through an increase in electrostatic repulsion (Blackburn et al. 2006, Viereggs 2010). Additionally, a higher pH increases the solubility of the 5-TAMRA labelled probe in water.

To examine the impact of high pH, we treated the *pre*-hybridization-labelled oligonucleotide mix with ammonia. Unfortunately, this additional treatment had no effect on the staining of the entire chromosomes (data not shown).

Thus, despite various attempts and several modifications of the protocol aimed to minimize the uniform chromosome staining of the CuAAC-labelled oligonucleotide FISH probe mix; we did not identify the reason of uniformly distributed fluorescence. Notably, a similar problem was not experienced with any of the high-copy oligonucleotide FISH probes labelled *via* CuAAC. Thus, the observed phenomenon is specific for our single copy gene probes and should therefore be taken into account particularly in applications with single copy detection.

2.6 Discussion

2.6.1 CuAAC-labelled probes are suitable for reliable detection of repetitive sequences

FISH is a powerful technique to visualize the chromosomal location of a sequence of interest within a genome. Since its first use in *Drosophila* polytene chromosomes in 1982, many variations of FISH have been developed for different applications, e.g. the detection of repetitive elements and single copy genes on chromosomes, integration of physical and genetic maps, or the detection of chromosomal translocations (Langer-Safer et al. 1982, Khrustaleva et al. 2001, Szinay et al. 2008, Ren et al. 2009, Tang et al. 2014). Besides, requirement of appropriately prepared specimens, availability of robust probes is an ultimate prerequisite for successful FISH. As the cost of DNA synthesis substantially dropped in the last years, fluorescent 3'- and/or 5'-end labelled oligonucleotides became an attractive alternative to the frequently used NT-labelled FISH probes. Fluorescently-labelled nucleotides offer several advantages, including more consistent probe quality, and reduction of cost and time needed for probe preparation (Cox et al. 2004, Fu et al. 2015, Jiang 2019). The end-labelling technique generally limits the amount of fluorescent labels to one or two, however the sensitivity of the oligonucleotide probe can be enhanced by increasing the labelling rate (Cox et al. 2004). To achieve higher degree of labelling, oligonucleotides can be rendered fluorescent by conjugation of modified nucleotides during synthesis (Danilova et al. 2012). In this study, we investigated the suitability of the CuAAC reaction for an efficient labelling of oligonucleotide FISH probes with fluorochromes. Furthermore, we employed such CuAAC-labelled FISH probes for the detection of repetitive and single copy sequences.

As a proof-of-principle, first we synthesized oligonucleotides of different length (21 bp/ 28 bp) and various fluorophor numbers (2-4) recognizing the *Arabidopsis*-type telomere sequence (TTTAGGG)_n. We limited the amount of modified nucleotides to a maximum of 4, as higher labelling rates caused a precipitation of the probes in aqueous solutions, which impedes an application for FISH protocols. Our *pre*-hybridization CuAAC-labelled probes reliably detected telomeres of barley and *A. thaliana*, thus corroborating recent study using 5'-end labelled oligonucleotide telomere probes (Waminal et al. 2018). We did not observe a qualitative difference in the efficiency of telomere detection between the two tested probe lengths and label amounts. Unfortunately, a precise quantification and direct comparison of fluorescence intensities of the telomere signals detected by the differently labelled probes were not feasible, primarily due to strong variability in signal density and telomere distribution, a pronounced 3D structure of sorted nuclei, as well as differences in the telomere size between individual chromosomes (Wang et al. 1991). Therefore, the detection of DNA target sequences of an invariable length requires further investigation.

Although, we could not confirm whether the amount of fluorescent tags in the oligonucleotide probes correlates with the telomere signal intensity, we verified that CuAAC-labelled probes are suitable for the detection of telomeres of barley and *A. thaliana*. To compare the efficiency of the CuAAC-labelled oligonucleotide probes with that of 5'-end labelled oligonucleotides and a NT-labelled telomere probe, next we performed FISH experiments using flow-sorted nuclei of two *A. thaliana* ecotypes that are characterized by either short (Hov, ~1 kb) or long (Pro, ~9.3 kb) telomeres (Fulcher et al. 2015). Regardless of the used labelling approach, we found significantly fewer FISH signals in the Hov ecotype as compared to the Pro ecotype. As the detection sensitivity of FISH is limited to approx. 700 bp (Khrustaleva et al. 2016), the lower number of telomere repeats in the ecotype Hov could, at least partially, reflect that their short length falls beyond the range of reliable detection. Furthermore, earlier studies in Syrian hamster fibroblasts and *Drosophila melanogaster* demonstrated that telomere clustering can also occur in interphase nuclei (Solovjeva et al. 2012, Wesolowska et al. 2013). Given that comparative data on the telomere organization of different *Arabidopsis* ecotypes at interphase are missing, one could speculate that the different numbers of signals detected in Hov and Pro could indicate differences in clustering of telomeres between these ecotypes. Nevertheless, in both *Arabidopsis* ecotypes we observed a lower performance for the NT-labelled probes. The enhanced performance of oligonucleotide probes found in our study was likely caused by their improved hybridization abilities due to the smaller size and the lower complexity as compared to NT-labelled probes (Bradley et al. 2009). It should also be noted that the efficiency of DNA polymerase I used in the NT to incorporate fluorescently labelled deoxynucleotides is low, reaching around 2-10% of labelling (Yu et al. 1994, Kato et al. 2006). In addition, CuAAC-labelled telomere probes possessing 2 to 4 fluorochromes have a higher labelling rate than the NT-labelled probes, which could also account for the improved probe performance. Same applies for the 5'-end labelled probes, since even a single fluorophore per oligonucleotide outcompetes the NT-labelled probes in terms of label number.

Oligonucleotide probes detecting simple sequence repeats are widely used to investigate the chromosomal organization of such repeats in plant genomes and to identify plant chromosomes (Schmidt et al. 1996, Cuadrado et al. 1998, Fuchs et al. 1998, Tang et al. 2014, Fu et al. 2015, Tang et al. 2016). We found that *pre*-hybridization CuAAC-labelled oligonucleotides directed against the simple sequence repeat (CTT)_n yielded robust signals on wheat metaphase chromosomes that are comparable to FISH signals reported earlier (Pedersen et al. 1997). Moreover, the *pre*-hybridization CuAAC-labelled telomere and (CTT)_n probes also detected the target sequences when combined with immunohistochemistry and DNA replication assay *via* EdU uptake. This finding provided an important evidence that these probes can serve as reliable tools also in combinatorical cytological analyses involving several approaches in a single experiment. Moreover, our study revealed that the

performance of the CuAAC reaction on-slide (*post*-hybridization CuAAC labelling) results in signals comparable to that of the *pre*-hybridization CuAAC-labelled telomere and (CTT)_n FISH probes. Unfortunately, we could not achieve a reliable *post*-hybridization labelling of the CuAAC telomere and (CTT)_n probes on chromosome preparations fixed by paraformaldehyde. Given that the fixation of cells with formaldehyde before *post*-hybridization CuAAC labelling is recommended in the DNA synthesis-based cell proliferation assays using EdU incorporation for labelling *de novo* synthesized DNA (see manual Click-iT™ EdU Alexa Fluor™ 488 HCS Assay, cat. No. C10350, Invitrogen), we therefore assume that a further modification of our protocol is needed to successfully perform *post*-hybridization CuAAC labelling on immunohistochemistry-compatible slides.

2.6.2 Single copy FISH using CuAAC-labelled oligonucleotide probes requires optimization

Despite the variety of probes, labelling techniques, signal-detection systems, and advanced imaging techniques, FISH detection of single copy sequences in a range of few kilobases and below remains challenging. The two factors that are crucial for successful high resolution FISH are the quality of chromosome preparations and the sensitivity and robustness of probes (Jiang 2019). Recently, several approaches to improve the technique of chromosome preparation, which is applicable for single copy FISH, have been reported for several plants including barley (Aliyeva-Schnorr et al. 2015, Jiang 2019). On the other hand, synthetic oligonucleotide FISH probes were proven to be suitable for the detection of single copy DNA sequences and to offer an enhanced performance over clone-based FISH probes (Boyle et al. 2011, Yamada et al. 2011, Beliveau et al. 2012).

Using a reliable protocol to perform single copy FISH in barley previously established in our laboratory (Aliyeva-Schnorr et al. 2015), in this study we investigated whether *pre*-hybridization CuAAC-labelled oligonucleotides are suitable for detection of a 7670 bp single copy sequence of the barley chromosome 3H. A pool of 67 oligonucleotides was reported earlier to be sufficient in human to generate FISH signals of a 7.8 kb single gene region (Yamada et al. 2011). However, our probe mixture containing 95 oligonucleotides did not result in specific signals, but yielded rather in a uniform distribution of signals across all chromosomes. In contrast, we successfully detected the same 7670 bp-long sequence using NT-labelled probes and thereby ruled out the quality of slides and the FISH procedure as potential causes of the problem with the oligonucleotide probe-based detection.

To our knowledge, this phenomenon of uniform oligonucleotide binding to DNA was not described in literature yet. Several causes could account for the observed unspecific staining. First, the unspecific fluorescence could arise due to the oligonucleotide probe mixture detecting noise-generating repetitive elements. Indeed, additional purification of the oligonucleotides to remove potential

leftovers of the click reaction did not improve the FISH results. Moreover, our observation that the intensity of the all over staining of chromosomes and nuclei depends on the concentration of the pooled CuAAC-labelled oligonucleotide probes favours the assumption that the oligonucleotides themselves cause the uniform hybridization or DNA binding. However, splitting the initial probe mix into smaller sets of oligonucleotides did not result in an identification of single oligonucleotides responsible for the observed staining along the chromosomes. The *in silico* prediction of problematic oligonucleotide sequences using the Kmasker tool also revealed no repetitive sequence motif. Kmasker evaluates the frequency of the oligonucleotide sequences within a reference genome. Considering a frequency of one as a unique sequence, our calculated low values of the oligonucleotides ranged 1 to 5.5 provided no indication of repetitive sequences. It is tempting to speculate that a more stringent selection of oligonucleotides having frequencies in a range of 1 to 2 might lead to an improvement of the probe quality. The complete sequence data of the barley genome was not available at the time of analysis, hence the calculated frequencies can be considered only as an approximation. Moreover, the Kmasker tool was not designed to analyse short sequences. Thus, our result should be considered with certain caution.

Importantly, the hybridization of the oligonucleotide probe mix to rye chromosomes showed a similar uniform labelling. Either rye also possesses the same repetitive elements that are detected by the CuAAC-labelled probes, or the observed all over staining is caused by an unspecific binding to the chromosomes. The fact that neither modification of the FISH procedure (e.g., the change of the pH and the slide preparation or post-hybridization CuAAC labelling) improved the FISH results implies a strong interaction of the oligonucleotide probes with the DNA. Since all 95 alkyne-labelled FISH probes derived from the same batch of synthesis, we cannot rule out the possibility that the observed uniform staining of the chromosomes stems from an unknown mistake during the probe synthesis. In this context, a comparison of the CuAAC-labelled 95 oligonucleotides to the same mixture of probes labelled by e.g., end labelling would allow to evaluate whether the CuAAC labelling itself causes the observed problems.

Further optimization of our protocol is required to judge whether a specific single copy FISH signal of the 7670 bp long sequence was present but was masked by unspecific staining. A promising direction for such optimization involves the optimization of the probe design. In several studies, the detection of specific chromosomal regions or entire chromosomes relied on the optimization of the oligonucleotide probe design using single copy sequence prediction tools such as *Chorus* or *OligoArray 2.0* (Rouillard et al. 2003, Beliveau et al. 2012, Beliveau et al. 2015, Han et al. 2015). Whereas the *Chorus* software is able to predict repetitive sequence-free oligonucleotides suitable as FISH probes, in the *OligoArray 2.0* software the thermodynamic parameters, including

oligonucleotide length, melting temperature and GC content, are taken into account to achieve an optimization of the probes.

Lastly, the observed uniform labelling could be also caused by a yet unknown biochemical reaction(s). Identification and characterization of such reaction(s) would require an extensive analysis of biochemical interactions that falls far beyond the scope of our study. In future experiments, the causes of the unspecific chromosome labelling will be addressed in detail and additional efforts will be invested into the optimization of the probe design by aforementioned tools.

2.6 Summary

Here, we tested an alternative technique to label double and single stranded DNA probes by use of the Cu(I)-catalysed azide-alkyne cycloaddition (CuAAC) for its suitability for FISH. We showed that CuAAC-labelled probes represent a reliable tool to detect different types of repetitive sequences on chromosomes and nuclei. Comparison between different labelling techniques revealed a comparable sensitivity of CuAAC probes to that of conventionally labelled probes. Importantly, we demonstrated that the CuAAC reaction-based labelling technique can be combined with immunohistochemistry and cell proliferation assays *via* 5-Ethynyl-deoxyuridine (EdU) without loss of sensitivity. Thus the CuAAC reaction-based labelling technique could be considered as a valid and flexible tool in cytogenetics and cell biology. The application of CuAAC probes to detect a single copy sequence unfortunately resulted in a uniform labelling along the entire chromosomes and needs further studies to be optimized.

2.7 Outlook

The data derived from this study imply the following questions to be addressed in future:

2. Development of CuAAC-labelled probes to detect also repetitive sequences with a longer monomer length than microsatellites.
3. Optimization of single copy sequence detection through probe design using software tools such as *Chorus* or *OligoArray 2.0* or design of probes with a longer oligonucleotide length.
4. Application of CuAAC labelling to RNA for detection of gene transcripts *in situ*.
4. Evaluation of the nick translation method as an alternative procedure to label FISH probes with alkyne-modified dNTPs.

3. References

- Abirached-Darmency, M., Zickler, D. and Cauderon, Y.** (1983). Synaptonemal complex and recombination nodules in rye (*Secale cereale*). *Chromosoma* 88, 299-306
- Aliyeva-Schnorr, L., Beier, S., Karafiatova, M., Schmutzer, T., Scholz, U., Dolezel, J., et al.** (2015). Cytogenetic mapping with centromeric bacterial artificial chromosomes contigs shows that this recombination-poor region comprises more than half of barley chromosome 3H. *Plant J* 84, 385-394
- Aliyeva-Schnorr, L., Ma, L. and Houben, A.** (2015). A fast air-dry dropping chromosome preparation method suitable for FISH in plants. *J Vis Exp*, e53470
- Appels, R., L. B. Moran and J. P. Gustafson** (1986). Rye heterochromatin. I. Studies on clusters of the major repeating sequence and the identification of a new dispersed repetitive sequence element. *Canadian Journal of Genetics and Cytology* 28, 645-657
- Armstrong, S. J., Caryl, A. P., Jones, G. H. and Franklin, F. C.** (2002). Asy1, a protein required for meiotic chromosome synapsis, localizes to axis-associated chromatin in *Arabidopsis* and *Brassica*. *J Cell Sci* 115, 3645-3655
- Armstrong, S. J., Franklin, F. C. and Jones, G. H.** (2001). Nucleolus-associated telomere clustering and pairing precede meiotic chromosome synapsis in *Arabidopsis thaliana*. *J Cell Sci* 114, 4207-4217
- Armstrong, S. J., Fransz, P., Marshall, D. F. and Jones, G. H.** (1998). Physical mapping of DNA repetitive sequences to mitotic and meiotic chromosomes of *Brassica oleracea* var. *alboglabra* by fluorescence in situ hybridization. *Heredity* 81, 666-673
- Bahler, J., Wyler, T., Loidl, J. and Kohli, J.** (1993). Unusual nuclear structures in meiotic prophase of fission yeast: a cytological analysis. *J Cell Biol* 121, 241-256
- Banaei-Moghaddam, A. M., Schubert, V., Kumke, K., Weibeta, O., Klemme, S., Nagaki, K., et al.** (2012). Nondisjunction in favor of a chromosome: the mechanism of rye B chromosome drive during pollen mitosis. *Plant Cell* 24, 4124-4134
- Baroux, C. and V. Schubert** (2018). "Technical review: microscopy and image processing tools to analyze plant chromatin: practical considerations." *Methods Mol Biol* 1675, 537-589
- Bass, H. W., Marshall, W. F., Sedat, J. W., Agard, D. A. and Cande, W. Z.** (1997). Telomeres cluster *de novo* before the initiation of synapsis: a three-dimensional spatial analysis of telomere positions before and during meiotic prophase. *J Cell Biol* 137, 5-18
- Beliveau, B. J., Boettiger, A. N., Avendano, M. S., Jungmann, R., McCole, R. B., Joyce, E. F., et al.** (2015). Single-molecule super-resolution imaging of chromosomes and *in situ* haplotype visualization using Oligopaint FISH probes. *Nat Commun* 6, 7147
- Beliveau, B. J., Joyce, E. F., Apostolopoulos, N., Yilmaz, F., Fonseka, C. Y., McCole, R. B., et al.** (2012). Versatile design and synthesis platform for visualizing genomes with Oligopaint FISH probes. *Proc Natl Acad Sci U S A* 109, 21301-21306
- Bennett, M. D. and Kaltsike.Pj** (1973). Duration of Meiosis in a Diploid Rye, a Tetraploid Wheat and Hexaploid Triticale Derived from Them. *Canadian Journal of Genetics and Cytology* 15, 654-654

- Bhalla, N. and Dernburg, A. F.** (2008). Prelude to a division. *Annu Rev Cell Dev Biol* 24, 397-424
- Bickel, J. S., Chen, L., Hayward, J., Yeap, S. L., Alkers, A. E. and Chan, R. C.** (2010). Structural maintenance of chromosomes (SMC) proteins promote homolog-independent recombination repair in meiosis crucial for germ cell genomic stability. *PLoS Genet* 6, e1001028
- Blackburn, G. M., Gait, M. J., Loakes, D. and M., W. D.** (2006). Nucleic Acids in Chemistry and Biology. *The Royal Society of Chemistry Publishing, Dorset, United Kingdom* 3rd Edition
- Blunden, R., Wilkes, T. J., Forster, J. W., Jimenez, M. M., Sandery, M. J., Karp, A., et al.** (1993). Identification of the E3900 family, a 2nd family of rye chromosome-B specific repeated sequences. *Genome* 36, 706-711
- Bolcun-Filas, E., Costa, Y., Speed, R., Taggart, M., Benavente, R., De Rooij, D. G., et al.** (2007). SYCE2 is required for synaptonemal complex assembly, double strand break repair, and homologous recombination. *J Cell Biol* 176, 741-747
- Bolcun-Filas, E., Hall, E., Speed, R., Taggart, M., Grey, C., de Massy, B., et al.** (2009). Mutation of the mouse *Syce1* gene disrupts synapsis and suggests a link between synaptonemal complex structural components and DNA repair. *PLoS Genet* 5, e1000393
- Bougourd, S. M. and Parker, J. S.** (1975). B chromosome system of *Allium schoenoprasum* .1. B distribution. *Chromosoma* 53, 273-282
- Boveri, T.** (1892). Befruchtung. *Ergebnisse der Anatomie und Entwicklungsgeschichte* 1, 1981
- Boyle, S., Rodesch, M. J., Halvensleben, H. A., Jeddloh, J. A. and Bickmore, W. A.** (2011). Fluorescence *in situ* hybridization with high-complexity repeat-free oligonucleotide probes generated by massively parallel synthesis. *Chromosome Res* 19, 901-909
- Bradley, S., Zamechek, L. and Aurich-Costa, J.** (2009). Oligonucleotide FISH Probes. *Fluorescence In Situ Hybridisation (FISH)- Application Guide* 1, 67-73
- Bugrov, A. G., Karamysheva, T. V., Perepelov, E. A., Elisaphenko, E. A., Rubtsov, D. N., Warchalowska-Sliwa, E., et al.** (2007). DNA content of the B chromosomes in grasshopper *Podisma kanoi* Storozh. (*Orthoptera, Acrididae*). *Chromosome Res* 15, 315-326
- Burley, G. A., Gierlich, J., Mofid, M. R., Nir, H., Tal, S., Eichen, Y., et al.** (2006). Directed DNA metallization. *J Am Chem Soc* 128, 1398-1399
- Burrows, C. J. and Muller, J. G.** (1998). Oxidative nucleobase modifications leading to strand scission. *Chem Rev* 98, 1109-1152
- Byers, B. and L. Goetsch** (1975). Electron microscopic observations on the meiotic karyotype of diploid and tetraploid *Saccharomyces cerevisiae*. *Proc Natl Acad Sci U S A* 72, 5056-5060
- Cahoon, C. K. and R. S. Hawley** (2016). Regulating the construction and demolition of the synaptonemal complex. *Nat Struct Mol Biol* 23, 369-377
- Cai, X., Dong, F., Edelman, R. E. and Makaroff, C. A.** (2003). The *Arabidopsis* SYN1 cohesin protein is required for sister chromatid arm cohesion and homologous chromosome pairing. *J Cell Sci* 116, 2999-3007

- Carchilan, M., Delgado, M., Ribeiro, T., Costa-Nunes, P., Caperta, A., Morais-Cecilio, L., et al.** (2007). Transcriptionally active heterochromatin in rye B chromosomes. *Plant Cell* 19, 1738-1749
- Carlton, P. M. and Cande, W. Z.** (2002). Telomeres act autonomously in maize to organize the meiotic bouquet from a semipolarized chromosome orientation. *J Cell Biol* 157, 231-242
- Carlton, P. M., Cowan, C. R. and Cande, W. Z.** (2003). Directed motion of telomeres in the formation of the meiotic bouquet revealed by time course and simulation analysis. *Mol Biol Cell* 14, 2832-2843
- Caryl, A. P., Armstrong, S. J., Jones, G. H. and Franklin, F. C.** (2000). A homologue of the yeast HOP1 gene is inactivated in the *Arabidopsis* meiotic mutant *asy1*. *Chromosoma* 109, 62-71
- Chan, T. R., Hilgraf, R., Sharpless, K. B. and Fokin, V. V.** (2004). Polytriazoles as copper(I)-stabilizing ligands in catalysis. *Org Lett* 6, 2853-2855
- Chelysheva, L., Vezon, D., Chambon, A., Gendrot, G., Pereira, L., Lemhemdi, A., et al.** (2012). The *Arabidopsis* HEI10 is a new ZMM protein related to Zip3. *PLoS Genet* 8, e1002799
- Cheng, Y. M. and Lin, B. Y.** (2003). Cloning and characterization of maize B chromosome sequences derived from microdissection. *Genetics* 164, 299-310
- Chikashige, Y., Ding, D. Q., Funabiki, H., Haraguchi, T., Mashiko, S., Yanagida, M., et al.** (1994). Telomere-led premeiotic chromosome movement in fission yeast. *Science* 264, 270-273
- Cleland, R. E.** (1951). Extra, Diminutive Chromosomes in *Oenothera*. *Evolution* 5, 165-176
- Colas, I., Darrier, B., Arrieta, M., Mittmann, S. U., Ramsay, L., Sourdille, P., et al.** (2017). Observation of extensive chromosome axis remodeling during the "diffuse-phase" of meiosis in large genome cereals. *Front Plant Sci* 8, 1235
- Collins, K. A., Unruh, J. R., Slaughter, B. D., Yu, Z., Lake, C. M., Nielsen, R. J., et al.** (2014). Corolla is a novel protein that contributes to the architecture of the synaptonemal complex of *Drosophila*. *Genetics* 198, 219-228
- Colmsee, C., Beier, S., Himmelbach, A., Schmutzer, T., Stein, N., Scholz, U., et al.** (2015). BARLEX - the Barley Draft Genome Explorer. *Mol Plant* 8, 964-966
- Comadran, J., Kilian, B., Russell, J., Ramsay, L., Stein, N., Ganai, M., et al.** (2012). Natural variation in a homolog of *Antirrhinum* CENTRORADIALIS contributed to spring growth habit and environmental adaptation in cultivated barley. *Nat Genet* 44, 1388-1392
- Conrad, M. N., Lee, C. Y., Chao, G., Shinohara, M., Kosaka, H., Shinohara, A., et al.** (2008). Rapid telomere movement in meiotic prophase is promoted by NDJ1, MPS3, and CSM4 and is modulated by recombination. *Cell* 133, 1175-1187
- Copsey, A., Tang, S., Jordan, P. W., Blitzblau, H. G., Newcombe, S., Chan, A. C., et al.** (2013). Smc5/6 coordinates formation and resolution of joint molecules with chromosome morphology to ensure meiotic divisions. *PLoS Genet* 9, e1004071
- Covert, S. F.** (1998). Supernumerary chromosomes in filamentous fungi. *Current Genetics* 33, 311-319

- Cowan, C. R. and Cande, W. Z.** (2002). Meiotic telomere clustering is inhibited by colchicine but does not require cytoplasmic microtubules. *J Cell Sci* 115, 3747-3756
- Cox, W. G. and Singer, V. L.** (2004). Fluorescent DNA hybridization probe preparation using amine modification and reactive dye coupling. *Biotechniques* 36, 114-122
- Cuadrado, A. and Schwarzacher, T.** (1998). The chromosomal organization of simple sequence repeats in wheat and rye genomes. *Chromosoma* 107, 587-594
- D'Ambrosio, U., Alonso-Lifante, M. P., Barros, K., Kovařík, A., Mas de Xaxars, G. and Garcia, S.** (2017). B-chrom: a database on B-chromosomes of plants, animals and fungi. *New Phytologist* 216, 635-642
- Danilova, T. V., Friebe, B. and Gill, B. S.** (2012). Single-copy gene fluorescence *in situ* hybridization and genome analysis: Acc-2 loci mark evolutionary chromosomal rearrangements in wheat. *Chromosoma* 121, 597-611
- De Muyt, A., Zhang, L., Piolot, T., Kleckner, N., Espagne, E. and Zickler, D.** (2014). E3 ligase Hei10: a multifaceted structure-based signaling molecule with roles within and beyond meiosis. *Genes Dev* 28, 1111-1123
- de Vries, F. A., de Boer, E., van den Bosch, M., Baarends, W. M., Ooms, M., Yuan, L., et al.** (2005). Mouse Sycp1 functions in synaptonemal complex assembly, meiotic recombination, and XY body formation. *Genes Dev* 19, 1376-1389
- Demidov, D., Hesse, S., Tewes, A., Rutten, T., Fuchs, J., Ashtiyani, R. K., et al.** (2009). Aurora1 phosphorylation activity on histone H3 and its cross-talk with other post-translational histone modifications in *Arabidopsis*. *Plant J* 59, 221-230
- Dhar, M. K., Friebe, B., Koul, A. K. and Gill, B. S.** (2002). Origin of an apparent B chromosome by mutation, chromosome fragmentation and specific DNA sequence amplification. *Chromosoma* 111, 332-340
- Diez, M., Jimenez, M. M. and Santos, J. L.** (1993). Synaptic patterns of rye B chromosomes .2. The effect of the standard B chromosomes on the pairing of the a set. *Theoretical and Applied Genetics* 87, 17-21
- Dolezel, J., Binarova, P. and Lucretti, S.** (1989). Analysis of nuclear DNA content in plant cells by flow cytometry. *Biologia Plantarum* 31, 113-120
- Egel-Mitani, M., Olson, L. W. and Egel, R.** (1982). Meiosis in *Aspergillus nidulans*: another example for lacking synaptonemal complexes in the absence of crossover interference. *Hereditas* 97, 179-187
- Eisen, G.** (1900). The spermatogenesis of *Batrachoseps*. Polymorphous spermatogonia, auxocytes, and spermatocytes. *Journal of Morphology* 17, 1-117
- El-Sagheer, A. H. and Brown, T.** (2010). Click chemistry with DNA. *Chem Soc Rev* 39, 1388-1405
- Endo, T. R., Nasuda, S., Jones, N., Dou, Q., Akahori, A., Wakimoto, M., et al.** (2008). Dissection of rye B chromosomes, and nondisjunction properties of the dissected segments in a common wheat background. *Genes Genet Syst* 83, 23-30

- Esponda, P. and Gimenez-Martin, G.** (1972). The attachment of the synaptonemal complex to the nuclear envelope. An ultrastructural and cytochemical analysis. *Chromosoma* 38, 405-417
- Farmer, J. B. and Moore, J. E. S.** (1905). Memoirs: On the meiotic phase (reduction divisions) in animals and plants. *Quarterly Journal of Microscopical Science* s2-48, 489-558
- Fawcett, D. W.** (1956). The fine structure of chromosomes in the meiotic prophase of vertebrate spermatocytes. *J Biophys Biochem Cytol* 2, 403-406
- Fedotova, Y. S., Kolomiets, O. L. and Bogdanov, Y. F.** (1989). Synaptonemal complex transformations in rye microsporocytes at the diplotene stage of meiosis. *Genome* 32, 816-823
- Ferdous, M., Higgins, J. D., Osman, K., Lambing, C., Roitinger, E., Mechtler, K., et al.** (2012). Inter-homolog crossing-over and synapsis in *Arabidopsis* meiosis are dependent on the chromosome axis protein AtASY3. *PLoS Genet* 8, e1002507
- Francki, M. G.** (2001). Identification of Bilby, a diverged centromeric Ty1-copia retrotransposon family from cereal rye (*Secale cereale* L.). *Genome* 44, 266-274
- Fröst, S.** (1959). The cytological behaviour and mode of transmission of accessory chromosomes in *Plantago serria*. *Hereditas* 45, 191-210
- Fu, S., Chen, L., Wang, Y., Li, M., Yang, Z., Qiu, L., et al.** (2015). Oligonucleotide Probes for ND-FISH Analysis to Identify Rye and Wheat Chromosomes. *Sci Rep* 5, 10552
- Fuchs, J., Kuhne, M. and Schubert, I.** (1998). Assignment of linkage groups to pea chromosomes after karyotyping and gene mapping by fluorescent in situ hybridization. *Chromosoma* 107, 272-276
- Fukui, K., Kamisugi, Y. and Sakai, F.** (1994). Physical mapping of 5S rDNA loci by direct-cloned biotinylated probes in barley chromosomes. *Genome* 37, 105-111
- Fulcher, N., Teubenbacher, A., Kerdaffrec, E., Farlow, A., Nordborg, M. and Riha, K.** (2015). Genetic architecture of natural variation of telomere length in *Arabidopsis thaliana*. *Genetics* 199, 625-635
- Geci, I., Filichev, V. V. and Pedersen, E. B.** (2007). Stabilization of parallel triplexes by twisted intercalating nucleic acids (TINAs) incorporating 1,2,3-triazole units and prepared by microwave-accelerated click chemistry. *Chemistry* 13, 6379-6386
- Gelei, J.** (1922). Weitere Studien über die Oogenese des *Dendrocoelum lacteum*. III Die Konjugation der Chromosomen in der Literatur und meine Befunde. *Archiv f. Zellforsch.* 16, 299-370
- Gerton, J. L. and Hawley, R. S.** (2005). Homologous chromosome interactions in meiosis: diversity amidst conservation. *Nat Rev Genet* 6, 477-487
- Gierlich, J., Burley, G. A., Gramlich, P. M., Hammond, D. M. and Carell, T.** (2006). Click chemistry as a reliable method for the high-density postsynthetic functionalization of alkyne-modified DNA. *Org Lett* 8, 3639-3642
- Gill, J. J. B., Marchant, C. J., Mcleish, J., Jones, B. M. G. and Ockendon, D. J.** (1972). Distribution of Chromosome Races of *Ranunculus-Ficaria* L in British-Isles. *Annals of Botany* 36, 31-47
- Gillies, C. B.** (1974). The nature and extent of synaptonemal complex formation in haploid barley. *Chromosoma* 48, 441-453

- Gillies, C. B.** (1981). Electron microscopy of spread maize pachytene synaptonemal complexes. *Chromosoma* 83, 575-591
- Golubovskaya, I. N., Hamant, O., Timofejeva, L., Wang, C. J., Braun, D., Meeley, R., et al.** (2006). Alleles of *afd1* dissect REC8 functions during meiotic prophase I. *J Cell Sci* 119, 3306-3315
- Golubovskaya, I. N., Harper, L. C., Pawlowski, W. P., Schichnes, D. and Cande, W. Z.** (2002). The *pam1* gene is required for meiotic bouquet formation and efficient homologous synapsis in maize (*Zea mays* L.). *Genetics* 162, 1979-1993
- Golubovskaya, I. N., Wang, C. J., Timofejeva, L. and Cande, W. Z.** (2011). Maize meiotic mutants with improper or non-homologous synapsis due to problems in pairing or synaptonemal complex formation. *J Exp Bot* 62, 1533-1544
- Gomez, R., Jordan, P. W., Viera, A., Alsheimer, M., Fukuda, T., Jessberger, R., et al.** (2013). Dynamic localization of SMC5/6 complex proteins during mammalian meiosis and mitosis suggests functions in distinct chromosome processes. *J Cell Sci* 126, 4239-4252
- Gotoh, K.** (1924). Über die Chromosomenzahl von *Secale cereale* L. *Botanical Magazine-Tokyo* 38, 135-152
- Gramlich, P. M., Warncke, S., Gierlich, J. and Carell, T.** (2008). Click-click-click: single to triple modification of DNA. *Angew Chem Int Ed Engl* 47, 3442-3444
- Gramlich, P. M., Wirges, C. T., Manetto, A. and Carell, T.** (2008). Postsynthetic DNA modification through the copper-catalyzed azide-alkyne cycloaddition reaction. *Angew Chem Int Ed Engl* 47, 8350-8358
- Grun, P.** (1959). Variability of accessory chromosomes in native populations of *Allium cernuum*. *American Journal of Botany* 46, 218-224
- Hamant, O., Ma, H. and Cande, W. Z.** (2006). Genetics of meiotic prophase I in plants. *Annu Rev Plant Biol* 57, 267-302
- Hamer, G., Wang, H., Bolcun-Filas, E., Cooke, H. J., Benavente, R. and Hoog, C.** (2008). Progression of meiotic recombination requires structural maturation of the central element of the synaptonemal complex. *J Cell Sci* 121, 2445-2451
- Han, Y., Zhang, T., Thammapichai, P., Weng, Y. and Jiang, J.** (2015). Chromosome-specific painting in *Cucumis* Species using bulked oligonucleotides. *Genetics* 200, 771-779
- Harper, L., Golubovskaya, I. and Cande, W. Z.** (2004). A bouquet of chromosomes. *J Cell Sci* 117, 4025-4032
- Hasegawa, N.** (1934). A cytological study on 8-chromosome rye. *Cytologia* 6, 68-77
- Heckmann, S., Jankowska, M., Schubert, V., Kumke, K., Ma, W. and Houben, A.** (2014). Alternative meiotic chromatid segregation in the holocentric plant *Luzula elegans*. *Nat Commun* 5, 4979
- Hernandez-Hernandez, A., Masich, S., Fukuda, T., Kouznetsova, A., Sandin, S., Daneholt, B., et al.** (2016). The central element of the synaptonemal complex in mice is organized as a bilayered junction structure. *J Cell Sci* 129, 2239-2249

- Hertwig, O.** (1876). Beiträge zur Kenntniss der Bildung, Befruchtung und Theilung des thierischen Eies. *Morphol. Jahrbuch* 1, 347-434
- Higgins, J. D., Sanchez-Moran, E., Armstrong, S. J., Jones, G. H. and Franklin, F. C.** (2005). The *Arabidopsis* synaptonemal complex protein ZYP1 is required for chromosome synapsis and normal fidelity of crossing over. *Genes Dev* 19, 2488-2500
- Himo, F., Lovell, T., Hilgraf, R., Rostovtsev, V. V., Noodleman, L., Sharpless, K. B., et al.** (2005). Copper(I)-catalyzed synthesis of azoles. DFT study predicts unprecedented reactivity and intermediates. *J Am Chem Soc* 127, 210-216
- Hiraoka, T.** (1952). Observational and experimental studies of meiosis with special reference to the bouquet Stage. XIII Further experimental study of the nucleolar movement. *Cytologica* 17, 287-291
- Hiraoka, Y. and Dernburg, A. F.** (2009). The SUN rises on meiotic chromosome dynamics. *Dev Cell* 17, 598-605
- Hobolth, P.** (1981). Chromosome pairing in allohexaploid wheat var. Chinese Spring. Transformation of multivalents into bivalents, a mechanism for exclusive bivalent formation. *Carlsberg Research Communications* 46, 129
- Hollingsworth, N. M. and Ponte, L.** (1997). Genetic interactions between HOP1, RED1 and MEK1 suggest that MEK1 regulates assembly of axial element components during meiosis in the yeast *Saccharomyces cerevisiae*. *Genetics* 147, 33-42
- Holm, P. B.** (1977). Three-dimensional reconstruction of chromosome pairing during the zygotene stage of meiosis in *Lilium longiflorum* (thunb.). *Carlsberg Research Communications* 42, 103
- Houben, A., Field, B. L. and Saunders, V.** (2001). Microdissection and chromosome painting of plant B chromosomes. *Methods Cell. Sci.* 23, 115-124
- Houben, A., Kynast, R. G., Heim, U., Hermann, H., Jones, R. N. and Forster, J. W.** (1996). Molecular cytogenetic characterisation of the terminal heterochromatic segment of the B-chromosome of rye (*Secale cereale*). *Chromosoma* 105, 97-103
- Hoyle, C. E. and Bowman, C. N.** (2010). Thiol-ene click chemistry. *Angewandte Chemie-International Edition* 49, 1540-1573
- Humphries, N., Leung, W. K., Argunhan, B., Terentyev, Y., Dvorackova, M. and Tsubouchi, H.** (2013). The Ecm11-Gmc2 complex promotes synaptonemal complex formation through assembly of transverse filaments in budding yeast. *PLoS Genet* 9, e1003194
- Ijdo, J. W., Wells, R. A., Baldini, A. and Reeders, S. T.** (1991). Improved telomere detection using a telomere repeat probe (TTAGGG)_n generated by PCR. *Nucleic Acids Res* 19, 4780
- Janssens, F. A.** (1909). "La Theorie de la Chiasmotypie. Nouvelle interprétation des cinèses de maturation." *La Cellule* 25, 389-411
- Jenkins, G.** (1985). Synaptonemal complex formation in hybrids of *Lolium temulentum* × *Lolium perenne* (L.). *Chromosoma* 92, 81-88
- Jiang, J.** (2019). Fluorescence *in situ* hybridization in plants: recent developments and future applications. *Chromosome Res*

- Jiang, J. M. and Gill, B. S.** (1994). Nonisotopic *in situ* hybridization and plant genome mapping- the first 10 years. *Genome* 37, 717-725
- Jimenez, G., Manzanero, S. and Puertas, M. J.** (2000). Relationship between pachytene synapsis, metaphase I associations, and transmission of 2B and 4B chromosomes in rye. *Genome* 43, 232-239
- Jimenez, M., Diez, M. and Santos, J. L.** (1994). Synaptic patterns of rye B chromosomes. III. The deficient B. *Chromosome Res* 2, 93-98
- Jimenez, M. M., Romera, F., GonzalezSanchez, M. and Puertas, M. J.** (1997). Genetic control of the rate of transmission of rye B chromosomes .3. Male meiosis and gametogenesis. *Heredity* 78, 636-644
- John, H. A., Birnstiel, M. L. and Jones, K. W.** (1969). RNA-DNA hybrids at the cytological level. *Nature* 223, 582-587
- Jones, G. H.** (1967). Control of chiasma distribution in rye. *Chromosoma* 22, 69-90
- Jones, N. and Pasakinskiene, I.** (2005). Genome conflict in the gramineae. *New Phytol* 165, 391-409
- Jones, R. N. and Puertas, M. J.** (1993). The B chromosomes of rye (*Secale cereale* L.). *In: Dhir, K.K., Sareen, T.S. eds. Frontiers in Plant Science Research. Dehli (India): Bhagwati Enterprises*, 81-112
- Jones, R. N. and Rees, H.** (1982). B chromosomes. *1st edn. Academic Press, London New York*
- Jong, J. H. d., Havekes, F., Roca, A. and Naranjo, T.** (1991). Synapsis and chiasma formation in a ditelo-substituted haploid of rye. *Genome* 34, 109-120
- Kartavtseva, i. V. R., G.V.; Pavlenko, M.V.; Amachaeva, E.Yu.; Sawaguchi, S.; Obara, Y.** (2000). The B chromosome system of the Korean field mouse *Apodemus peninsulae*. *Chromosome Science* 4, 21-29
- Kato, A., Albert, P. S., Vega, J. M. and Birchler, J. A.** (2006). Sensitive fluorescence *in situ* hybridization signal detection in maize using directly labeled probes produced by high concentration DNA polymerase nick translation. *Biotech Histochem* 81, 71-78
- Kato, A., Lamb, J. C. and Birchler, J. A.** (2004). Chromosome painting using repetitive DNA sequences as probes for somatic chromosome identification in maize. *Proc Natl Acad Sci U S A* 101, 13554-13559
- Kayano, H.** (1957). Cytogenetic studies in *Lilium callosum*. III Preferential segregation of a supernumary chromosome in EMCs. *Proceedings of the Japan Academy* 33, 553-558
- Kayano, H.** (1971). Accumulation of B chromosomes in germ line of *Locusta-migratoria*. *Heredity* 27, 119-123
- Kishikawa, H.** (1965). Cytogenetic studies of B-chromosomes in rye, *Secale cereale* L. *Agricultural Bulletin of Saga University* 21, 1-81
- Klemme, S., Banaei-Moghaddam, A. M., Macas, J., Wicker, T., Novak, P. and Houben, A.** (2013). High-copy sequences reveal distinct evolution of the rye B chromosome. *New Phytol* 199, 550-558

- Kolb, H. C., Finn, M. G. and Sharpless, K. B.** (2001). Click chemistry: Diverse chemical function from a few good reactions. *Angew Chem Int Ed Engl* 40, 2004-2021
- Kolomiets, O. L., Borbiev, T. E., Safronova, L. D., Borisov, Y. M. and Bogdanov, Y. F.** (1988). Synaptonemal complex analysis of B-chromosome behavior in meiotic prophase I in the East-Asiatic mouse *Apodemus peninsulae* (Muridae, Rodentia). *Cytogenetic and Genome Research* 48, 183-187
- Kosar, T. F. and Phillips, R. J.** (1995). Measurement of protein diffusion in Dextran solutions by holographic interferometry. *AIChE Journal* 41, 701-711
- Kuwada, Y.** (1925). On the number of chromosomes in maize. *Botanical Magazine-Tokyo* 39, 227-234
- Lahann, J.** (2009). Click-chemistry for biotechnology and material science. *John Wiley & Sons (Publ.)*
- Langer-Safer, P. R., Levine, M. and Ward, D. C.** (1982). Immunological method for mapping genes on *Drosophila* polytene chromosomes. *Proc Natl Acad Sci U S A* 79, 4381-4385
- Lavania, U. C.** (1998). Fluorescence *in situ* hybridization in genome, chromosome and gene identification in plants. *Current Science* 74, 126-133
- Lee, C. Y., Conrad, M. N. and Dresser, M. E.** (2012). Meiotic chromosome pairing is promoted by telomere-led chromosome movements independent of bouquet formation. *PLoS Genet* 8, e1002730
- Lee, D. H., Kao, Y. H., Ku, J. C., Lin, C. Y., Meeley, R., Jan, Y. S., et al.** (2015). The axial element protein DESYNAPTIC2 mediates meiotic double-strand break formation and synaptonemal complex assembly in Maize. *Plant Cell* 27, 2516-2529
- Lewis, H.** (1951). The origin of supernumerary chromosomes in natural populations of *Clarkia elegans*. *Evolution* 5, 142-157
- Liehr, T.** (2018). Chromothripsis detectable in small supernumerary marker chromosomes (sSMC) using fluorescence *in situ* hybridization (FISH). *Methods Mol Biol* 1769, 79-84
- Lilienthal, I., Kanno, T. and Sjogren, C.** (2013). Inhibition of the Smc5/6 complex during meiosis perturbs joint molecule formation and resolution without significantly changing crossover or non-crossover levels. *PLoS Genet* 9, e1003898
- Lima-De-Faria, A.** (1962). Genetic interaction in rye expressed at the chromosome phenotype. *Genetics* 47, 1455-1462
- Lutz, A. M.** (1916). *Oenothera* mutants with diminutive chromosomes. *Am. J. Bot.* 3, 502-526
- Luxton, G. W. and Starr, D. A.** (2014). KASHing up with the nucleus: novel functional roles of KASH proteins at the cytoplasmic surface of the nucleus. *Curr Opin Cell Biol* 28, 69-75
- Ma, L., Vu, G. T., Schubert, V., Watanabe, K., Stein, N., Houben, A., et al.** (2010). Synteny between *Brachypodium distachyon* and *Hordeum vulgare* as revealed by FISH. *Chromosome Res* 18, 841-850

- Ma, W., Schubert, V., Martis, M. M., Hause, G., Liu, Z., Shen, Y., et al.** (2016). The distribution of alpha-kleisin during meiosis in the holocentromeric plant *Luzula elegans*. *Chromosome Res* 24, 393-405
- Mamat, C., Flemming, A., Kockerling, M., Steinbach, J. and Wuest, F. R.** (2009). Synthesis of benzoate-functionalized phosphanes as novel building blocks for the traceless Staudinger ligation. *Synthesis-Stuttgart*, 3311-3321
- Manuelidis, L., Langer-Safer, P. R. and Ward, D. C.** (1982). High-resolution mapping of satellite DNA using biotin-labeled DNA probes. *J Cell Biol* 95, 619-625
- Marques, A., Klemme, S., Guerra, M. and Houben, A.** (2012). Cytomolecular characterization of *de novo* formed rye B chromosome variants. *Molecular Cytogenetics* 5
- Marques, A., Ribeiro, T., Neumann, P., Macas, J., Novak, P., Schubert, V., et al.** (2015). Holocentromeres in *Rhynchospora* are associated with genome-wide centromere-specific repeat arrays interspersed among euchromatin. *Proc Natl Acad Sci U S A* 112, 13633-13638
- Marques, A., Schubert, V., Houben, A. and Pedrosa-Harand, A.** (2016). Restructuring of holocentric centromeres during meiosis in the plant *Rhynchospora pubera*. *Genetics* 204, 555-568
- Martis, M. M., Klemme, S., Banaei-Moghaddam, A. M., Blattner, F. R., Macas, J., Schmutzer, T., et al.** (2012). Selfish supernumerary chromosome reveals its origin as a mosaic of host genome and organellar sequences. *Proc Natl Acad Sci U S A* 109, 13343-13346
- Matthews, R. B. and Jones, R. N.** (1983). Dynamics of the B chromosome polymorphism in rye .2. estimates of parameters. *Heredity* 50, 119-137
- McClintock, B.** (1931). Cytological observations of deficiencies involving known genes, translocations and an inversion in *Zea mays*. *Missouri Agr. Exp. Sta. Res. Bull.* 163, 1-48
- McClintock, B.** (1938). The production of homozygous deficient tissues with mutant characteristics by means of the aberrant mitotic behavior of ring-shaped chromosomes. *Genetics* 23, 315-376
- McClintock, B.** (1939). The behavior in successive nuclear divisions of a chromosome broken at meiosis. *Proc Natl Acad Sci U S A* 25, 405-416
- McClintock, B.** (1941). The stability of broken ends of chromosomes in *Zea Mays*. *Genetics* 26, 234-282
- Mendelson, D. and Zohary, D.** (1972). Behavior and transmission of supernumerary chromosomes in *Aegilops speltoides*. *Heredity* 29, 329-&
- Meuwissen, R. L., Offenbergh, H. H., Dietrich, A. J., Riesewijk, A., van Iersel, M. and Heyting, C.** (1992). A coiled-coil related protein specific for synapsed regions of meiotic prophase chromosomes. *EMBO J* 11, 5091-5100
- Mikhailova, E. I., Phillips, D., Sosnikhina, S. P., Lovtsyus, A. V., Jones, R. N. and Jenkins, G.** (2006). Molecular assembly of meiotic proteins Asy1 and Zyp1 and pairing promiscuity in rye (*Secale cereale* L.) and its synaptic mutant sy10. *Genetics* 174, 1247-1258
- Moens, P. B.** (1969). The fine structure of meiotic chromosome polarization and pairing in *Locusta migratoria* spermatocytes. *Chromosoma* 28, 1-25

- Moore, J. E. S.** (1895). On the structural changes in the reproductive cells in the spermatogenesis of *Elasmobranchs*. *Q J Microsc Sci* 38, 275-313
- Moses, M. J.** (1956). Chromosomal structures in crayfish spermatocytes. *J Biophys Biochem Cytol* 2, 215-218
- Moses, M. J.** (1968). Synaptonemal Complex. *Annual Review of Genetics* 2, 363-412
- Muller, H. J.** (1938). The remaking of chromosomes. *The Collecting Net (Wood's Hole)* 13, 181-195
- Müntzing, A.** (1945). Cytological studies of extra fragment chromosomes in rye. II. Transmission and multiplication of standard fragments and iso-fragments. *Hereditas* 31, 457-477
- Müntzing, A.** (1946). Cytological studies of extra fragment chromosomes in rye .III. The mechanism of non-disjunction at the pollen mitosis. *Hereditas* 32, 97-119
- Müntzing, A.** (1948). Cytological studies of extra fragment chromosomes in rye .IV. The position of various fragment types in somatic plates. *Hereditas* 34, 161-180
- Müntzing, A.** (1948). Cytological studies of extra fragment chromosomes in rye .V. A new fragment type arisen by deletion. *Hereditas* 34, 435-442
- Müntzing, A. and Lima-de-Faria, A.** (1952). Pachytene analysis of a deficient accessory chromosome in rye. *Hereditas* 38, 1-10
- Müntzing, A. and Lima-De-Faria, A.** (1953). Pairing and transmission of a small accessory iso-chromosome in rye. *Chromosoma* 6, 142-148
- Müntzing, A. and Lima-De-Faria, A.** (1953). Pairing and transmission of a small accessory iso-chromosome in rye. *Chromosoma* 6, 142-148
- Murphy, S. P., Gumber, H. K., Mao, Y. and Bass, H. W.** (2014). A dynamic meiotic SUN belt includes the zygotene-stage telomere bouquet and is disrupted in chromosome segregation mutants of maize (*Zea mays* L.). *Front Plant Sci* 5, 314
- Nakao, M.** (1911). Cytological studies on the nucleus division of the pollen mother cells of some cereals and their hybrids. *Journal of the College of Agriculture, Tohoku Imperial University Sapporo* 4, 173-190
- Niklas, K.J., Cobb, E.D., and Kutschera, U.** (2014). Did meiosis evolve before sex and the evolution of eukaryotic life cycles? *Bioessays* 36, 1091-1101
- Niwa, K. and Sakamoto, S.** (1995). Origin of B chromosomes in cultivated rye. *Genome* 38, 307-312
- Nonomura, K., Nakano, M., Eiguchi, M., Suzuki, T. and Kurata, N.** (2006). PAIR2 is essential for homologous chromosome synapsis in rice meiosis I. *J Cell Sci* 119, 217-225
- Nur, U.** (1963). A mitotically unstable supernumerary chromosome with an accumulation mechanism in a grasshopper. *Chromosoma* 14, 407-422
- Olson, L. W., Eden, U., Egelmitani, M. and Egel, R.** (1978). Asynaptic meiosis in fission yeast. *Hereditas* 89, 189-199

- Olszewska, M., Wanowska, E., Kishore, A., Huleyuk, N., Georgiadis, A. P., Yatsenko, A. N., et al.** (2015). Genetic dosage and position effect of small supernumerary marker chromosome (sSMC) in human sperm nuclei in infertile male patient. *Sci Rep* 5, 17408
- Osman, K., Higgins, J. D., Sanchez-Moran, E., Armstrong, S. J. and Franklin, F. C.** (2011). Pathways to meiotic recombination in *Arabidopsis thaliana*. *New Phytol* 190, 523-544
- Östergren, G.** (1945). Parasitic nature of extra fragment chromosomes. *Bot. Notiser* 2, 157-163
- Page, B. T., Wanous, M. K. and Birchler, J. A.** (2001). Characterization of a maize chromosome 4 centromeric sequence: evidence for an evolutionary relationship with the B chromosome centromere. *Genetics* 159, 291-302
- Page, S. L. and Hawley, R. S.** (2001). c(3)G encodes a *Drosophila* synaptonemal complex protein. *Genes Dev* 15, 3130-3143
- Page, S. L. and Hawley, R. S.** (2004). The genetics and molecular biology of the synaptonemal complex. *Annu Rev Cell Dev Biol* 20, 525-558
- Page, S. L., Khetani, R. S., Lake, C. M., Nielsen, R. J., Jeffress, J. K., Warren, W. D., et al.** (2008). Corona is required for higher-order assembly of transverse filaments into full-length synaptonemal complex in *Drosophila* oocytes. *PLoS Genet* 4, e1000194
- Palecek, J., Vidot, S., Feng, M., Doherty, A. J. and Lehmann, A. R.** (2006). The Smc5-Smc6 DNA repair complex. bridging of the Smc5-Smc6 heads by the KLEISIN, Nse4, and non-Kleisin subunits. *J Biol Chem* 281, 36952-36959
- Palestis, B. G., Trivers, R., Burt, A. and Jones, R. N.** (2004). The distribution of B chromosomes across species. *Cytogenetic and Genome Research* 106, 151-158
- Pardue, M. L. and Gall, J. G.** (1969). Molecular Hybridization of Radioactive DNA to DNA of Cytological Preparations. *Proceedings of the National Academy of Sciences of the United States of America* 64, 600-604
- Pebernard, S., McDonald, W. H., Pavlova, Y., Yates, J. R., 3rd and Boddy, M. N.** (2004). Nse1, Nse2, and a novel subunit of the Smc5-Smc6 complex, Nse3, play a crucial role in meiosis. *Mol Biol Cell* 15, 4866-4876
- Pedersen, C. and Langridge, P.** (1997). Identification of the entire chromosome complement of bread wheat by two-colour FISH. *Genome* 40, 589-593
- Phillips, D., Mikhailova, E. I., Timofejeva, L., Mitchell, J. L., Osina, O., Sosnikhina, S. P., et al.** (2008). Dissecting meiosis of rye using translational proteomics. *Ann Bot* 101, 873-880
- Phillips, D., Nibau, C., Ramsay, L., Waugh, R. and Jenkins, G.** (2010). Development of a molecular cytogenetic recombination assay for barley. *Cytogenet Genome Res* 129, 154-161
- Phillips, D., Nibau, C., Wnetrzak, J. and Jenkins, G.** (2012). High resolution analysis of meiotic chromosome structure and behaviour in barley (*Hordeum vulgare* L.). *PLoS One* 7, e39539
- Platner, G.** (1886). Ueber die Entstehung des Nebenkerns und seine Beziehung zur Kerntheilung. *Archiv Mikrosk. Anat.* 26, 343-369

- Puertas, M. J.** (1973). La transmisión de los cromosomas B en polinización natural en el centeno. *Ph.D. Thesis, Universidad Complutense*
- Puertas, M. J., Gonzalez-Sanchez, M., Manzanero, S., Romera, F. and Jimenez, M. M.** (1998). Genetic control of the rate of transmission of rye B chromosomes. IV. Localization of the genes controlling B transmission rate. *Heredity* 80, 209-213
- Qiao, H., Lohmiller, L. D. and Anderson, L. K.** (2011). Cohesin proteins load sequentially during prophase I in tomato primary microsporocytes. *Chromosome Res* 19, 193-207
- Qiao, H., Prasada Rao, H. B., Yang, Y., Fong, J. H., Cloutier, J. M., Deacon, D. C., et al.** (2014). Antagonistic roles of ubiquitin ligase HEI10 and SUMO ligase RNF212 regulate meiotic recombination. *Nat Genet* 46, 194-199
- Rabl, C.** (1885). Über Zelltheilung. *Morphol. Jahrbuch* 10, 214-330
- Rao, H. B., Qiao, H., Bhatt, S. K., Bailey, L. R., Tran, H. D., Bourne, S. L., et al.** (2017). A SUMO-ubiquitin relay recruits proteasomes to chromosome axes to regulate meiotic recombination. *Science* 355, 403-407
- Rayburn, A. L. and Gill, B. S.** (1985). Use of biotin-labeled probes to map specific DNA sequences on wheat chromosomes. *Journal of Heredity* 76, 78-81
- Ren, Y., Zhang, Z., Liu, J., Staub, J. E., Han, Y., Cheng, Z., et al.** (2009). An integrated genetic and cytogenetic map of the cucumber genome. *PLoS One* 4, e5795
- Reynolds, A., Qiao, H., Yang, Y., Chen, J. K., Jackson, N., Biswas, K., et al.** (2013). RNF212 is a dosage-sensitive regulator of crossing-over during mammalian meiosis. *Nat Genet* 45, 269-278
- Ribeiro, T., Pires, B., Delgado, M., Viegas, W., Jones, N. and Morais-Cecilio, L.** (2004). Evidence for 'cross-talk' between A and B chromosomes of rye. *Proc Biol Sci* 271 Suppl 6, S482-484
- Richards, D. M., Greer, E., Martin, A. C., Moore, G., Shaw, P. J. and Howard, M.** (2012). Quantitative dynamics of telomere bouquet formation. *Plos Computational Biology* 8
- Rimpau, J. and Flavell, R. B.** (1975). Characterization of rye B chromosome DNA by DNA-DNA hybridization. *Chromosoma* 52, 207-217
- Roberts, N. Y., Osman, K. and Armstrong, S. J.** (2009). Telomere distribution and dynamics in somatic and meiotic nuclei of *Arabidopsis thaliana*. *Cytogenet Genome Res* 124, 193-201
- Rocha, D. M., Marques, A., Andrade, C. G., Guyot, R., Chaluvadi, S. R., Pedrosa-Harand, A., et al.** (2016). Developmental programmed cell death during asymmetric microsporogenesis in holocentric species of *Rhynchospora* (Cyperaceae). *J Exp Bot* 67, 5391-5401
- Rocha, R., Santos, R. S., Madureira, P., Almeida, C. and Azevedo, N. F.** (2016). Optimization of peptide nucleic acid fluorescence *in situ* hybridization (PNA-FISH) for the detection of bacteria: The effect of pH, dextran sulfate and probe concentration. *Journal of Biotechnology* 226, 1-7
- Rog, O. and Dernburg, A. F.** (2013). Chromosome pairing and synapsis during *Caenorhabditis elegans* meiosis. *Curr Opin Cell Biol* 25, 349-356
- Rog, O. and Dernburg, A. F.** (2015). Direct visualization reveals kinetics of meiotic chromosome synapsis. *Cell Rep*

- Romera, F., Vega, J. M., Diez, M. and Puertas, M. J.** (1989). B chromosome polymorphism in Korean rye populations. *Heredity* 62, 117
- Rostovtsev, V. V., Green, L. G., Fokin, V. V. and Sharpless, K. B.** (2002). A stepwise Huisgen cycloaddition process: copper(I)-catalyzed regioselective "ligation" of azides and terminal alkynes. *Angew Chem Int Ed Engl* 41, 2596-2599
- Rouillard, J. M., Zuker, M. and Gulari, E.** (2003). OligoArray 2.0: design of oligonucleotide probes for DNA microarrays using a thermodynamic approach. *Nucleic Acids Res* 31, 3057-3062
- Rozkiewicz, D. I., Gierlich, J., Burley, G. A., Gutmiedl, K., Carell, T., Ravoo, B. J., et al.** (2007). Transfer printing of DNA by "click" chemistry. *ChemBiochem* 8, 1997-2002
- Rückert, J.** (1882). Zur Entwicklungsgeschichte des Ovarialeies bei Selachiern. *Anat Anz* 7, 107-118
- Rückert, J.** (1894). Zur Eireifung bei Copepoden. *Anatomische Hefte* 4, 261-351
- Ruban, A., Schmutzer, T., Scholz, U. and Houben, A.** (2017). How next-generation sequencing has aided our understanding of the sequence composition and origin of B chromosomes. *Genes (Basel)* 8
- Sadaie, M., Naito, T. and Ishikawa, F.** (2003). Stable inheritance of telomere chromatin structure and function in the absence of telomeric repeats. *Genes Dev* 17, 2271-2282
- Sanchez-Moran, E., Osman, K., Higgins, J. D., Pradillo, M., Cunado, N., Jones, G. H., et al.** (2008). ASY1 coordinates early events in the plant meiotic recombination pathway. *Cytogenet Genome Res* 120, 302-312
- Sandery, M. J., Forster, J. W., Blunden, R. and Jones, R. N.** (1990). Identification of a family of repeated sequences on the rye B-chromosome. *Genome* 33, 908-913
- Sanei, M., Pickering, R., Kumke, K., Nasuda, S. and Houben, A.** (2011). Loss of centromeric histone H3 (CENH3) from centromeres precedes uniparental chromosome elimination in interspecific barley hybrids. *Proc Natl Acad Sci U S A* 108, E498-505
- Santos, J. L., Jimenez, M. M. and Diez, M.** (1993). Synaptic patterns of rye B chromosomes. I: The standard type. *Chromosome Res* 1, 145-152
- Santos, J. L., Jimenez, M. M. and Diez, M.** (1995). Synaptic patterns of rye B chromosomes. IV. The B isochromosomes. *Heredity (Edinb)* 74 (Pt 1), 100-107
- Santos, J. L., M. M. Jiménez and M. Díez** (1994). "Meiosis in haploid rye: extensive synapsis and low chiasma frequency." *Heredity* 73, 580.
- Sapre, B. and Deshpande, S.** (1987). Origin of B chromosomes in Coix L. through spontaneous interspecific hybridisation. *J Hered* 78, 191-196
- Scherthan, H.** (2001) A bouquet makes ends meet. *Nat Rev Mol Cell Biol* 2, 621-627.
- Scherthan, H.** (2007). Telomere attachment and clustering during meiosis. *Cell Mol Life Sci* 64, 117-124.
- Scherthan, H., J. Bahler, J. and Kohli, J.** (1994). Dynamics of chromosome organization and pairing during meiotic prophase in fission yeast. *J Cell Biol* 127, 273-285

- Scherthan, H., Wang, H., Adelfalk, C., White, E. J., Cowan, C., Cande, W. Z., et al.** (2007). Chromosome mobility during meiotic prophase in *Saccharomyces cerevisiae*. *Proc Natl Acad Sci U S A* 104, 16934-16939
- Schmidt, T. and Heslop-Harrison, J. S.** (1996). The physical and genomic organization of microsatellites in sugar beet. *Proc Natl Acad Sci U S A* 93, 8761-8765
- Schmutzer, T., Ma, L., Pousarebani, N., Bull, F., Stein, N., Houben, A., et al.** (2014). Kmasker--a tool for in silico prediction of single-copy FISH probes for the large-genome species *Hordeum vulgare*. *Cytogenet Genome Res* 142, 66-78
- Schramm, S., Fraune, J., Naumann, R., Hernandez-Hernandez, A., Hoog, C., Cooke, H. J., et al.** (2011). A novel mouse synaptonemal complex protein is essential for loading of central element proteins, recombination, and fertility. *PLoS Genet* 7, e1002088
- Schubert, V., Weissleder, A., Ali, H., Fuchs, J., Lermontova, I., Meister, A., et al.** (2009). Cohesin gene defects may impair sister chromatid alignment and genome stability in *Arabidopsis thaliana*. *Chromosoma* 118, 591-605
- Seela, F. and Sirivolu, V. R.** (2006). DNA containing side chains with terminal triple bonds: Base-pair stability and functionalization of alkynylated pyrimidines and 7-deazapurines. *Chem Biodivers* 3, 509-514
- Semple, J. C.** (1989). Geographical-Distribution of B-Chromosomes of *Xanthisma-Texanum* (*Compositae, Astereae*) .2. Local Variation within and between Populations and Frequency Variation through Time. *American Journal of Botany* 76, 769-776
- Shao, T., Tang, D., Wang, K., Wang, M., Che, L., Qin, B., et al.** (2011). OsREC8 is essential for chromatid cohesion and metaphase I monopolar orientation in rice meiosis. *Plant Physiol* 156, 1386-1396
- Sheehan, M. J. and Pawlowski, W. P.** (2009). Live imaging of rapid chromosome movements in meiotic prophase I in maize. *Proc Natl Acad Sci U S A* 106, 20989-20994
- Shi, L., Tang, L., Ma, K. and Ma, C.** (1988). Synaptonemal complex formation among supernumerary B chromosomes: an electron microscopic study on spermatocytes of Chinese raccoon dogs. *Chromosoma* 97, 178-183
- Simanovsky, S. A., Matveevsky, S. N., Iordanskaya, I. V., Spangenberg, V. E., Kolomiets, O. L. and Bogdanov, Y. B.** (2014). Spiral cores of synaptonemal complex lateral elements at the diplotene stage in rye include the ASY1 protein. *Genetika* 50, 1250-1253
- Smith, A. V. and Roeder, G. S.** (1997). The yeast Red1 protein localizes to the cores of meiotic chromosomes. *J Cell Biol* 136, 957-967
- Solovjeva, L. V., Demin, S. J., Pleskach, N. M., Kuznetsova, M. O. and Svetlova, M. P.** (2012). Characterization of telomeric repeats in metaphase chromosomes and interphase nuclei of Syrian Hamster Fibroblasts. *Mol Cytogenet* 5, 37
- Speicher, M. R. and Carter, N. P.** (2005). The new cytogenetics: blurring the boundaries with molecular biology. *Nat Rev Genet* 6, 782-792
- Starr, D. A.** (2011). KASH and SUN proteins. *Curr Biol* 21, R414-415

- Starr, D. A. and Fridolfsson, H. N.** (2010). Interactions between nuclei and the cytoskeleton are mediated by SUN-KASH nuclear-envelope bridges. *Annu Rev Cell Dev Biol* 26, 421-444
- Stevens, N. M.** (1908). The chromosomes in *Diabrotica vittata*, *Diabrotica soror*, and *Diabrotica 12-punctata*. A contribution to the literature on heterochromosomes and sex determination. *J. Exp. Zool.* 5, 453-470
- Storlazzi, A., Gargano, S., Ruprich-Robert, G., Falque, M., David, M., Kleckner, N., et al.** (2010). Recombination proteins mediate meiotic spatial chromosome organization and pairing. *Cell* 141, 94-106
- Strasburger, E.** (1888). "Ueber Kern- und Zelltheilung im Pflanzenreiche, nebst einem Anhang über Befruchtung." *Jena, G. Fischer*
- Świtoński, M., Gustavsson, I., Höjer, K. and Plöen, L.** (1987). Synaptonemal complex analysis of the B-chromosomes in spermatocytes of the silver fox (*Vulpes fulvus* Desm.). *Cytogenetic and Genome Research* 45, 84-92
- Sybenga, J. and DeVries, J. M.** (1972). Chromosome pairing and chiasma formation in polysomic B-chromosomes in rye, *Secale cereale*. *Biol. Zent. bl.* 91, 181-192
- Sym, M., Engebrecht, J. A. and Roeder, G. S.** (1993). ZIP1 is a synaptonemal complex protein required for meiotic chromosome synapsis. *Cell* 72, 365-378
- Szinay, D., Chang, S. B., Khrustaleva, L., Peters, S., Schijlen, E., Bai, Y., et al.** (2008). High-resolution chromosome mapping of BACs using multi-colour FISH and pooled-BAC FISH as a backbone for sequencing tomato chromosome 6. *Plant J* 56, 627-637
- Tang, S., Qiu, L., Xiao, Z., Fu, S. and Tang, Z.** (2016). New oligonucleotide probes for ND-FISH analysis to identify barley chromosomes and to investigate polymorphisms of wheat chromosomes. *Genes (Basel)* 7
- Tang, Z., Yang, Z. and Fu, S.** (2014). Oligonucleotides replacing the roles of repetitive sequences pAs1, pSc119.2, pTa-535, pTa71, CCS1, and pAWRC.1 for FISH analysis. *Journal of Applied Genetics* 55, 313-318
- Taylor, E. M., Copsey, A. C., Hudson, J. J., Vidot, S. and Lehmann, A. R.** (2008). Identification of the proteins, including MAGEG1, that make up the human SMC5-6 protein complex. *Mol Cell Biol* 28, 1197-1206
- Thyagarajan, S., Murthy, N. N., Narducci Sarjeant, A. A., Karlin, K. D. and Rokita, S. E.** (2006). Selective DNA strand scission with binuclear copper complexes: implications for an active Cu₂O₂ species. *J Am Chem Soc* 128, 7003-7008
- Timmis, J. N., Deumling, B. and Ingle, J.** (1975). Localisation of satellite DNA sequences in nuclei and chromosomes of two plants. *Nature* 257, 152-155
- Toby, G. G., Gherraby, W., Coleman, T. R. and Golemis, E. A.** (2003). A novel RING finger protein, human enhancer of invasion 10, alters mitotic progression through regulation of cyclin B levels. *Mol Cell Biol* 23, 2109-2122
- Tornøe, C. W., Christensen, C. and Meldal, M.** (2002). Peptidotriazoles on solid phase: [1,2,3]-triazoles by regioselective copper(i)-catalyzed 1,3-dipolar cycloadditions of terminal alkynes to azides. *J Org Chem* 67, 3057-3064

- Trivers, R., Burt, A. and Palestis, B. G.** (2004). B chromosomes and genome size in flowering plants. *Genome* 47, 1-8
- Tsujimoto, H. and Niwa, K.** (1992). DNA structure of the B-chromosome of rye revealed by *in situ* hybridization using repetitive sequences. *Japanese Journal of Genetics* 67, 233-241
- van Gijswijk, R. P., Wiegant, J., Raap, A. K. and Tanke, H. J.** (1996). Improved localization of fluorescent tyramides for fluorescence *in situ* hybridization using dextran sulfate and polyvinyl alcohol. *Journal of Histochemistry & Cytochemistry* 44, 389-392
- Varas, J., Graumann, K., Osman, K., Pradillo, M., Evans, D. E., Santos, J. L., et al.** (2015). Absence of SUN1 and SUN2 proteins in *Arabidopsis thaliana* leads to a delay in meiotic progression and defects in synapsis and recombination. *Plant J* 81, 329-346
- Vershinin, A. V., Schwarzacher, T. and Heslop-Harrison, J. S.** (1995). The large-scale genomic organization of repetitive DNA families at the telomeres of rye chromosomes. *Plant Cell* 7, 1823-1833
- Verver, D. E., Hwang, G. H., Jordan, P. W. and Hamer, G.** (2016). Resolving complex chromosome structures during meiosis: versatile deployment of Smc5/6. *Chromosoma* 125, 15-27
- Verver, D. E., Langedijk, N. S., Jordan, P. W., Repping, S. and Hamer, G.** (2014). The SMC5/6 complex is involved in crucial processes during human spermatogenesis. *Biol Reprod* 91, 22
- Vieregg, J. R.** (2010). Nucleic acid structural energetics. *Encyclopedia of Analytical Chemistry*
- Voet, T., Liebe, B., Labaere, C., Marynen, P. and Scherthan, H.** (2003). Telomere-independent homologue pairing and checkpoint escape of accessory ring chromosomes in male mouse meiosis. *J Cell Biol* 162, 795-807
- Vujosevic, M. and Blagojevic, J.** (2004). B chromosomes in populations of mammals. *Cytogenetic and Genome Research* 106, 247-256
- Waminal, N. E., Pellerin, R. J., Kim, N. S., Jayakodi, M., Park, J. Y., Yang, T. J., et al.** (2018). Rapid and efficient FISH using *pre*-labeled oligomer probes. *Sci Rep* 8, 8224
- Wang, K., Wang, M., Tang, D., Shen, Y., Miao, C., Hu, Q., et al.** (2012). The role of rice HEI10 in the formation of meiotic crossovers. *PLoS Genet* 8, e1002809
- Wang, K., Wang, M., Tang, D., Shen, Y., Qin, B., Li, M., et al.** (2011). PAIR3, an axis-associated protein, is essential for the recruitment of recombination elements onto meiotic chromosomes in rice. *Mol Biol Cell* 22, 12-19
- Wang, N. and Dawe, R. K.** (2018). Centromere size and its relationship to haploid formation in plants. *Mol Plant* 11, 398-406
- Wang, S., Lapitan, N. and Tsuchiya, T.** (1991). Characterization of telomeres in *Hordeum vulgare* chromosomes by *in situ* hybridization. I. Normal diploid barley. *The Japanese Journal of Genetics*. 66, 313-316.
- Wang, X.** (1988). Chromosome pairing analysis in haploid wheat by spreading of meiotic nuclei. *Carlsberg Research Communications* 53, 135

- Ward, J. O., Reinholdt, L. G., Motley, W. W., Niswander, L. M., Deacon, D. C., Griffin, L. B., et al.** (2007). Mutation in mouse HEI10, an E3 ubiquitin ligase, disrupts meiotic crossing over. *PLoS Genet* 3, e139
- Watanabe, K., Pacher, M., Dukowic, S., Schubert, V., Puchta, H. and Schubert, I.** (2009). The STRUCTURAL MAINTENANCE OF CHROMOSOMES 5/6 complex promotes sister chromatid alignment and homologous recombination after DNA damage in *Arabidopsis thaliana*. *Plant Cell* 21, 2688-2699
- Wehrkamp-Richter, S., Hyppa, R. W., Prudden, J., Smith, G. R. and Boddy, M. N.** (2012). Meiotic DNA joint molecule resolution depends on Nse5-Nse6 of the Smc5-Smc6 holocomplex. *Nucleic Acids Res* 40, 9633-9646
- Weismann, A.** (1887). "Über die Zahl der Richtungkörper und über ihre Bedeutung für die Vererbung." *Jena, Gustav Fischer*
- Weisshart, K., Fuchs, J. and Schubert, V.** (2016). Structured illumination microscopy (SIM) and photoactivated localization microscopy (PALM) to analyze the abundance and distribution of RNA polymerase II molecules on flow-sorted *Arabidopsis* nuclei. *Bio-protocol* 6, e1725
- Wesolowska, N., Amariei, F. L. and Rong, Y. S.** (2013). Clustering and protein dynamics of *Drosophila melanogaster* telomeres. *Genetics* 195, 381-391
- Westergaard, M. and von Wettstein, D.** (1972). The synaptonemal complex. *Annu Rev Genet* 6, 71-110
- Whitby, M. C.** (2005). Making crossovers during meiosis. *Biochem Soc Trans* 33, 1451-1455
- White, E. J., Cowan, C., Cande, W. Z. and Kaback, D. B.** (2004). *In vivo* analysis of synaptonemal complex formation during yeast meiosis. *Genetics* 167, 51-63
- Wiessler, M., Waldeck, W., Kliem, C., Pipkorn, R. and Braun, K.** (2010). The Diels-Alder-Reaction with inverse-Electron-Demand, a very efficient versatile Click-Reaction Concept for proper Ligation of variable molecular Partners. *International Journal of Medical Sciences* 7, 19-28
- Wilkes, T. M., Francki, M. G., Langridge, P., Karp, A., Jones, R. N. and Forster, J. W.** (1995). Analysis of rye B-chromosome structure using fluorescence *in situ* hybridization (FISH). *Chromosome Res* 3, 466-472
- Wilkins, A.S., and Holliday, R.** (2009). The evolution of meiosis from mitosis. *Genetics* 181, 3-12.
- Wilson, E. B.** (1907). The supernumerary chromosomes of *Hemiptera*. *Science* XXVI, 870
- Winiwarter, H. v.** (1901). "Recherches sur l'Ovogenèse et l'Organogenèse de l'ovaire des Mammifères (Lapin et Homme)." *Arch de Biolog* 17: 33-199.
- Xaver, M., Huang, L., Chen, D. and Klein, F.** (2013). Smc5/6-Mms21 prevents and eliminates inappropriate recombination intermediates in meiosis. *PLoS Genet* 9, e1004067
- Xu, J. and Earle, E. D.** (1996). High resolution physical mapping of 45S (5.8S, 18S and 25S) rDNA gene loci in the tomato genome using a combination of karyotyping and FISH of pachytene chromosomes. *Chromosoma* 104, 545-550

- Yamada, D., Koyama, Y., Komatsubara, M., Urabe, M., Mori, M., Hashimoto, Y., et al.** (2004). Comprehensive search for chicken W chromosome-linked genes expressed in early female embryos from the female-minus-male subtracted cDNA macroarray. *Chromosome Res* 12, 741-754
- Yamada, N. A., Rector, L. S., Tsang, P., Carr, E., Scheffer, A., Sederberg, M. C., et al.** (2011). Visualization of fine-scale genomic structure by oligonucleotide-based high-resolution FISH. *Cytogenet Genome Res* 132, 248-254
- Yu, H., Chao, J., Patek, D., Mujumdar, R., Mujumdar, S. and Waggoner, A. S.** (1994). Cyanine dye dUTP analogs for enzymatic labeling of DNA probes. *Nucleic Acids Res* 22, 3226-3232
- Zeleny, V.** (1974). B-Chromosomes of *Leucanthemum* (Asteraceae) in Czechoslovakia. *Plant Systematics and Evolution* 123, 55-60
- Zelkowski, M., Zelkowska, K., Conrad, U., Hesse, S., Lermontova, I., Marzec, M., et al.** (2019). Arabidopsis NSE4 proteins act in somatic nuclei and meiosis to ensure plant viability and fertility. *Frontiers in Plant Science* 10
- Zhang, L., J.Zhang, L., Tao, J., Wang, S., Chong, K. and Wang, T.** (2006). The rice OsRad21-4, an orthologue of yeast Rec8 protein, is required for efficient meiosis. *Plant Mol Biol* 60, 533-554
- Zhou, X. and Meier, I.** (2013). How plants LINC the SUN to KASH. *Nucleus* 4, 206-215
- Zickler, D.** (2006). From early homologue recognition to synaptonemal complex formation. *Chromosoma* 115, 158-174
- Zickler, D. and Kleckner, N.** (1998). The leptotene-zygotene transition of meiosis. *Annu Rev Genet* 32, 619-697
- Zickler, D. and Kleckner, N.** (1999). Meiotic chromosomes: integrating structure and function. *Annu Rev Genet* 33, 603-754
- Zickler, D. and Kleckner, N.** (2015). Recombination, pairing, and yynapsis of homologs during meiosis. *Cold Spring Harb Perspect Biol* 7
- Zickler, D. and Kleckner, N.** (2016). A few of our favorite things: Pairing, the bouquet, crossover interference and evolution of meiosis. *Semin Cell Dev Biol* 54, 135-148
- Ziolkowski, P. A., Underwood, C. J., Lambing, C., Martinez-Garcia, M., Lawrence, E. J., Ziolkowska, L., et al.** (2017). Natural variation and dosage of the HEI10 meiotic E3 ligase control *Arabidopsis* crossover recombination. *Genes Dev* 31, 306-317

Curriculum vitae

PERSONAL DETAILS

Name: Susann Hesse-Bikbaeva
Nationality: German
Date of birth: 21st July 1982

EDUCATION

- 03/2017- 08/ 2018** **Leibniz Institute of Plant Genetics and Crop Plant Research (IPK)**
Gatersleben, Germany
Guest scientist in the research group Chromosome Structure and Function
(Prof. Dr. Andreas Houben)
- 04/2013 – 02/2017** **Leibniz Institute of Plant Genetics and Crop Plant Research (IPK)**
Gatersleben, Germany and
baseclick GmbH
Neuried (Munich), Germany
PhD Student in the group Chromosome Structure and Function
Supervisors: Prof. Andreas Houben and Dr. Antonio Manetto
- 10/2010- 03/2013** **Leibniz Institute for Neurobiology (LIN)**
Magdeburg, Germany
Research associate in the research group Extracellular Matrix
(Dr. Renato Frischknecht)
- 12/2009- 09/2010** **Leibniz Institute for Neurobiology (LIN)**
Magdeburg, Germany
Graduiertenkolleg 1167 scholarship holder in the research group Neuralomics
(Prof. Dr. Daniela Dieterich)
- 10/2009- 11/2009** **Leibniz Institute for Neurobiology (LIN)**
Magdeburg, Germany
Scientific assistance in the research group Neuralomics
(Prof. Dr. Daniela Dieterich)
- 10/2002- 07/2008** **Kassel University**
Kassel, Germany and
Leibniz Institute of Plant Genetics and Crop Plant Research (IPK)
Gatersleben, Germany
Diploma in genetics, biochemistry, human biology, developmental biology
Thesis: 'Characterization of potential interactors of the plant Aurora kinase
AtAurora 1'
-

STAYS IN ANOTHER RESEARCH CENTERS AND OTHER RESEARCH EXPERIENCE

15-16 June 2015

University of Regensburg

Regensburg, Germany

Cell Biology and Plant Biochemistry group

Supervisor: Dr. Andrea Bleckmann

4-23 September 2011

Bordeaux FENS-IBRO Training Centre at University of Bordeaux

Bordeaux, France

European Synapse Summer School (ESCube)

POSTER PRESENTATIONS

Hesse S., Raddaoui N., Manetto A., Houben A. Fluorescent labelling of DNA by click-chemistry based *in situ* hybridization. Plant science student conference (2- 5 June 2015) IPK, Gatersleben, Germany

Hesse S., Schubert V., Houben A. The behaviour of rye B chromosomes in early Meiosis. Plant Molecular Cytogenetics in Genomic and Postgenomic Era (23-24 September 2014) University of Silesia, Katowice, Poland

Hesse S., Schubert V., Houben A. The behavior of rye B chromosomes in Meiosis. Plant science student conference (2- 5 June 2014) IPK, Gatersleben, Germany

Hesse S., Kreutz M.R., Frischknecht R. Correlation of synaptic activity and synaptic protein composition. 8th FENS Forum of Neuroscience (14-18 July 2002) Barcelona, Spain

ATTENDED CONFERENCES

2- 5 June 2015 Plant Science student Conference, Martin Luther University Halle-Wittenberg, Halle, Germany

23- 24 September 2014 Symposium Plant molecular cytogenetics in genomic and postgenomic era, Katowice, Poland

2- 5 June 2014 Plant science student conference, IPK Gatersleben, Germany

7- 9 April 2014 3rd B-chromosome conference, IPK Gatersleben, Germany

14-18 July 2002 8th FENS Forum of Neuroscience, Barcelona, Spain

PUBLICATION LIST

Hesse S., Zelkowski M., Mikhailova E., Keijzer C., Houben A., Schubert V. (2019) Ultrastructure and dynamics of synaptonemal complex components during meiotic pairing/ synapsis of standard (A) and accessory (B) rye chromosomes. *Frontiers in Plant Science* 10 (774). DOI:

Zelkowski M., Zelkowska K., Conrad U., **Hesse S.,** Lermontova I., Marzec M., Meister A., Houben A., Schubert V. (2019). *Arabidopsis* NSE4 proteins act in somatic nuclei and meiosis to ensure plant viability and fertility. *Frontiers in Plant Science* 10 (774). DOI: 10.3389/fpls.2019.00774

Hesse S., Manetto A., Cassinelli V., Fuchs J., Ma L., Raddaoui N. and Houben A. (2016). Fluorescent labelling of *in situ* hybridization probes through the copper-catalysed azide-alkyne cycloaddition reaction. *Chromosome Research* 24 (3), 299-307. DOI: 10.1007/s10577-016-9522-z

Badaeva E., Ruban A. S., Aliyeva-Schnorr L., Municio C., **Hesse S.**, Houben A. (2016). *In situ* hybridization to plant chromosomes. *Liehr, T. (Ed.): Fluorescence In Situ Hybridization (FISH): Application Guide, 2nd edition (Springer)*. DOI: 10.1007/978-3-662-52959-1

Demidov D., **Hesse S.**, Tewes A., Rutten T., Fuchs J., Karimi R., Vlasenko L., Lein S., Fischer A., Reuter G. and Houben A. (2009). Aurora 1 phosphorylation activity on histone H3 and its cross-talk with other post-translational histone modifications in *Arabidopsis*. *The Plant Journal* 59, 221-230. DOI: 10.1111/j.1365-313X.2009.03861.x

Eidesstattliche Erklärung/ Declaration under Oath

Hiermit erkläre ich an Eides statt, dass ich die vorliegende Arbeit selbstständig und ohne fremde Hilfe verfasst habe. Es wurden keine anderen als die in der Arbeit angegebenen Quellen und Hilfsmittel benutzt. Die den benutzten Werken wörtlich oder inhaltlich entnommenen Stellen sind als solche kenntlich gemacht.

I declare under penalty of perjury that this thesis is my own work entirely and has been written without any help from other people. I used only the sources mentioned and included all the citations correctly both in word or content.

Quedlinburg, 29.06.2019

Susann Hesse-Bikbaeva

Erklärung über bestehende Vorstrafen und anhängige Ermittlungsverfahren / Declaration concerning Criminal Record and Pending Investigations

Hiermit erkläre ich, Susann Hesse-Bikbaeva, dass ich weder vorbestraft bin noch dass gegen mich Ermittlungsverfahren anhängig sind.

I hereby declare that I, Susann Hesse-Bikbaeva, have no criminal record and that no preliminary investigations are pending against me.

Quedlinburg, 29.06.19

Susann Hesse-Bikbaeva

Appendix

Table 2 Synthesized FISH probes for the barley 3H single copy gene.

Name	Sequence	Normalized k-mer frequency
A1	<u>I</u> AGGTA <u>A</u> T <u>A</u> T <u>T</u> CC <u>C</u> I <u>G</u> CTGACT	0
A2	<u>I</u> G <u>T</u> AGG <u>A</u> I <u>C</u> TTCTG <u>C</u> I <u>C</u> AA <u>A</u> CA	<u>2</u>
A3	<u>I</u> CA <u>A</u> ATG <u>T</u> TT <u>C</u> TATAT <u>C</u> A <u>I</u> T <u>C</u> A	<u>2</u>
A4	<u>I</u> T <u>A</u> T <u>A</u> CCAG <u>T</u> T <u>A</u> AG <u>T</u> T <u>A</u> AG <u>A</u> C	<u>2</u>
A5	<u>I</u> A <u>A</u> CAT <u>A</u> I <u>A</u> TG <u>T</u> G <u>T</u> TG <u>A</u> I <u>T</u> ATG	<u>4</u>
A6	<u>I</u> T <u>C</u> TTT <u>C</u> T <u>I</u> G <u>C</u> TAT <u>A</u> T <u>I</u> AG <u>A</u> A	<u>4</u>
A7	<u>I</u> C <u>C</u> T <u>A</u> I <u>C</u> CA <u>A</u> AG <u>T</u> G <u>T</u> I <u>G</u> ATTAT	<u>1</u>
A8	<u>I</u> AGG <u>A</u> AT <u>I</u> ACG <u>T</u> TT <u>A</u> TTTT <u>T</u> A	<u>4</u>
A9	<u>I</u> TAGATG <u>T</u> I <u>A</u> ATTTT <u>G</u> T <u>I</u> ACTG	<u>4</u>
A10	<u>I</u> AGAGTT <u>C</u> C <u>I</u> ATGATAGG <u>C</u> I <u>C</u> A	0
A11	<u>I</u> TAAT <u>I</u> AGAT <u>C</u> A <u>I</u> GCATTT <u>C</u> TT	1
A12	<u>I</u> AACGCT <u>A</u> ITTCCCT <u>I</u> TTATAT	1
A13	<u>I</u> TGGGAT <u>A</u> TTATAATG <u>I</u> GTGCC	5
A14	<u>I</u> TCTAAGAT <u>I</u> TTCAAG <u>I</u> TGTTA	1
A15	<u>I</u> GTGTTT <u>A</u> TATATGTAGTTTAT	3
A16	<u>I</u> TTTCACATG <u>I</u> GTGTAT <u>I</u> ATTG	1
A17	<u>I</u> AAAAAT <u>A</u> TATAATG <u>A</u> TAGTTC	1
A18	<u>I</u> TCGTAGT <u>I</u> ATCTAAGA <u>A</u> C <u>I</u> AC	1
A19	<u>I</u> GCATA <u>A</u> I <u>G</u> AACTGAGAAAT <u>A</u> T	1
A20	<u>I</u> CATTATACAAGAGAGA <u>A</u> CAT <u>C</u>	<u>5</u>
A21	<u>I</u> TAACAATAATTAGCTAT <u>I</u> GAG	<u>3,5</u>
A22	<u>I</u> TTTGTCT <u>I</u> AAACTTAAC <u>I</u> GGT	<u>1</u>
A23	<u>I</u> AGGGTCAATGTCCTTT <u>I</u> CATT	<u>1</u>
A24	<u>I</u> GCACA <u>I</u> CAACCC <u>I</u> C <u>C</u> AAATC	<u>3</u>
A25	<u>I</u> AAGGCCAGG <u>C</u> I <u>C</u> GCGGG <u>I</u> TGG	<u>3,5</u>
A26	<u>I</u> TGTGAAGGGGG <u>I</u> TGTG <u>I</u> ATCC	<u>5</u>
A27	<u>I</u> GCAAAA <u>A</u> TAGGACTG <u>I</u> GCAAG	<u>2</u>
A28	<u>I</u> CTAGGG <u>I</u> AGAGTAGAA <u>I</u> CGGA	<u>1</u>
A29	<u>I</u> CCT <u>I</u> GGCGGCAGGGAC <u>I</u> GCC	<u>1</u>
A30	<u>I</u> CGGGGCAAGG <u>C</u> I <u>A</u> CTCG <u>C</u> I <u>A</u> C	<u>1</u>
A31	<u>I</u> GCTGCAG <u>C</u> I <u>A</u> ACTGCTA <u>I</u> GCG	<u>1</u>
A32	<u>I</u> CACCCAGGG <u>I</u> CCCT <u>I</u> GGGACA	<u>3</u>
A33	<u>I</u> GTGGAAG <u>C</u> I <u>C</u> TCTCCACG <u>I</u> CC	<u>1</u>
A34	<u>I</u> GAT <u>I</u> GCCACCAGAGG <u>I</u> GCCGA	<u>5</u>
A35	<u>I</u> GTGAGGCAAG <u>I</u> AGCGG <u>I</u> CAGG	<u>1</u>
A36	<u>I</u> TGTGCG <u>C</u> I <u>G</u> GCTGGG <u>C</u> I <u>G</u> GAG	<u>2</u>

A37	<u>I</u> TCGTAGTTATCTAAGAACT <u>A</u> C	<u>1</u>
A38	<u>I</u> AGCGTTA <u>T</u> GAACTATCG <u>T</u> ATC	<u>5.5</u>
A39	<u>I</u> CTAATCCAC <u>I</u> TCTGC <u>I</u> CATCA	<u>1</u>
A40	<u>T</u> ATTAACCT <u>I</u> ACCAGAC <u>I</u> GAGCC	<u>3</u>
A41	<u>I</u> AGAGAT <u>A</u> AAGGAC <u>I</u> CAAACCAC	<u>1</u>
A42	<u>I</u> TTAGTATATGTGTGAAAGGAT	<u>1</u>
A43	<u>I</u> CGAGCGACCGCTGAAAT <u>A</u> ATC	<u>1</u>
A44	<u>I</u> CCGGACA <u>T</u> AAGAAAAAGG <u>I</u> TG	<u>4</u>
A45	<u>I</u> ACCATATGTATATGCA <u>I</u> TAGC	<u>1</u>
A46	<u>I</u> GAACGTAAG <u>I</u> GTAGAACCA <u>I</u> C	<u>3</u>
A47	<u>I</u> CCTTT <u>I</u> CATTGATCACCACGA	<u>3</u>
A48	<u>I</u> GGAATAAGACCTATTGTAT <u>A</u> C	<u>1</u>
A49	GCG <u>I</u> CGACAGGAAATCTCAG <u>I</u> G	<u>1</u>
A50	<u>I</u> GAGAAACT <u>I</u> ATATATGT <u>A</u> AAT	<u>5</u>
A51	<u>I</u> GTAGGGTCA <u>I</u> GTCCTTT <u>I</u> CA	<u>2</u>
A52	<u>I</u> CAAGAC <u>I</u> GAACGTAAG <u>I</u> GTAG	<u>4</u>
A53	<u>I</u> CGTTT <u>I</u> CTGAGT <u>I</u> CAACCGGG	<u>1</u>
A54	<u>I</u> CCGGACA <u>T</u> AAGAAAAAGG <u>I</u> TG	<u>3</u>
A55	<u>I</u> TTGCTAT <u>I</u> GGTGTGAGC <u>I</u> GAA	<u>1</u>
A56	<u>I</u> TCAT <u>I</u> GGAAATCAGT <u>I</u> GGTTC	<u>1</u>
A57	<u>I</u> GTTCTAA <u>I</u> CATTATACAAGAG	<u>5.5</u>
A58	<u>I</u> CTCAGCGCC <u>I</u> GCAGAAAT <u>C</u> AA	<u>1</u>
A59	<u>I</u> GCACATGTCTGAATATCTAC	<u>1</u>
A60	<u>I</u> ATTTGCAATGTTAGTAGGA <u>I</u> C	<u>4.5</u>
A61	<u>I</u> ACGGATGAG <u>I</u> TGATAAC <u>I</u> CCA	<u>4</u>
A62	<u>I</u> GGTAGGTTAA <u>I</u> ATTTCCCT <u>I</u> GC	<u>2</u>
A63	<u>I</u> GCTTG <u>I</u> GGTTTGAG <u>I</u> CCTTAT	<u>2</u>
A64	<u>I</u> AGGAATTACG <u>I</u> TTATTTTT <u>I</u> A	<u>4</u>
A65	<u>I</u> ATTCTACAAGTACAGC <u>I</u> T	<u>1</u>
A66	<u>I</u> ATCCAAAGT <u>I</u> TGATTATT <u>I</u> C	<u>2</u>
A67	<u>I</u> CGGCAA <u>I</u> AGTTAGTGGT <u>I</u> GGG	<u>2</u>
A68	<u>I</u> TCCACG <u>I</u> GATACATG <u>I</u> ACATA	<u>2</u>
A69	<u>I</u> TGCAC <u>I</u> TGAAAGGC <u>I</u> AATGCA	<u>2</u>
A70	<u>I</u> GTGTG <u>I</u> CATAATG <u>I</u> CCCCGG <u>I</u>	<u>1</u>
A71	<u>I</u> AACCAAT <u>I</u> CTTAGTTGT <u>I</u> ACT	<u>2</u>
A72	<u>I</u> CATGATT <u>I</u> ATGTGCAC <u>I</u> CGAG	<u>3</u>
A73	<u>I</u> AATCTCAGCCAAG <u>I</u> ATG <u>I</u> GTA	<u>1</u>
A74	<u>I</u> AGAATTC <u>I</u> CCTGCTAGC <u>I</u> ATG	<u>2</u>
A75	<u>I</u> CCATAGCCAGC <u>I</u> CATCC <u>I</u> GAG	<u>2.5</u>
A76	<u>I</u> CGTTGT <u>I</u> CGC <u>I</u> TGAAGG <u>I</u> GGCG	<u>2</u>
A77	<u>I</u> AGGCCCAATCCA <u>I</u> GAAGAG <u>I</u> G	<u>3</u>

A78	<u>T</u> CAGTGACA <u>T</u> CATCACTGAT <u>T</u> A	<u>3</u>
A79	<u>T</u> ATTGGCC <u>T</u> TTTTCT <u>T</u> CCACGT	<u>2.5</u>
A80	<u>T</u> GATTTGACA <u>T</u> AACAAATT <u>G</u> IT	<u>3.5</u>
A81	<u>T</u> GTGGGCAGAT <u>G</u> GGCCG <u>T</u> CCCG	<u>2</u>
A82	<u>T</u> GGAACGGA <u>A</u> T <u>C</u> AGTCGG <u>T</u> GGA	<u>4</u>
A83	<u>T</u> CGTCGTAG <u>T</u> AGGG <u>T</u> CACCGCA	<u>4</u>
A84	<u>T</u> CT <u>T</u> CCCGGGCCCG <u>T</u> TCGCAT	<u>5</u>
A85	<u>T</u> GAAACAGGGAT <u>T</u> CAGAGTCA <u>T</u> C	<u>4</u>
A86	<u>T</u> GACGTGCG <u>T</u> CGTGC <u>T</u> GGCATT	<u>1</u>
A87	<u>T</u> GAGATTTTT <u>T</u> ACATGGG <u>T</u> TGG	<u>1</u>
A88	<u>T</u> CTTGTCTG <u>T</u> CTTAAT <u>T</u> AGATC	<u>1</u>
A89	<u>T</u> AGCTAAT <u>T</u> ATTGT <u>T</u> AAGCATT	<u>1</u>
A90	<u>T</u> CACTTG <u>T</u> ATGTATG <u>T</u> GTTAAT	<u>5</u>
A91	<u>T</u> AGTCATA <u>T</u> TCTACAAC <u>T</u> AGTA	<u>1</u>
A92	<u>T</u> TATG <u>G</u> CCCAACAAGAGT <u>C</u> IT	<u>2</u>
A93	<u>T</u> GACAAT <u>T</u> AATGTTCCACCTTC	<u>3</u>
A94	<u>T</u> TTTAG <u>T</u> AAAGAGT <u>G</u> TGTCA	<u>1</u>
A95	<u>T</u> GACCC <u>T</u> ACACCC <u>T</u> CGATCTC	<u>2</u>

Sequence of the barley chromosome 3H single copy sequence

Length: 7670bp

5'-3'

ACCCGTGCTCCTCAACTACAGTATAACAATAGGTCTTATTCCATCTCCCGTGCATCTTCAATTCTGTACTTGTATCA
CTAATAGGTAATATTCCCTGCTGACTCCACCCATCCTTGTTTTCCCTTGCCGACAACATCTTAATTACAAGCTACA
ACACCGATGGATCACATCCTCACTGAGATTTCCCTGTGACGCAACAACACATGCTAATTTCAAACCTACTAAGTT
TTCCTAGTTTATTTGCATAATTTAAGTGAAGCATTACATATATAAGTTTCTCAGTGAAAAAATGTAGGATCTT
CTGCTCAAACATTGAACAAAGAGAAAAGATGGTTTTTGCAGAGAGATAACAAGTTGATGAATGTGTCAAGAA
GATCACTAAATTGAGAAATAAGGTATTCTACTTACTGTGCAGCCATGCTCTCTCTCTCTTTGGCAAATATTGTG
CTCAAATGTTTCTATATCATTGAGTTTTTTTAGGGAGTGACAATAATTCGTGGTGATCAATGAAAAGGACATT
GACCCTACACCCCTCGATCTCCTAAGTAGAGCAGGGGTAACCAATTCCTAGTTGTTACTACATGATGGTTCTAC
ACTTACGTTGAGTCTTGTCTGTTGGGTTCCATTTTAGTAAAGAGTGTGTGCATAATGTCCCGGTTGAACTC
AGAAAACGAAAGTTGTTTGACATTATACATAATGGTACTCTATAAGCCACAATATAACCAGTTAAGTTTAAGAC
AAAACCAATGTAGAAATACAAGTTTCAGCAACCTTTTTTTGGGCGGGCTTGCATTGAAAGGCTAATGCATATA
CATATGGTATGTAATATATAACAATGACCAAAGCATGACAATTAATGTTCCACCTTCACGTGATACATGTACATA
TCTCTATGGCCCAACAACCTTTTTCTTATGTCCGGAACATGAAGTAACATATATGTGTTGATTATGGCCCAACAA
AGAGTCTTACTAATTAACATCGGCAATAGTTAGTGGTTGGGTACATATAAATTTATTTTACAACCTGTCATATTCC
AATGCCGACCAAGCTTCTTTCTTGCTATTATTAGAAATAAAGATTCAACAATAAAAGTTGTACTGCGCCATACGC
TCCTATCCAAAGTGTGATTATTTAGCGGGTGCCTCGAGTTCAGCTCACACCAATAGCAAACTAGTCATATTCT
ACAACCTAGTACAGCTTCGACTAGCAAAATAAATCATAATTAATCCTTTACACATATACTAAAATAGGAATTAC
GTTTATTTTTTATGATTCACTTGTATGTATGTGTTAATTCAGGAAGAATGTTGTATCGCATTTCCTCAATAGC
TAATTATTGTTAAGCATTAGATGTTAATTTGTTACTGCCATCCCGTGGAAACCAACTGATTTCCAATGAATCCCT

GCTTGTGGTTTGAGTCCTTATCTCTACTTGGTGTGGCGCTGCAAGATCAGACGGTAATTAGAGTTCCTATGATA
GGCTCAGTCTGGTAGGTTAATATTTCCCTGCCGCGAAGGAATTATTTTTGATGTTCTCTCTTGTATAATGATTA
GAACATGCTCTTGTCTGTCTTAATTAGATCATGCATTTCTCCAGGTCGAGTCAGCGGCTAAGGGTAGGCGTGA
TGATGAGCAGAAGTGGATTAGAAAGTATGACGAGCAGATGTGGATACGATAGTTCATAACGCTATTTCCCTTT
TATATTTCTCAGTTCATTATGCACGTCTTCTTTTTACGGATGAGTTGATAACTCCAAGTCCCAAAATGTGATGAT
TCTTTTTGTATTGTTGATTTCTGCAGGCGCTGAGATTTTTTACATGGGTTGGGATATTATAATGTGTGCCTTTGT
AGTTCCTAGATAACTACGAAGTCTTGCCTGATGTTGATTATTCTAAGATTTTCAAGTTGTTAGCACTAGGTACAC
CATAGCAAGCATGACTAATGAACCATCCCAAGCATAAGTAGTAAATGTCCTTAGCTTACAAAGTAAGGGTAAA
CCTGTGTTTATATATGTAGTTTATTATATGAAGCAGCCGTAGATATTCAGAACATGTGCAGGGCAATTAAGTGA
AATAGAATATCCTCGGTTTACAAAGTAATGGTGAAGACTCGAAGTCTCTCTTGTACTTCATAGCATGGTGA
TGACCTTTTACATGTGTGATTATTGTTATTTCTTTGCCGGGTGATCCTACTAACATTGCAAATAGCTACAGTTT
CCCTTTCTCGACTATGGTCTTTTTAATAGACTGGAACTAAAAATATAATGATAGTTCATATAGTTTTGAGC
GGATGTAAGATGCTCACGCAAGACTTCGTAGTTATCTAAGAACTACAAAGGCACACATTATAATATCCCAACCC
ATGTAAAAAATCTCAGCGCTGCAGAAATCAACAATACAAAAAAGAATCATCACATTTGGGGCAGTTGGAGTT
ATCAACTCATCCGTAAGAAAGACGTGCATAATGAACTGAGAAATATAAAAGGGAAATAGCGTTATGAACTA
TCGTATCCACATCTGCTCGTCATACTTTCTAATCCACTTCTGCTCATCATCACGCCTACCTTAGCCGCTGACTCG
ACCTGGAAGAAATGCATGATCTAATTAAGACAGACAAGAGCATGTTCTAATCATTATACAAGAGAGAACATCA
AAAAATAATTCCTTCGCGGCAGGGAAATATTAACCTACCAGACTGAGCCTATCATAGGAACTCTAATTACCGTC
TGATCTTGACGCGCCACACCAAGTAGAGATAAGGACTCAAACCACAAGCAGGGATTTCATTGGAATCAGTTGG
TTCCACGGGATGGCAGTAACAAAATTAACATCTAATGCTTAACAATAATTAGCTATTGAGGAAATGCGATACAA
CATTCTTCTGAATTAACACATACATAAAGTATGAAATCAAAAAATAAACGTAATTCCTATTTTAGTATATG
TGTGAAAGGATTAATTATGATTTATTTGCTAGTACGAAGCTGTACTAGTTGTAGAATATGACTAGTTTTGCTAT
TGGTGTGAGCTGAACTCGAGCGACCGCTGAAATAATCAACACTTTGGATAGGAGCGTATGGCGCAGTACAAC
TTTATTGTTGAATCTTTATTTCTAATAATAGCAAGAAAGAAGCTTGGTCGGCATTGGAATATGACAGTTGTA
ATAAATTTATATGTACCAACCACTAATGCTGATGTTAATTAGTAAGACTCTTTGTTGGGCCATAATCAAC
ACATATATGTTACTTCATGTTCCGGACATAAGAAAAAGGTTGTTGGGCCATAGAGATATGTACATGTATCACGT
GGAAGGTGGAACATTAATTGTCATGCTTTGGTCATTGTATATATTACATACCATATGTATATGCATTAGCCTTTC
AAGTGCAAGCCCGCCAAAAAAGGTTGCTGAACTTGTATTTCTACATTGGTTTTGTCTTAACTTAACTGGTT
ATATTGTGGCTTATAGAGTACCATTATGTATAATGTCAAACAACCTTCGTTTTCTGAGTTCAACCGGGGACATTA
TGACACACACTCTTTACTAAAATGGAACCCAAACAGATCAAGACTGAACGTAAGTGTAGAACCATCATGTAGT
AACAATAAGAATTGGTTACCCCTGCTCTACTTAGGAGATCGAGGGGTGAGGGTCAATGTCCTTTTCATTGAT
CACCACGAAATTATTGTCCTCCACATTGTTCCCTTCTGAGATTTTTCTTGATCAACACATGGAGAAGCGTT
GAGAGAATTTGGTTTGTACCTTCTGATCAGTCTCTATTCTAATGACGTTGTTATCTTTGCAAACCAATAAAA
CAGGAGGTGACGCTCGAGTGCACATAAATCATGATTTTGGACCATCCACGGGCCTGCACATCAACCCCTCCA
AATCCATGGCGCTACCCATTATATGTGAAAATATAAACCTCACAGAGGTGCTCTTGGACAGTTCCAGCCACCT
ACCTGGGGCTCCACATACATACTTGGCTGAGATTAGCTAATACGTAGTTCATCATAGATAGGACTAAGGCC
AGGCTCGCGGGTTGGAAAAGGAAGTTTCTACCCATAGCTAGCAGGAGAATTCTAGTCAGGTGTGTCTCAGCG
GCATGCCAACATTGCGTATATCTTCTTTGAGTACCAAAGAAGCTCCTCGAGGAAATAGACAAATGTAGGCAT
AGATTTGTACGGAAGCAAACAATAGATCACTCGGGGCAGTTGCAAGGTGAACTGGTGCACGGTCTGCACA
CCGACCTTGTGAAGGGGGTTGTGTATCCTAGACCTGGAGCGCTTAAACCGCGCACTCAGGATGAGCTGGCTAT
GGATTGCTTGGGCTGACTTGGGCAGCCATGGGTGGGCCCAGCCACCTTCAAGCGACAACGAGAATGCTA
TTTTGCACCGACAACCACTATCACAATCGGCGAAGGTTACTCAGCCTTGTCTGGCACTCTTCATGGATTGGGC
CTAACACCCTCGCTGTTGCCTACCCTCTGCTCTAAAAACACTCTTGATGCAAAAAATAGGACTGTGCAAGATGTG
CTTCATGATGAACTTGGCTACAAGATTTTAGGAATGGGGACGTGCAACCTTCTAGAAAGAGTTCATTTGTCC
TCATCGTTAATCAGTGATGATGTCCTGAGCTTATGGAGGGCAGTACACACCAAATTTGTTGGAACGTGGAA
GAAAAAGGCAATACAAGACAAGCTCAGCTTATAGAGCGCAATTCTAGGGTAGAGTAGAATCGGATTTGGAG

AAGCTCATTGGCAGTCCAATGTACCATAGAACATCGAGATATTCATATGTCCACTAGTGCAAAAACCGCCTCTT
GACAAATGTCGCTTGCAAAGGCATGGCTAGCCCAACATCTATTTTTCCCACTTTACGTCTGCAACCTAGCAGAA
CCAGATATCAAGCACAACAATTTGTTATGTCAAATCACTATCATCTGTATTGTCAAATCATTTTTTTATTAACATG
TTGCATGCAAACATGCACCTGCATGCCTGTAACATGCTTATCAATATGTTGCATGCCGCCAGTATGGGTGGCGG
GACGGCCCATCTGCCACAGCCTGCCGCTGGCTGTGTGGCGGCAGGGTCCACCGACTGATTCCGTTCCATCG
TCGTTTGCATGTTCCGTTAACATATGGCCTGCCGCTGGTCTCTGGCGGCAGGGACTGCCGCTCCGCTCGTG
GCGGCACGAGCGGCAGGTGCCACGTGTGACTCGCGCGCCGACGCCACGATTTAGGTGATTTTTTCTCGTAA
TTTGATTGGGGGTGGTTTTTTTATCAACTGCGCTCGATAGGCGGTCTTTTTAGACAAAATTCGCAGCAGAGA
AGCAAGATTGCGGTGACCCTACTACGACGAGCCGGGACTCGATGTGACACTCGGGGCAAGGCTACTCGCTA
CATCTGCGATGTGCTGCAATGGCTACCAATTGCTTTTGTGCTGACGCTAACTGCTATGCGGCGGCAAAGGGCGGG
CAGCACAGCTACGCGACTGCAACTGCAACACACGCTCGCACACATAGAGGCCATGGAAAAGGGTGCTCACCC
AGGGTCCCTTGGGACATAATAGGTAGACGGGGACGATGCGAACGGGGCCCGGAAGAGGCGATGCTGCGG
ACAGGCTTCTGGAGCGGATAGCGACGCTAACGGCGCTGACGATGTGGAAGCTCTCTCCACGTCCTAGCGTC
GGGAATTGGACGCGAGCGTCTGCATGAACCACCCGACATCTCGGACGGAGCGGTGATTGCCACCAGAGGTG
CCGATGACGACGAGGAAGCCGGTGATCCTCACTGCTCTCTCTAACTCCTTTGAACATACTCTCTGATGACTC
TGAATCCCTGTTCAAGTGGAAGGAAGGAGGGAGAGGAAGGAGATGGCGGCAACGCAAGGGAAGGGGAAAA
CCCTAGACGAAGGGGGCGCGAACGCCGAGGCTAAATAGGCCGGGGATGATGGTGTGGCTGCATTGTCGTCC
GTCAAATGCCAGCACGACGCACGTACACCCTCTCTCTGACGAGGACAACGATGTGAGGCAAGTAGCGGT
CAGGAGGGAAGCTGGGCCGGGCACTCGGGTGTGAGAGTGAGCGGTTGTGCGCTGGCTGGGCTGGAGAGGG
AGAGAACCCAGGTAGGCCTCTCTCCCAACAAGCAAATTTAATCAACATCACGCAAGACTTCGTAGTTATCTA
AGAACTACAAAGGCACACATTATAATATCCCAACCCATGTAAAAAATCTCAGCGCCTGCAGAAATCAACAATAC
AAAAAGAATCATCATTGGGGCAGTTGGAGTTATCAACTCATCCGTAAAAAGAAGACGTGCATAATGAAC
TGAGAAATATAAAAGGGAATAGCGTTATGAACTATCGTATCCACATCTGCTCGTCATACTTTCTAATCCACTTC
TGCTCATCATCACGCCTACCCTTAGCCGCTGACTCGACCTGGAAGAAATGCATGATCTAATTAAGACAGACAAG
AGCATGTTCTAATCATTATAACAAGAGAGAACATCAAAAAATAATTCCTTCGCGGCAGGGAAATATTAACCTACC
AGACTGAGCCTATCATAGGAACTCTAATTACCGTCTGATCTTGCAGCGCCACACCAAGTAGAGATAAGGACTC
AAACCACAAGCAGGGATTCAATTGGAAATCAGTTGGTCCACGGGATGGCAGTAACAAAATTAACATCTAATGC
TTAACAATAATTAGCTATTGAGGAAATGCGATACAACATTCTCCTGAATTAACACATACATACAAGTGATGAA
TCATAAAAAATAAACGTAATTCCTATTTTAGTATATGTGTGAAAGGATTAATTATGATTTATTTGCTAGTACGA
AGCTGTACTAGTTGTAGAATATGACTAGTTTTGCTATTGGTGTGAGCTGAACTCGAGCGACCGCTGAAATAATC
AACACTTTGGATAGGAGCGTATGGCGCAGTACAACTTTTATTGTTGAATCTTTATTTCTAATAATAGCAAGAAA
GAAGCTTGGTCGGCATTGGAATATGACAGTTGTAATAAATTTATATGTACCCAACCACTAACTATTGCCGAT
GTTAATTAGTAAGACTCTTTGTTGGGCCATAATCAACACATATATGTTACTTCATGTTCCGGACATAAGAAAA
GGTTGTTGGGCCATAGAGATATGTACATGTATCACGTGGAAGGTGGAACATTAATTGTCATGCTTTGGTCATT
GTATATATTACATACCATATGTATATGCATTAGCCTTTCAAGTGCAAGCCCGCCAAAAAAGGTTGCTGAAAC
TTGTATTTCTACATTGGTTTTGTCTTAACTTAACTGGTTATATTGTGGCTTATAGAGTACCATTATGTATAATGT
CAAACAACCTTCGTTTTCTGAGTTCAACCGGGACATTATGACACACACTCTTACTAAAATGGAACCCAAACA
GATCAAGACTGAACGTAAGTGTAGAACCATCATGTAGTAACAACCTAAGAATTGGTTACCCCTGCTCTACTTAGG
AGATCGAGGGGTGTAGGGTCAATGTCTTTTTATTGATCACCACGAAATTATTG